UNCLASSIFIED

UCRL 8887

UNIVERSITY OF CALIFORNIA

Ernest O. Lawrence

Radiation Laboratory

CONTROLLED THERMONUCLEAR RESEARCH

QUARTERLY REPORT

June, July, August 1959

DISCLAIMER

UCRL-8887
Controlled Thermonuclear
Process
TID-4500 (15th Ed.)

UNIVERSITY OF CALIFORNIA
Lawrence Radiation Laboratory
Berkeley and Livermore, California

Contract No. W-7405-eng-48

CONTROLLED THERMONUCLEAR RESEARCH QUARTERLY REPORT

June, July, August 1959

September 10, 1959

Printed for the U. S. Atomic Energy Commission

Printed in USA. Price $2.75. Available from the
Office of Technical Services
U. S. Department of Commerce
Washington 25, D.C.

CONTROLLED THERMONUCLEAR RESEARCH QUARTERLY REPORT

June, July, August 1959

Contents

*Preceding reports: UCRL-8775 and UCRL-8682

UCRL-8887

CONTROLLED THERMONUCLEAR RESEARCH QUARTERLY REPORT

June, July, August 1959

Lawrence Radiation Laboratory
University of California
Berkeley and Livermore, California

September 10, 1959

GENERAL INTRODUCTION

C. M. Van Atta

During the period of this report significant progress has been made in several of the applied aspects of the controlled fusion program and interesting results have been obtained in a variety of fundamental plasma experiments. Activities during the past quarter are described under the following headings:

I. Pyrotron (Magnetic Mirror) Program
II. High-Energy Injection
III. Astron Program
IV. Livermore Pinch Program
V. Berkeley Pinch Program
VI. Theoretical Research
VII. Basic Experimental Research
VIII. Engineering and Technological Development

A listing of recent talks and publications of the controlled thermonuclear group is given at the end of the report.

A number of distinguished visitors spent the academic vacation period at Livermore and Berkeley. Since their contributions to the program are not necessarily reflected in the authorships of the sections of the report, a brief description of their activities is given below.

Dr. Chieh-Chien Chang, Professor of Aeronautical Engineering, University of Minnesota. Series of lectures on magnetohydrodynamics; hydromagnetic study of the rotating plasma in E×H devices, such as the Homopolar; description of a hydromagnetic injector for the Astron; description of a pulsed form of the Astron.

Dr. Herman A. Haus, Electronic Research Laboratory and Department of Electrical Engineering, Massachusetts Institute of Technology. Study of plasma oscillations excited by the streaming of the E-layer electrons through the plasma of an Astron device (study still in progress at Vienna, where Dr. Haus is spending about a year on a fellowship).

Dr. Norman L. Oleson, Professor of Physics, Naval Postgraduate School, Monterey. (Part-time consultant during the academic year.) Study of the characteristics of the P-4 plasma by various diagnostic means.

Dr. Robert H. McFarland, Professor of Physics, Kansas State College. Comparison of surface adsorption of hydrogen and other gases by well outgassed ribbons of titanium, molybdenum, and tungsten and on the vacuum-evaporated films of various metals.

Dr. Forrest I. Boley, Professor of Physics, Wesleyan University. Experimental and theoretical study of initiation, propagation, and attenuation of hydromagnetic waves in plasma.

The manpower assigned to controlled thermonuclear research for the period May, June, and July (lagging the technical report period by one month, as usual) is given in the following table.

Approximate Direct Heads

	Livermore	Berkeley	Total
May 1959	266	64	330
June 1959	278	75	353
July 1959	267	76	343

I. PYROTRON (MAGNETIC MIRROR) PROGRAM

INTRODUCTION AND SUMMARY

Richard F. Post

The efforts of the Pyrotron group in this quarter again were concentrated on injection studies and on the analysis of plasmas produced by slow magnetic compression. Experimental results since the September 1958 Geneva Conference were reported at an International Conference at Uppsala, Sweden.

Some of the results (reported in greater detail in the following section) that seem worthy of note are:

(1) More detailed analysis of trapped plasmas in the experiments by Coensgen et al., showing the effect of magnetic field intensity.

(2) The determination of radial distributions of the escaping electron fluxes in Table Top, from which information on radial plasma diffusion can be gleaned (Robert Ellis). This shows that the indicated role of radial diffusion is very small, and that the plasma density falls rapidly to a very small value outside a central core about 1-1/2 in. in diameter.

(3) The refinement of buildup calculations for the ALICE energetic neutral injection experiment, showing the role of the chamber wall in the buildup and establishing limits on the required pumping.

It is worth noting that Ellis's results on the slowness of radial diffusion, coupled with the long "single-particle" confinement times reported in the β-ray experiment (Lauer et al.) show that truly stable confinement of an adiabatic plasma of high electron temperature is a fact. But in the experiments by Ellis, and in almost all previous Mirror experiments by this group, the ion temperatures are known to have been much lower than the electron temperature. Thus the important question of whether stable confinement will still be observed in the more interesting case of ions hotter than electrons is yet unanswered. This explains our continued emphasis on perfecting injection methods that will allow the attainment of such a condition.

MAGNETIC HIGH-COMPRESSION EXPERIMENTS

Frederic H. Coensgen

A. Injection Studies

1. Angular Distributions

Angular distributions have been obtained for plasma ions for conditions discussed below by the method described in previous reports.

(a) Longitudinal injection (axis of source aligned with magnetic field) into a uniform magnetic field

Angular distributions have been determined for several magnetic field values in the range from 50 to 1000 gauss. The distribution is broader at higher magnetic fields but the amount of plasma is less. The number of ions for which the angle between the velocity and the magnetic field vectors is greater than 20 degrees remains nearly constant. Modifications in the injector construction or operation could possibly increase the quantity of plasma injected into the high magnetic fields.

(b) Longitudinal injection with a local magnet

This configuration has been studied at 200, 400, 700, and 1000 gauss base field. The effect of the local field, both in aiding and in opposing the base field, was studied extensively for base-field values of 700 and 1000 gauss. The broadest distributions were obtained for 1000 gauss base field and the highest opposing local field (~ 2000 gauss). Again the number of ions with high angular momentum remained about constant because of a decrease in the amount of injected plasma. Moreover, modifications of the injector or pulsing conditions may increase the quantity of injected plasma.

(c) Longitudinal injection through a magnetic cusp (i. e., base-field direction reversed at injector)

The angular distribution is found to be broader for injection through the cusp than injection into a uniform field. Although the amount of injected plasma is decreased for the cusp injection, the method can be utilized at low magnetic fields, which is advantageous for high-compression experiments.

(d) Radial injection

A number of radial configurations were investigated as the method for observation of the angular distribution was developed. The result of one run with two sources at 90 deg to the magnetic field agrees with the previous qualitative observations that the angular distribution is sharply peaked along the field lines and that the ion energies, as judged from time of flight, are lower. The change in ion energy may be due to a difference in operation of the injectors in transverse magnetic fields. However, the angular distribution may indicate that the simple ideas concerning cross-field injection of plasma beams are not correct. This problem is of fundamental importance and

should be fully investigated, particularly as there are proposals for extensive programs based on injection of high-energy plasmas (Robert E. Ellis's memo to Richard F. Post, April 14, 1959; John Luce, ORNL-CF-59-3-70).

2. Colliding Plasma Streams

Plasma injectors have been inserted at both ends of the dc test facility and preliminary investigations are under way to determine what phenomena occur upon the collision of two plasma streams confined by a longitudinal magnetic field. Considerable theoretical work has been done by E. N. Parker and F. D. Kahn which should apply to our conditions. In particular the translational velocity of the plasma may be converted to random motion in a very small distance. If this were true, such collisions would be a good injection mechanism.

B. Plasma Injectors

1. Toy Top Injectors

The parametric study of the plasma injector operation has been completed and a report is being written.

2. Gas-Fed Injector

This injector is based on the reported observation of high translational ion velocities from the first section of John Marshall's (LASL) experiment. It consists of a pulsed gas valve and a single-turn coil. In operation a pulse of gas is injected into the coil where it is ionized and heated by the rapidly changing magnetic fields. In the first setup there was considerable arcing around the insulators and coil connections as well as a failure of the coil in the pulsed gas valve. The system is being reworked.

C. Instrumentation

1. Ion Coupling from System to Analyzer

Several angular distributions have been obtained which are adequate for an initial plasma which is to be magnetically compressed, provided the ion energies are of the order measured along the field lines and provided the ions with high angular momentum are deuterium.

The measurement of the energy of the ions that have high angular momentum is, at present, our most important problem, and must be solved before magnetic compression can be investigated more completely than previously. For study of the coupling problem by using the injection methods that have been developed, provisions have been made to mount six sources off axis. This provision is necessary as the angular distribution from the source is sharply peaked along the magnetic field line through the axis of the source. Thus the analyzer slit and source should be radially displaced.

The twelve-channel analyzer was connected to the system early in August. The calibration of the analyzer as determined from "bias runs" has been compared with the previous calibrations using an rf ion source. It was found that the quantity and density of the plasma entering the analyzer slit had to be reduced in order to eliminate polarization and space-charge effects. This change resulted in reduced signal and thus in increased noise problems. Consequently the shielding of the analyzer and of the firing circuits is being improved.

An angular-distribution run was made with the analyzer before the modifications were started. The bias runs of the 100- and 250-ev channels were in reasonable agreement with the previous calibrations. From the angular distributions for these channels the behavior of the ions appears to be adiabatic. If this result is found for higher energies, then the coupling can be accomplished by allowing space for adiabatic ion behavior, with the normal decay of the magnetic field at the end of the system. Some short sections of large diameter may be needed, but a long tapered guiding field and long large-diameter vacuum sections would not be needed.

2. Data-Handling System

Four men are needed to operate the experiment and analyzer, and about 10 man-days to reduce one analyzer run. A data-handling system that will present the data in digital form is being developed by David R. Branum of the Electronic Engineering Department.

This system should eliminate the need for one man from the operating crew and should reduce the data-reduction time to 1/2 man-day per run. One channel of a twelve-channel system should be ready for testing within 2 weeks.

3. Electron-Multiplier-Equipped Analyzer

Dr. Herman Bandel of the Sylvania Laboratory has been equipping one of the magnetic-electrostatic analyzers with a following accel-decel electrode system and an electron multiplier. The acceleration system is used to adjust the energies of the ions to the same value at the first dynode of the electron multiplier. The resolution of the instrument is quite good compared with other instruments of this type in the laboratory and the effects of space charge have been very apparent. Considerable work has been done in eliminating these effects. It is possible that the instrument could be used to determine the maximum density of a plasma at an analyzer slit for which space-charge effects are negligible. The present plan is to put the instrument at one end of Table Top and determine the energy spectrum of the ions scattered out of that system.

D. Multistage Compression

Arthur E. Sherman has been working on the design for a multistage experiment to be built in the Toy Top area. The design problem is quite involved, as we wish to maximize the final plasma "temperature" within the limitations of the available dc power, stored energy, floor area, floor loading, and glass vacuum parts. Some modifications of the small banks and building partitions may be acceptable.

ELECTRON-DISTRIBUTION ANALYSIS

Robert E. Ellis and Walton A. Perkins

50-kev Electron Accelerator (for Fluor Calibration)

The accelerator, without the deflector plates and deflector-voltage pulsing circuit, has been assembled and tested at voltages up to ~ 10 kv. This low-voltage limitation will be overcome by replacement of the Victoreen resistors in the accelerator stack with larger ones capable of holding 10 kv each. The replacement resistors have been received and tested for use in vacuum, and will be installed shortly. Although a small spot (~ 1/16-in.-diameter) has been obtained at a distance from the end of the accelerating tube corresponding to a desirable location for fluor testing, the dependence of focal length on the stack voltage and the distance between the gun and the first stack electrode may put an undesirably low limit on beam intensity with the present gun (Huggins Type HA-4). The use of guns with oxide-coated cathodes has been avoided because of deterioration when let up to air, but in order to obtain a large fraction of the original beam through the accelerator stack, we will investigate the possibility of using such guns with built-in focusing and deflecting anodes to replace the diverging-beam gun now used.

The electronic circuit for the pulsed deflector plates has been essentially designed and tested, but not yet used on the accelerator because of some unresolved difficulties with the voltage pulse shape. This circuit will provide a square pulsed deflection voltage of ± 3 kv on the ground-referenced deflector plates, with selected pulse widths of 10 μsec, 100 μsec, 1 msec and 10 msec, with the pulses occurring at intervals of 1, 10, and 100 sec. An initial test of the deflection circuit should be made in the next 10 days.

Scintillator Probe Measurements

The four-channel fluor probe has been tested and used for measurements of the radial distribution of electron energy flux due to electrons escaping through one of the magnetic mirrors of the Table Top machine; the field produced by this mirror was smaller than the other by about 10%, so that the escaping electrons were directed out this mirror. Satisfactory signals were found at various distances from the plane of the mirror.

Since it was discovered that a lower noise level and more dynamic range in the unsaturated signal produced by the DuMont 6395 photomultiplier tubes and the transistorized gain-of-five preamplifiers would be desirable, the design and testing of such bases was put under way, and they should be available in about 1 month.

When two of the four probe channels were utilized as monitors, the signals from the other two gave the relative electron energy flux as a function of distance from the magnetic axis of the machine as the probe was moved along a line perpendicular to and intersecting the axis in a plane 5 in. from the mirror. If the energy distribution of electrons in the plasma is independent of radial distance from the axis, and if the time decay of the pulsed magnetic field is taken into account, an increase in the electron energy flux with time at some distance r from the axis, relative to the flux on the axis, may be taken as an indication of a radial drift of plasma electrons across magnetic

field lines. Our measurements indicate that at the position 5 in. outside the mirror the electron energy flux distribution has a width at half maximum of about 1 in., and the flux is reduced to 1/10 or less of its axial value at a radius of ~ 3/4 in. This would indicate that the plasma diameter at the mirror is about 3/4 in., and with a mirror ratio of 2, about 1 in. midway between the mirrors.

There was some indication of a slight increase in relative flux at radii of 1/8, 1/4, and 3/8 in. during a period from 1 to 3 msec after the magnetic field was initiated. At later times and greater radial distances the flux (relative to axial flux 1 msec after the field was pulsed on) was always less than the axial flux and decreased more rapidly with time. With a greater dynamic range of gain, as will be supplied by the new phototube bases, it will be possible to investigate the relative flux at greater distances from the magnetic axis and further outside the main body of compressed plasma--the region in which the radial drift of electrons, caused by fluctuating electric fields, is most likely to occur (as pointed out by Richard F. Post[1]).

A single-channel fluor probe (1-in.-diameter stainless steel probe stem) was also inserted radially into the Table Top machine at a position midway between the two mirrors. This probe would see electrons of energy greater than a few kilovolts which might diffuse radially outward from the plasma. No signal was obtained on this probe at distances up to within about 1 in. from the magnetic axis. At positions closer to the axis, the probe interfered with the formation of a plasma. An upper limit of radially diffusing electron energy flux of less than 1% of the flux observed near the axis, 5 in. outside the mirror, can be applied here, subject to the calibration of this probe against the four-channel probe signals with which the comparison of relative signal was made. This will soon be accomplished.

During the above measurements, a titanium washer stack source was fired axially into the region between the mirrors to establish the plasma. In addition to the usual crowbar ignitrons, a mechanical switch crowbar, in parallel with the ignitrons, was used to relieve the ignitrons of most of the current pulse from the capacitor bank. The mechanical switch crowbarred the coil circuit 1 msec after the bank was fired. This switch worked well for about 1700 pulses and then failed because of deterioration of the surface of the switch blade. The 1/e decay time of the magnetic field with the switch operating was about 12 msec, compared with about 9 msec without it. The switch has been repaired and is now ready for use again.

Utilizing titanium washer stack sources fired radially into a plasma established by pulsing the coils after an axial source was fired, we have observed the effect in the four-channel fluor probe to be a considerably enhanced signal produced by electrons escaping along the axis through the mirror. With the magnetic field initiated 20 μsec after the axial source was fired, it was possible to pulse the radial sources at any time during the 5-msec duration of the signal and observe--at, say, 500 μsec, 1, 2, 3, and 4 msec after the field was pulsed on--the subsequent increase in electron

[1] Richard F. Post, Summary of UCRL Pyrotron (Mirror Machine) Program, UCRL-5044, June 27, 1958.

energy flux out of the mirror. By putting a foil wheel in front of the probe, we were able to determine energy distribution of the escaping electrons both before and after the radial sources were fired. An analysis of the data should yield the relative spectra of electron energies in the original and perturbed plasmas. As mentioned below, a code for the analysis is now essentially completed and the results of this experiment may be interpreted in the next few weeks. As pointed out by Fred Coensgen, this procedure might be used for "dumping" a plasma through the mirrors at a given time to provide a time-independent analysis of the plasma components. The present data indicate that the signal from the perturbed plasma lasts about as long as the unperturbed signals from the axial source alone, although the relative magnitude may be considerably greater at times subsequent to firing of the radial sources.

An apparently satisfactory code for the 650 computer has been developed for the solution of the set of integral equations arising from the electron energy-distribution measurements with fluor probes. Tests on the accuracy of the matrix-inversion solutions, using a Maxwellian distribution as the function to be solved for, indicate that the solution is good to 5% or less in the range from 10 kev to 220 kev electron energy. Assumptions about the nature of the electron energy distribution at higher energies, as was previously believed to be required, do not appear to be necessary. A considerable amount of data previously taken may now be analyzed, including (a) data on the effects on the electron distribution--at different times during containment of a compressed plasma--of the introduction of an impurity gas (argon) into the plasma, as well as (b) the result of compressing plasmas which have been injected into different values of dc trapping fields, and thus determining for different compression ratios the variation in plasma electron mean temperature.

Electron and Deuteron Energy Analyzer

An accel-decel-accel type of energy-distribution analyzer for electrons and deuterons is now in the design stage. This analyzer is designed to look at the electrons or deuterons escaping through one mirror of a mirror machine, the electronic and ionic components being separated by means of repelling and accelerating voltages before they are accepted into the detector. All the electrons (or ions) above a given repelling voltage will be accepted by the detector. For electrons, the detector is a terphenyl-loaded plastic fluor. For deuterons, a plastic fluor with a deuterated foil in front of it will look at protons from the D(d, p)T fusion reaction produced in the deuterated foil. Accel and decel voltages of up to 150 kv will be required. Three cylindrical electrodes are located in a region from which the magnetic field produced by the mirror machine is excluded by means of magnetic shielding.

Vacuum Development

A titanium-evaporation pumping unit, utilizing resistance heating in the evaporation elements, has been fabricated. This unit is intended as a small-scale prototype of a larger unit (perhaps 30 in. in diameter and about 4 ft long) which, in conjunction with high-speed diffusion pumps, will be utilized in the first stage of a multistage high-compression mirror machine.

As soon as space becomes available, this unit will be set up and tested for pumping speed, reliability of operation, etc., along with the diffusion pump and associated equipment intended for use in the vacuum-development testing area.

ADIABATIC LOW-ENERGY INJECTION AND CAPTURE EXPERIMENT (ALICE)

Charles C. Damm in charge

Theoretical Considerations

Archer H. Futch, Charles C. Damm, and Victor Seeger

The buildup equation for neutral-atom injection discussed in the preceding progress report has been put in the form for machine computation and turned over to the computer group for coding and machine solution. An additional term describing the effect of charge exchange of the incoming beam with trapped ions has been included. The machine program is being set up so that different parameters may be varied and the problem recomputed.

An approximate analysis has been made of the requirements for plasma buildup, including the effect of the thermal gas flux resulting from wall bombardment by fast atoms. At high plasma densities, well above the "burn-out" range, the fraction of fast atoms returning to the plasma as thermal neutrals must be less than the ratio of the effective trapping cross section to the charge-exchange (neutralizing) cross section. (At a proton energy of 20 kev, this ratio is about 0.3.) At plasma densities near "burn-out" this requirement is more severe, depending on the excess of beam current over the minimum required for exponential buildup, and can be specified for any set of conditions.

It is clear that a plasma growth above about 5×10^{11} ions/cm^3 depends upon the presence of suitably active walls, for the energy range of the present experiment. Our preliminary vacuum work is oriented towards the preparation of such walls, and the measurement of their properties.

Grid Source Development

Frank J. Gordon and James F. Steinhaus

A solenoidal magnetic field supplied by two existing coils has been used in the grid source development to date. In order to check the feasibility of extracting the beam from this field, detailed field mapping was done at coil separations of 5, 10.5, and 18 in. By use of these field maps and a "mechanical particle analog,"[1] trajectories were plotted for particles emerging from the accelerating slit at 0 deg and ± 10 deg from the normal to the plane of the exit slit. Traces were made for particles from the center of the slit and from points 1 in. and 1.5 in. from the center.

From these studies in which space charge was neglected, it appears that with suitable tilting and shaping of the exit slits and with a slightly larger radius than we had hoped to use, a reasonable portion of the beam can be extracted. It would enter an iron tube which shields out the reverse external field with very little disturbance to the internal field. Equipment is now being assembled to check the beam after it has traveled down approximately 6 ft of shielding pipe.

The addition of a saturable-reactor type of arc-current regulator has stabilized operation so that beam characteristics can be studied readily. Stable operation for a period of several days can be expected provided the beam level is dropped somewhat below maximum. (The sparking that accompanies maximum beams wears out electrical equipment.)

Beam-divergence studies were made by scanning with an adjustable water-cooled target across the beam at the 90° point of the trajectory. These scans were made with variations in radius, magnetic field, and accelerating voltage but not in geometry. Analysis of these data is not yet complete, but typical curves are shown in Figs. 1 and 2. The beam profile shown in Fig. 1 was taken with high output current, which should emphasize divergence due to space-charge effects. In Fig. 2 the increase in output with increase in magnetic field while the accelerating voltage is held constant is easily seen. Unfortunately, good extraction from the magnetic field requires a radius greater than 4 in., which is on a lower curve when hydrogen is used. Deuterium will require a higher magnetic field but output will be down because of the greater mass.

The source was briefly operated with no change other than from hydrogen to deuterium gas. The beam was about 500 ma with deuterium, compared with 630 ma with hydrogen.

Highest output to date has been 848 ma of hydrogen beam from an exit grid of 0.314 in.^{2} Highest current density to date has been 730 ma from 0.250 in.^{2}, giving 2.92 amp/in.^{2}

Emphasis will now be to get a maximum amount of beam out of the magnetic field and into an acceptable angular spread.

---

[1] W. I. Linlor, "The Mechanical Particle," Engr. Note 4501-13 CVL-7, Nov. 8, 1955. The original inventor was Bayard Rankin, Berkeley (UCRL-2272); the present version was designed by Art Millman and John Turner of Livermore.

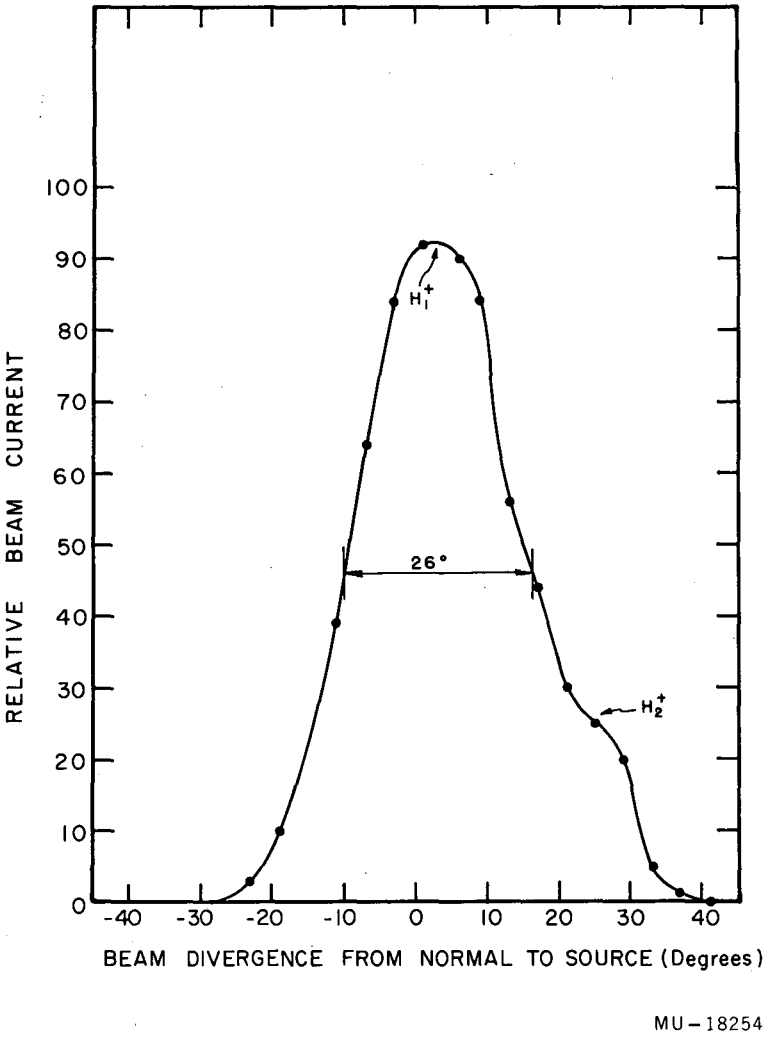

Fig. 1. Hydrogen beam profile. Magnetic field 2600 gauss; accelerating voltage 18 kv. Beam radius ρ=2.92 in. Total source output 767 ma. Hydrogen beam in profile 672 ma.

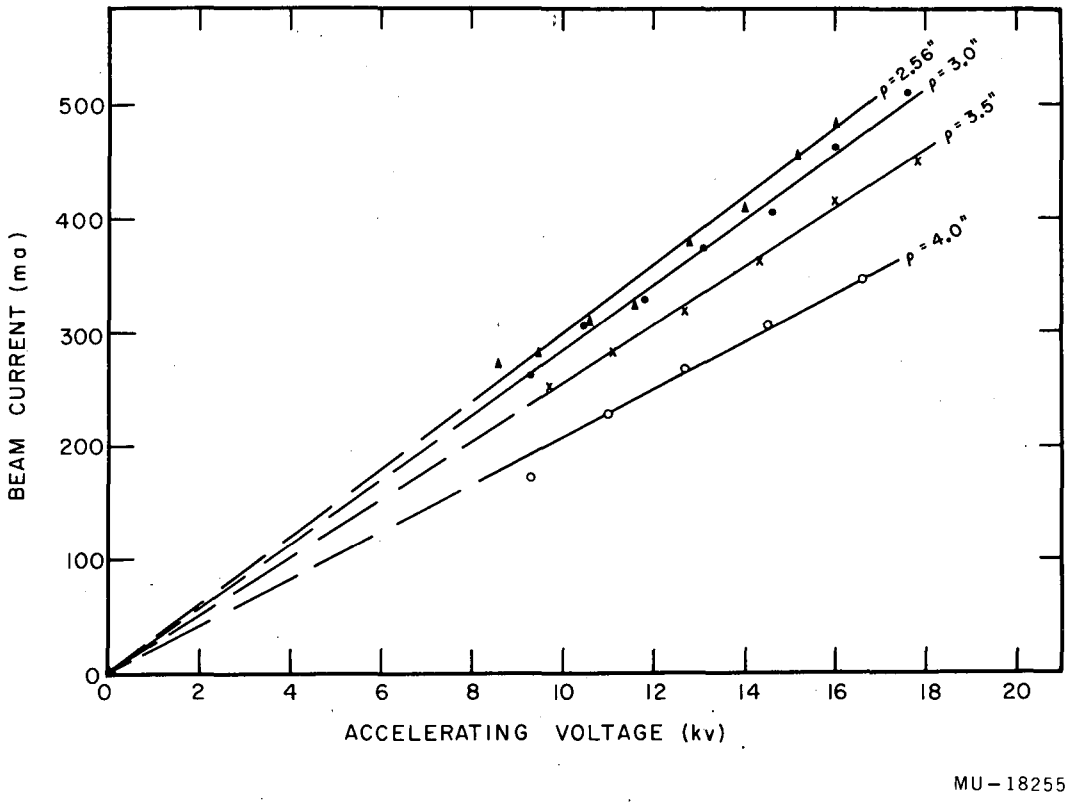

Fig. 2. Hydrogen ion current (H_1^+ plus H_2^+) for constant radii.

Beam Neutralization

Archer H. Futch

Hydrogen Jet Experiment

Experimental apparatus to determine the feasibility of a hydrogen jet as a beam neutralizer has been constructed. Preliminary runs indicate that the mass flow and the angle of divergence the jet makes at the nozzle exit agree approximately with aerodynamic flow calculations. With the mass flow approximately one tenth that which would give the required product of H_2 target density times thickness of 3×10^{15} atoms/cm^2, the gas pressure in regions outside the jet was higher than desired. The high gas density outside the beam is probably due to scattering of the beam molecules by the background gas. To decrease this scattering and to increase the pumping speed of the system, a 32-in. oil diffusion pump will be installed on the system.

To measure the distribution of density in the hydrogen jet, special Pirani gages of the type developed originally by Ellett and Zabel[1] have been built and now await testing and calibration. This project is being pursued by Victor Seeger.

Vacuum and Surface Studies

Charles C. Damm, Angus L. Hunt, Robert H. McFarland,* and Earl C. Popp

The activity reported under this heading includes the studies of gettering and getter pump development, mass-spectrometer studies in high vacuum, and the interaction of surfaces with energetic ions and atoms.

Getters and Getter-Pump Development

It has been reported previously that molybdenum can be evaporated from a simple filament wire in quantities sufficient to provide a large surface area for the adsorption of hydrogen. A pump operating on this principle is nearing completion, and information on the characteristics of this pump, as well as some basic information on the adsorption of hydrogen on the deposited molybdenum, is promised for the future.

Completion of the experiments on the evaporation of molybdenum by the electron-bombardment method has again been delayed by failure of the vacuum system. Although a preliminary test of the electron-bombardment mechanism was successful in the range 10^{-7} mm Hg, the copper-pinch seals did not survive the 400°C bake necessary to achieve ultrahigh-vacuum conditions and meaningful experimental results.

---

[1] A. Ellett and R. M. Zabel, Phys. Rev. 37, 1102-1112 (1931).

*Summer visitor from Kansas State University.

Further work on the gettering ability of molybdenum films deposited from a filament has been attempted by means of a comparative study of hydrogen adsorption on tungsten, molybdenum, and zirconium filaments, but it has been repeatedly delayed by the poor reliability of copper-pinch gasketing under bake-out at high temperature. As the cause for these gasketing failures is not known, a separate study of the gasket problem has been initiated.

The evaluation of an evaporated barium film as a getter for hydrogen at pressures of about 10^{-5} mm Hg has been discontinued. It is probable that no further work will be done with barium until the gettering characteristics of molybdenum have been determined.

The Bakable Mass Spectrometer

Many of the components for this instrument are now on hand. The vacuum systems have been assembled. In view of our recent experience with gasket failure under bake-out, these systems are currently undergoing extensive tests for reliability.

Surface Bombardment Studies

A surface Bombardment experiment has been undertaken. A controlled pulse of molecular and atomic hydrogen ions of up to 15 kev energy will strike an atomically clean metallic target. The ratio of molecular to atomic ions in the present beam has been measured and found to be 1.5:1, although this ratio is variable by adjustment of the source arc conditions.

The target is contained within a portion of an ultrahigh-vacuum chamber, and it is expected that pressure measurements as a function of time with an ionization gage of rapid response will provide values for sticking probabilities for these ions on the clean target. The ultrahigh-vacuum portion of the experiment is under construction.

P^4 (STEADY-STATE PLASMA) SYSTEM

William L. Barr, Daune M. Gall,* Andrew L. Gardner,
Laurence S. Hall, Raymond L. Kelly,† and Norman L. Oleson*

A substantial setback resulted when in the middle of June a rupture occurred in the water-cooled wall of the PIG discharge anode and several gallons of cooling water flooded into the vacuum system. Although the system was back in operation in about 3 weeks, its performance has only recently been fully restored to that experienced in the "preflood era."

Part of the down time was utilized to make needed magnetic-field measurements in the region of the PIG discharge.

Construction will commence soon on a tungsten lamp bank to be used in conjunction with the present (50-kw) nichrome ballast resistor for the PIG. The tungsten resistance characteristic will permit the load resistance to be more nearly optimum for both starting and running conditions.

Spectroscopy

A system capable of directly plotting the profiles of spectral lines has been assembled. The apparatus consists of a monochromator to isolate a spectral line, a Fabry-Perot interferometer to provide the necessary high resolution, and a photomultiplier tube to measure the intensity at the center of the interference pattern. Scanning is accomplished by varying the gas pressure (and hence the refractive index of the gas) between the interferometer mirrors.

This system has the advantage of both linear dispersion and linear response. It has the disadvantage of requiring an intense source of light that will remain steady for several minutes at a time. The P^4 machine meets these requirements.

The preceding progress report mentioned the production of spectra of refractory metals with P^4. We have observed the vacuum ultraviolet spectra of Mo, Ta, and W by evaporating material from a molten ball (using the P^4 beam as the heater), with the atoms undergoing subsequent ionization and excitation in the P^4 beam. Very rich spectra of these elements have been produced; the shortest wavelength recorded was 62 ev (λ 198.839, Mo VII). Plans are being considered for the production and classification of spectra.

In the vacuum ultraviolet region NV and OV spectra have also been observed which indicate substantial numbers of electrons with energies greater than 75 ev.

Probe Measurements

Measurements with a single electric probe have yielded clean voltage-current characteristic curves in the outer portions of the plasma column.

---

*U. S. Naval Postgraduate School.

†Stanford Research Institute.

Refinements in the technique now permit measurements as near as ~ 8 mm from the axis of the beam. It is hoped that a similar probe mounted as a spoke on a continuously rotating axle may have a sufficiently low duty cycle to probe to the axis without excessive heating.

Some measurements with a floating double probe gave satisfactory agreement with the single-probe data, but at present the single-probe method is simpler to apply to this experiment.

Measurements with the heated (constant-temperature) probe mentioned in the preceding report revealed experimental complications that led to deferring its use in favor of the simpler type.

A mock-up of a water-cooled probe for measuring energy flux in the beam performed satisfactorily in an oxygen-acetylene flame. Further evaluation of this technique is planned.

Microwave Measurements

A 70-kMc microwave beam transmitted through the plasma does not show appreciable attenuation (or reflection) by the plasma ($\leqslant$ 3db), whereas a 36-kMc signal becomes attenuated 24 db or so. These measurements rather well bracket the maximum electron density in the downstream portions of the plasma between 1.5 and 5×10^{13} electrons/cm^3 under present operating conditions.

The 10-cm receiver for measurement of radiation from the plasma is being relocated to improve the isolation from extraneous electrical noise near the plasma. No further measurements have been made.

Other Studies

Equipment is being assembled for the injection of an electron beam along the axis of the system. An Eimac klystron gun from a 4K 50,000 LQ tube will be employed.

Further measurements have not yet been made of propagation of hydromagnetic waves along the plasma column.

PLASMA POTENTIAL DIAGNOSTICS

Thomas O. Passell*

Assessment of electric potentials at the 180° focal plane of the hydrogen ion output from a hydride pulsed ion source has been completed. A report describing the results in detail is now in rough draft. The E×B electron beam-deflection scheme proved successful. It showed the ion beam to be less than 40% neutralized at the 180° focal plane region. This condition was for 15- to 45-ma 400- μsec 6.5-kev H^+ ion pulses. This confirms suspicions that space-charge electric potentials were present in the beam and were thus the source of beam blowup. Electric potentials measured as a function of background neutral gas pressure (hydrogen and argon) and time after pulse initiation showed the expected trends. Even for gas pressures up to 3×10^{-4} mm Hg and times up to 400 μsec after start of pulse, neutralization was not complete.

*Stanford Research Institute

II. HIGH-ENERGY INJECTION

ENERGY LOSS TO ARC ELECTRONS

Francis C. Gilbert, Warren Heckrotte, Ross E. Hester,
and John Killeen

The high-energy molecular ion injection scheme[1] as previously reported involves the use of an axial arc to dissociate the molecular ions. The presence of an arc in the center of a hot plasma will cause a serious drain on the hot ions, via the low-energy electrons in the arc. For example, a proton whose energy is 10^5 ev loses energy at the rate of 10^7 ev/sec in a Maxwellian electron energy distribution whose density is 10^{12} cm^{-3} and whose temperature is 10 ev.[2] In order to determine the effect of this energy loss upon the build-up of a hot plasma, the build-up equations have been modified to take account of this energy loss. The positive-ion energy distribution was divided in 11 intervals from 1 kev to 100 kev. The ion density n_i in the ith energy interval E_i is governed by

$$\frac{dn_i}{dt} = \frac{n_{i+1}}{(E_{i+1}-E_i)}\left(\frac{dE}{dt}\right)_{i+1} - \frac{n_i}{(E_i - E_{i-1})}\left(\frac{dE}{dt}\right)_i - n_i n_0 \sigma_i^{cx} v_i - n_i \sum_j m_{ij} n_j, \tag{1}$$

where the first term on the right represents the gain of ions from the $i+1$ energy interval and the second term represents the loss of ions to the $i-1$ interval. The third term gives the loss rate via charge exchange ($\sigma_i^{cx} v_i$) on the neutral gas of density n_0. The last term takes account of the loss of particles by scattering (m_{ij}) through the mirrors.

The neutral density is determined by

$$V_0 \frac{dn_0}{dt} = i + \beta I - S n_0 + (1-k) \sum_i n_i n_0 \sigma_i^{cx} v_i V - k \sum_i n_i n_0 \sigma_i^i v_i V \tag{2}$$

$$+ (1-k) \sum_i \sum_j m_{ij} n_i n_j V,$$

where $(i+\beta I)$ is the neutral leak current, V_0 is the machine volume, V is the plasma volume, S is the pumping speed, σ_i^i is the ionization cross section in the ith energy interval, and k is the efficiency factor for eliminating cold ions in the end conductances. The quantities are defined as reported in the preceding report,[1] Table I, Case A, except that where appropriate they are made energy-dependent. The large energy loss to the high-density arc in Case B eliminated it from consideration under these conditions.

---

[1] See preceding report, Controlled Thermonuclear Research Quarterly Report, UCRL-8775, June 1959, pp. 16-20.

[2] Lyman Spitzer, Jr., Physics of Fully Ionized Gases (Interscience Publishers, Inc., New York, pp. 76-79).

The results of a computer solution of the 12 coupled equations are shown in Figs. 3 and 4. Figure 3 displays the total ion density and the neutral density as a function of time. It is observed that the ion density levels at 5×10^{11} cm^{-3}, a factor of 10 lower than that for the energy-independent case. However, this density is considerably higher than the average arc density (10^{11} cm^{-3}) as seen by the molecular ions. Therefore, the arc may be turned off at this point and the build-up allowed to proceed on the trapped plasma.

The energy distribution above 1 kev of the trapped ions is shown in Fig. 4 at various stages of the build-up. It is apparent that at equilibrium the distribution is very broad. When the arc is turned off the distribution should shift to higher energies.

The foregoing problem involves a machine with a hydrogen arc. It may be possible to increase the break-up efficiency by using a helium or nitrogen arc. The cross section ratio $\sigma_{cx}/(\sigma_{cx}+\sigma_i)$ is favorable for "burn-out" for either gas. Figure 5 shows the solution to the three coupled equations necessary to describe such a system. (Energy loss to the arc was not considered.) The nitrogen gas load on the system was assumed to be 2×10^{17} atoms/sec, the same as the hydrogen leak. The other parameters are the same as those previously reported[1] with the addition of the appropriate nitrogen atom charge-exchange and ionization cross sections.

It is seen that the nitrogen background gas is exhausted very rapidly in comparison with the hydrogen background gas. This is because the H_2^+ beam represents the largest gas load on the system. In an actual machine the input flux of nitrogen gas would be terminated as soon as it was possible to transfer from arc trapping to plasma trapping, allowing the density of nitrogen to be exhausted to a very low value indeed. Nitrogen was chosen as an example, but consideration of charge exchange with the arc ions and the electron temperature one may be able to achieve in high-Z arcs might indicate helium to be a good compromise.

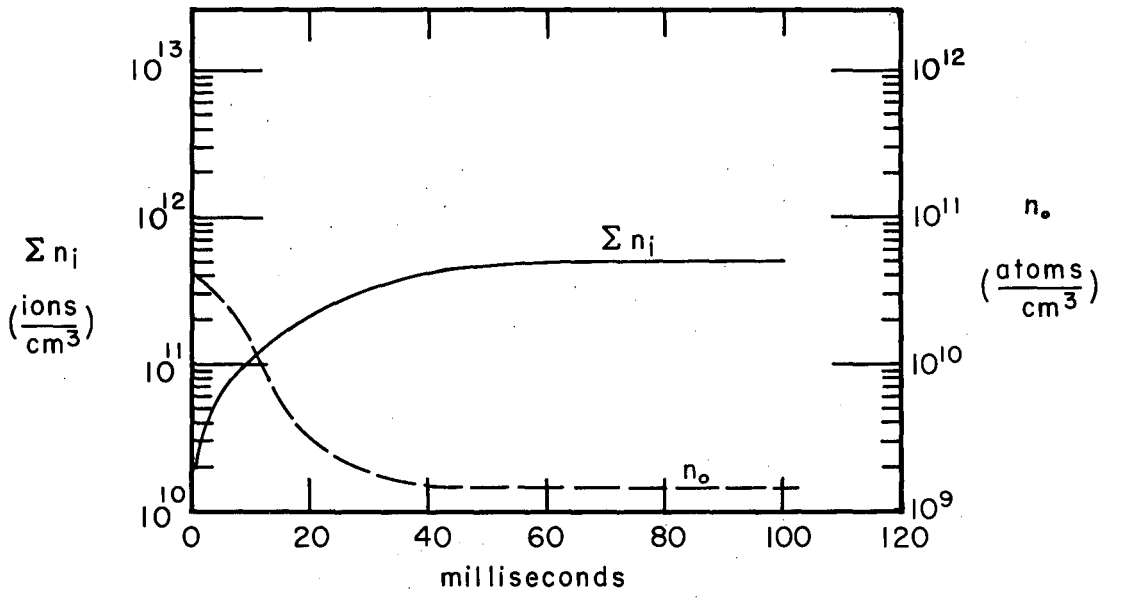

Fig. 3. Ion and neutral-atom density as a function of injection time.

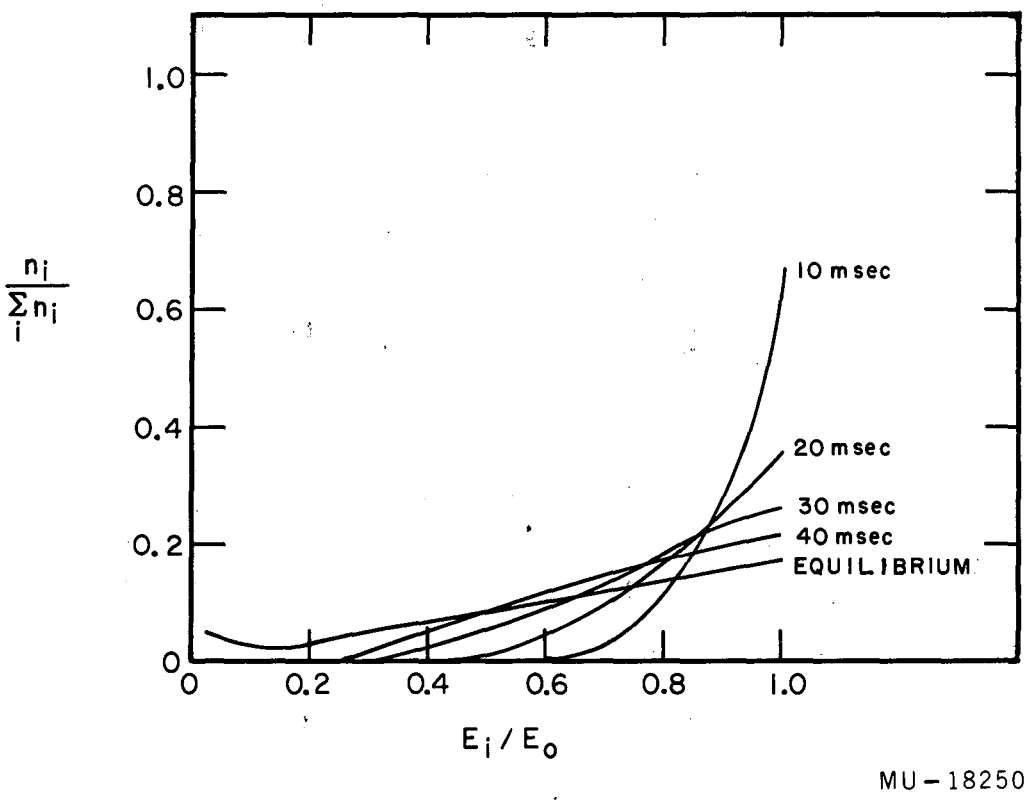

Fig. 4. Ion-energy distribution at various injection times.

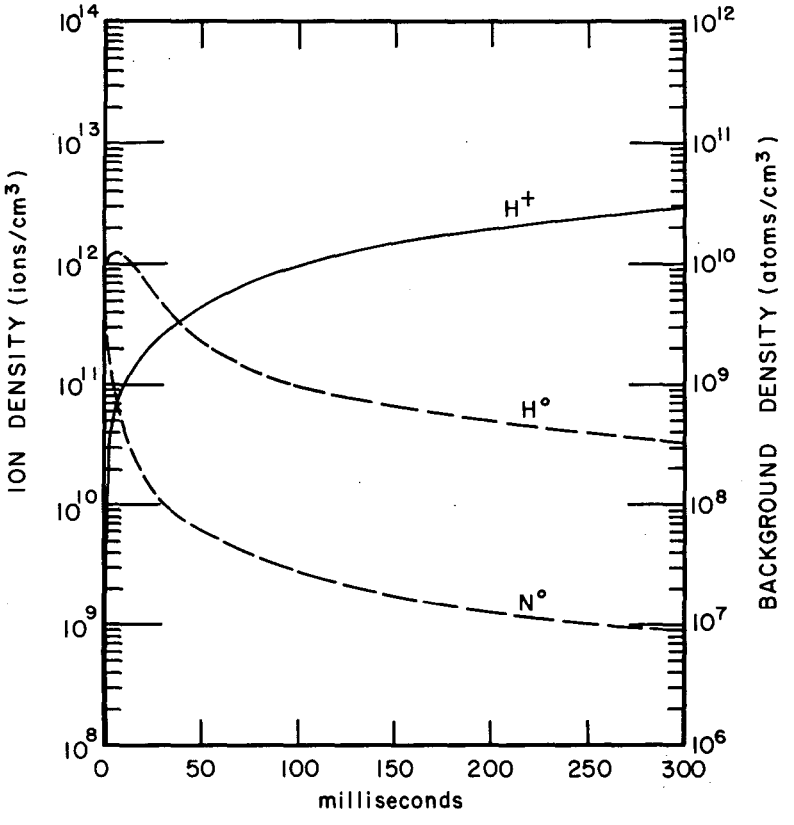

Fig. 5. Ion and background-gas atom density versus injection time for a system with a nitrogen arc.

BETA-RAY EXPERIMENT

Gordon Gibson,* Willard C. Jordan,† and Eugene J. Lauer

The steady-state bias curves and containment-time measurements[1] have been extended to other scattering gases (A and Xe). The observed steady-state bias curves do not agree satisfactorily at positive bias with the theoretical curve, and the emphasis at present is on experiments that will yield information on various effects that might be the cause of the discrepancy. For this reason, new information in this report will be limited to results associated with the time analysis of the counting rate.

The "dust-dumping" annoyance which was described in the preceding progress report[1] has been eliminated to the point where the probability of its occurrence is very small. Pump-out holes had previously been drilled in the hollow plastic fast-valve; by cleaning out the volume within the valve the source of most of the dust has been removed.

The measured containment times are in satisfactory agreement with the theoretical e-fold containment times obtained when multiple-scattering theory is applied to a simplified model.[2] From such theoretical considerations it may be shown (assumptions include neglecting spatial variations, energy loss, etc.) that a function, T, may be defined which depends only on the mirror ratio, R,

$$T = \tau_s (2\pi r_0^2 c) N_0 \ell n \left[\frac{0.05}{Z^{4/3} a^2} \quad \frac{(v/c)^2}{\sqrt{1-(v/c)^2}} \right] (Z^2 + Z) \quad \frac{1-(v/c)^2}{(v/c)^3} ,$$

where

τ_s is the dominant containment time after a time of order τ_s subsequent to removing the source,

r_0 is the classical electron radius,

c is the velocity of light,

v is the velocity of the positron,

N_0 is the particle density of the scattering gas,

Z is the nuclear charge of the scattering gas,

a is the fine-structure constant.

---

*Westinghouse Electric Co.

†Bendix Aviation Company

[1]Gordon Gibson, Willard C. Jordan, and Eugene J. Lauer, in Controlled Thermonuclear Research Quarterly Report, UCRL-8775, June 10, 1959 pp 20-28.

[2]Gordon Gibson and Eugene J. Lauer, "Confinement Time of a Lorentzian Gas in a Mirror Machine," to be published.

Fermi's formula for the root-mean-square angle of deflection of an electron beam in passing through a target[3] may be used if the root-mean-square angle when projected onto a plane is set equal to the complementary angle of the half angle defining the loss cone. In this case

$$T = \frac{1}{2}\left[\frac{\pi}{2} - \sin^{-1}\frac{1}{\sqrt{R}}\right]^2 .$$

The experimental data have been obtained for R = 1.8 with the counter on axis (see Fig. 6). The plotted points are the averages of several measurements at two different scattering gas pressures; the wings include all the measured values. The 1-Mev data were taken with the field at the center of the machine set at 1.3 kgauss. The 0.5-Mev points represent average values for two central magnetic field values 1.3 kg and 0.57 kg; the single-channel analyzer was set to accept a pulse-height spread of ± 10% and the energy resolution of the counter is ± 13% at 1 Mev and ± 19% at 1/2 Mev. Table I presents the containment times used for Fig. 6.

Table I

Measured mean containment times

Scattering gas	Pressure (mm/Hg)	τ(sec) At 0.5 Mev, 1.3 kgauss	At 0.5 Mev, 0.57 kgauss	At 1 Mev, 1.3 kgauss
neon	1.0×10^{-6}	4.7	3.9	3.0
	2.0×10^{-6}	2.4	2.1	1.9
argon	3.1×10^{-7}	3.4	2.9	3.8
	6.2×10^{-7}	2.1	0.88	1.8
xenon	4.3×10^{-8}	4.3	3.6	4.5
	8.5×10^{-8}	3.3	1.9	3.4

The 1-Mev cases agree with one another but are lower by a factor of 2.5 than the theoretical value obtained in the simplified model. The 0.5-Mev cases agree more closely with the theoretical value, but not as well with one another. The 0.5-Mev case with Ne as the scattering gas will be re-examined. The deviation of the experimental points at different energies may be associated with the energy degradation of the trapped positrons and their energy distribution. This correction has not been folded into the data as yet. Such effects could also cause deviations at a given energy for different scattering gases since the energy lost during a containment time is independent of gas pressure but proportional to $1/(Z+1)$. There is evidence of a radial loss of particles to the vacuum-chamber wall for all orbit diameters except the smallest (1/2 Mev, 1.3 kgauss central field).

[3]Enrico Fermi, "Nuclear Physics" (Univ. of Chicago Press, Chicago, 1950), p. 37.

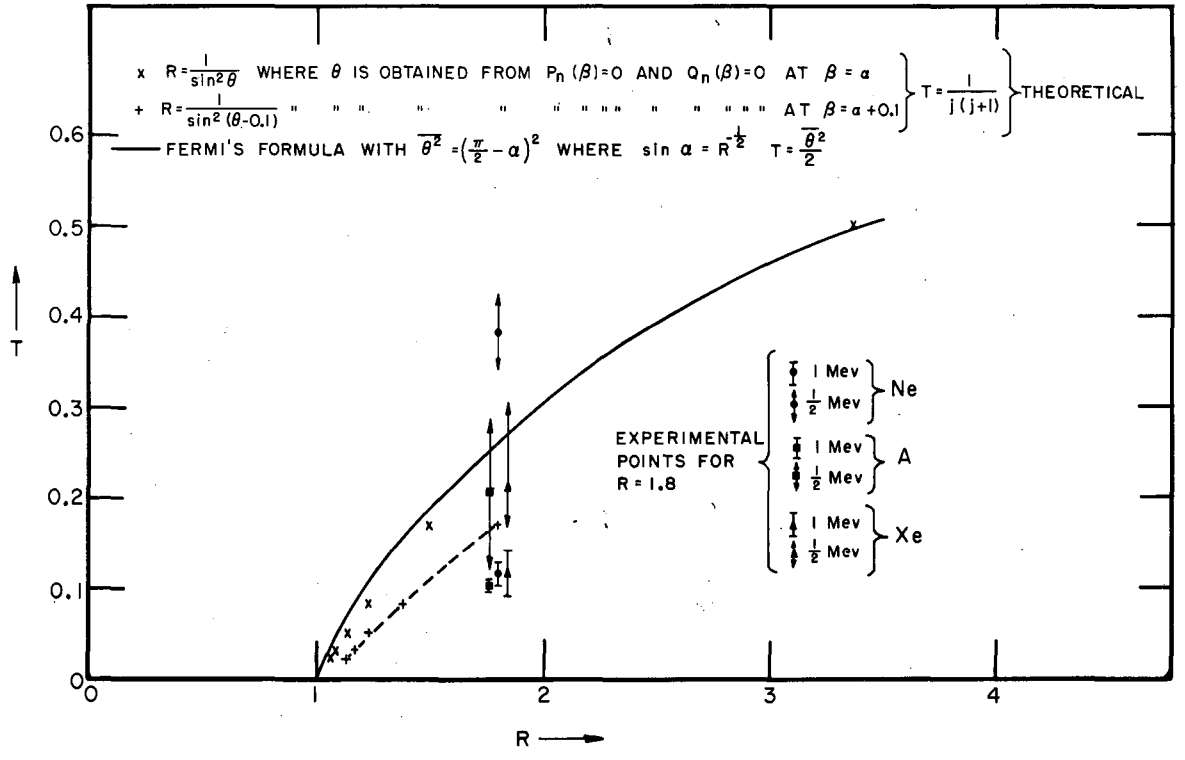

MU-18246

Fig. 6. T vs mirror ratio R.

In the preceding progress report[1] results were presented that demonstrated that the field within a particular "inhomogeneity coil," 1, located near the vacuum wall could be adjusted to cancel the field of the mirror machine within the coil without disturbing the containment time of the positrons which scatter out on the axis of the machine. Another inhomogeneity coil, 2, which is physically larger and capable of producing higher fields than 1, has been placed midway between the mirror coils with its axis parallel to the machine axis and separated from it by about 20 in. The field of this coil falls off less rapidly than the previous one, and hence has a greater effect on the particles located near the axis. Inhomogeneity coil 2 consists of 200 turns and has a 13-in. o.d., 6-in. i.d., and is 11 in. long. When the current through this coil is 200 amp the measured field inside it is 2.70 kgauss and the measured field on the axis of the mirror machine due to it is 27 gauss. The effect on the containment time of turning on this coil is shown in Fig. 7. Once again the particles which scatter out on axis are not appreciably perturbed when the current through the inhomogeneity coil 2 is equal to or less than the value (~ 100 amperes) which creates a field within the coil equal and opposite to the mirror-machine field. However, the containment time is affected when currents larger than this are passed through the coil. When everything is kept the same except that 1-Mev particles are detected, similar results are obtained. For 1-Mev particles and a mirror field on axis in the mid plane equal to 570 gauss a current of ~ 60 amp through inhomogenity coil 2 makes a detectable effect on the containment.

A paddle about 1 in. in diameter, attached to the end of a small-diameter rod which passed through a sliding vacuum seal into the vacuum tank, was positioned at various distances D from the axis along a radius in the plane midway between the mirror coils. The effect on the time-analyzed counting rates for the counter located on axis is shown in Fig. 8. The Larmor diameter of a 0.5-Mev positron whose velocity is normal to the field (~ 1.3 kgauss) in the central plane is $2\rho_{max}$ = 1.8 in. For $D \leqslant 2$ inches no trapped particles are observed. As the paddle is moved out radially, larger trapped fractions are observed until at $D \gtrsim 5.5$ in. there is no noticeable effect on the counting rate. The experiment was also carried out with the mirror-machine field on axis in the central plane equal to 570 gauss. In this case $2\rho_{max}$ = 4.3 in., and the paddle has no effect for $D \gtrsim 7.5$ in. There are no observed trapped particles for $D \leqslant 4$ in.

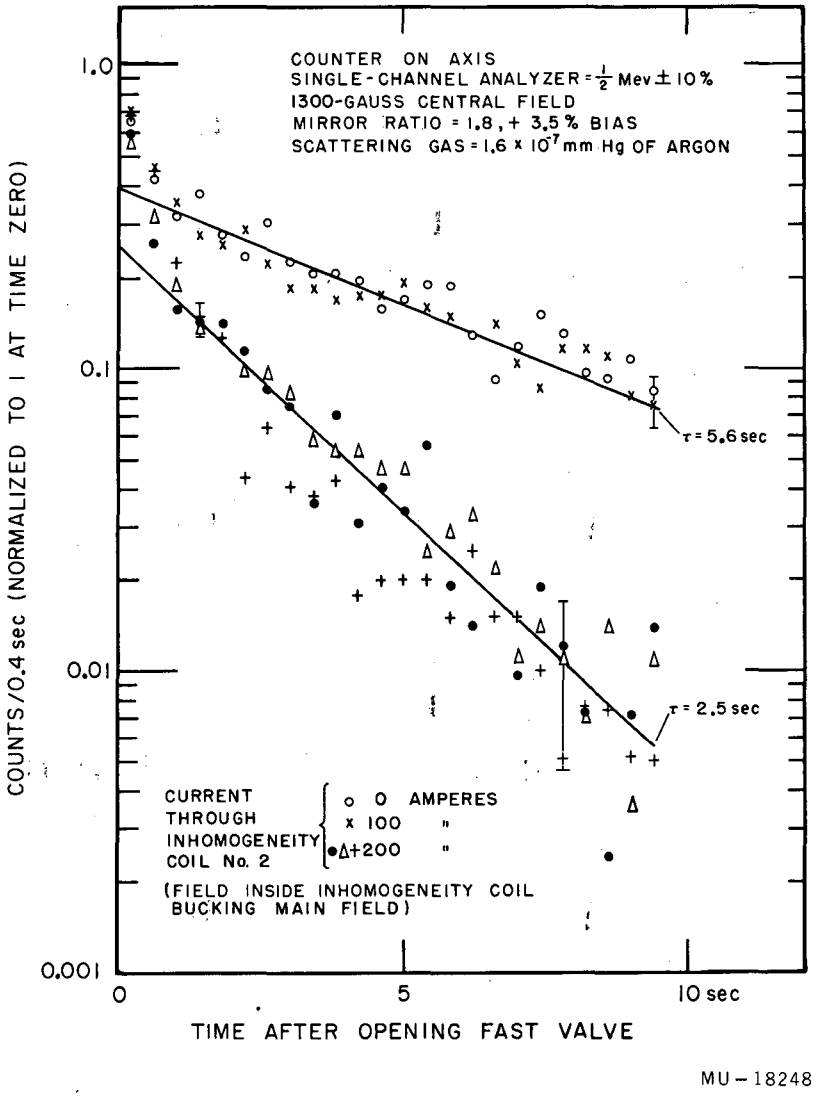

Fig. 7. Effect of inhomogeneity coil No. 2 on fast-emptying runs.

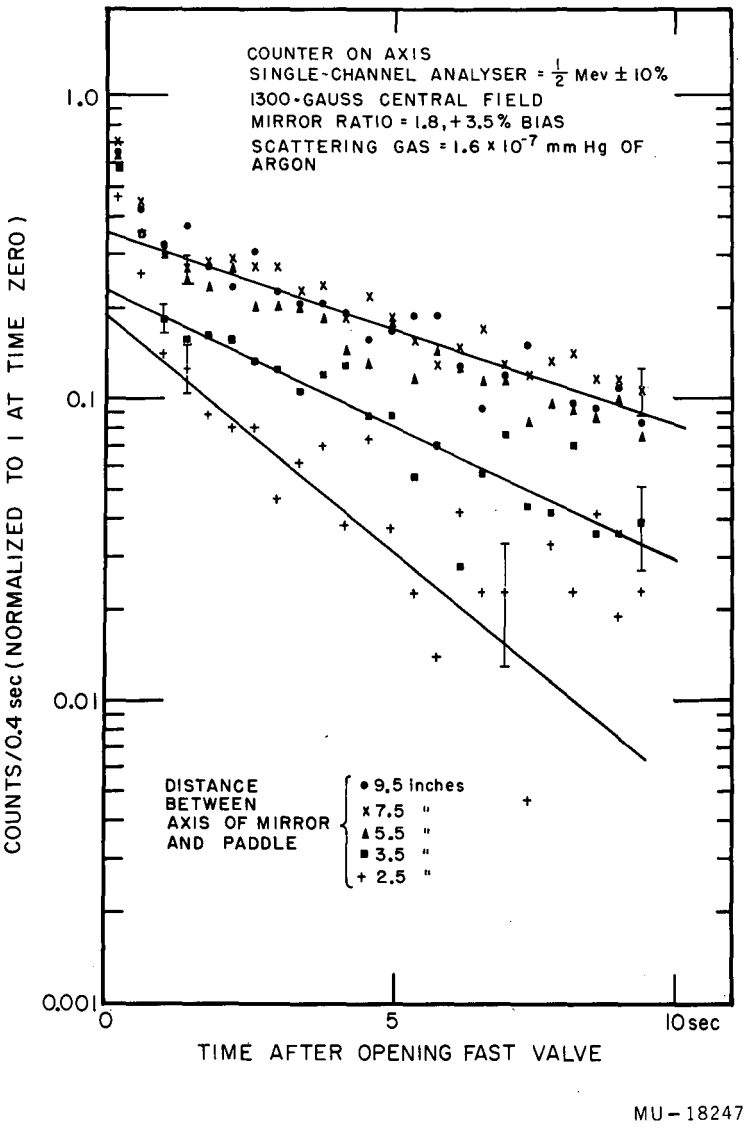

Fig. 8. Effect of paddle on fast-emptying runs.

THE BUMPY TORUS

Gordon Gibson,* Willard C. Jordan,† and Eugene J. Lauer

As mentioned in the preceding progress report, we are analyzing the Bumpy Torus, neglecting the effects of plasma fields. The analysis was undertaken to find out whether the geometry is closed in the following sense:

Is there a finite volume in configuration space in which there is no initial direction of the velocity that will result in escape (for the case of a single charged particle in the adiabatic approximation)?

It is assumed that the following quantities are constants of the motion:

(a) the kinetic energy, W;

(b) the magnetic moment, $\mu = W_\perp / H$; and

(c) the action integral, $J = \int p_{||}\, d\ell$ evaluated over a period (as defined later) of the longitudinal motion, where $p_{||}$ is the component of the momentum parallel to the field and $d\ell$ is the element of path length parallel to the field.[1]

The IBM 650 is being used[2] to calculate

(a) the magnitude of the magnetic field,

(b) the direction of the magnetic field, and

(c) the action integral for particular values of the magnetic moment and starting coordinates.

The code is set up to calculate these quantities in the symmetry plane, S (see Fig. 9) for N equally spaced circular current loops for which the ratio of major radius divided by current-loop radius is R/r. Because of the symmetry it is necessary to investigate only the region between a median plane and the plane of an adjacent current loop. Taking account of the constancy of the kinetic energy and of the magnetic moment, one may write the action integral as

---

*Westinghouse Electric Co.

†Bendix Aviation Company

[1]Ted G. Northrop and Edward Teller have recently shown that the action integral is an adiabatic invariant whether the field is axially symmetric or not; see Theodore G. Northrop and Edward Teller, Stability of the Adiabatic Motion of Charged Particles in the Earth's Field, UCRL-5615, June 24, 1959.

[2]The code (MALOF) was set up by Joseph L. Brady, Bart Williams, and Thomas N. Haratani.

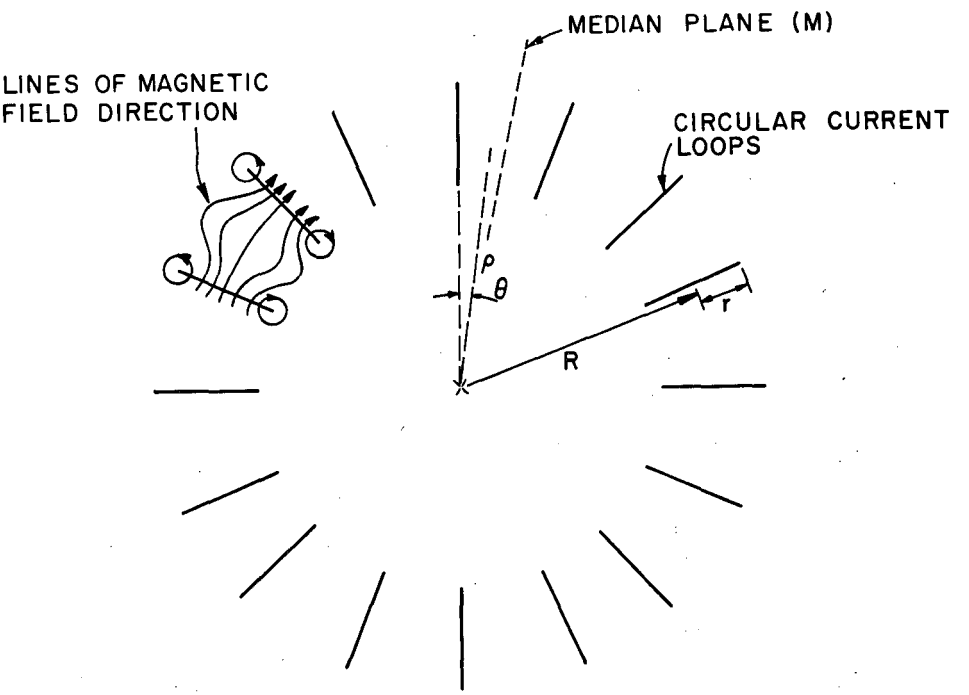

Fig. 9. Bumpy torus constructed with N=16 equally spaced circular current loops.

$$J = mv \int_{\substack{\rho = \rho_{final} \\ \theta = \theta_{final}}}^{\substack{\rho = \rho_0 \\ \theta = \pi/n}} \sqrt{1 - \frac{H}{H_0} \sin^2\delta} \; d\ell,$$

where mv is the momentum, H_0 is the initial field magnitude, and δ is the initial angle that the velocity makes with the field direction. The integrals are all started at the median plane (M) and are stopped

(a) at the turning point where $v_{||}$ has decreased to zero, or

(b) at the plane of the adjacent coil if there is no turning point.[3]

Figure 10 shows the results of the action-integral calculations and some of the field magnitude calculations that have been obtained for N = 16 and R/r = 5.44. All the action integral curves have a minimum. If a particular curve of μ = constant is chosen, then for a chosen value of J the two values of ρ (inner and outer) where the precessional surface intercepts the plane of symmetry S are uniquely determined.

For the particular case of a particle trapped midway between two mirrors with $v_{||} = 0$ (i.e., precessing in the median plane M), the action integral is zero for all ρ and therefore the action-integral theorem gives no information. However, this is just the case where the precessional curve can be predicted from a different point of view: namely, since μ is constant and $v_\perp = v_\perp$ = constant the precession is constrained to a path along which H is constant. Thus, inner and outer intercepts for the precessional curve with the plane of symmetry S may be found from the curve of H vs ρ in the median plane. In the limit, for a particle not trapped in the median plane, as μ approaches the value characteristic of a particle trapped in the median plane (holding the kinetic energy constant), the intercepts predicted by the J curves should approach those predicted by the median-plane H curve. The cases shown in Fig. 10 indicate that this indeed happens.

---

[3] The justification for this assumption is that it makes J approach the same value in two limiting cases (holding the kinetic energy and the magnetic moment constant):

(a) for a particle that is trapped between two adjacent mirrors as the turning point approaches the mirror,

(b) for an untrapped particle as $v_{||}$ at the mirror approaches zero.

We would prefer to have a more detailed analysis of this case because the longitudinal period becomes very long as the above limit is approached, and the action-integral theorem is not proven for this case.

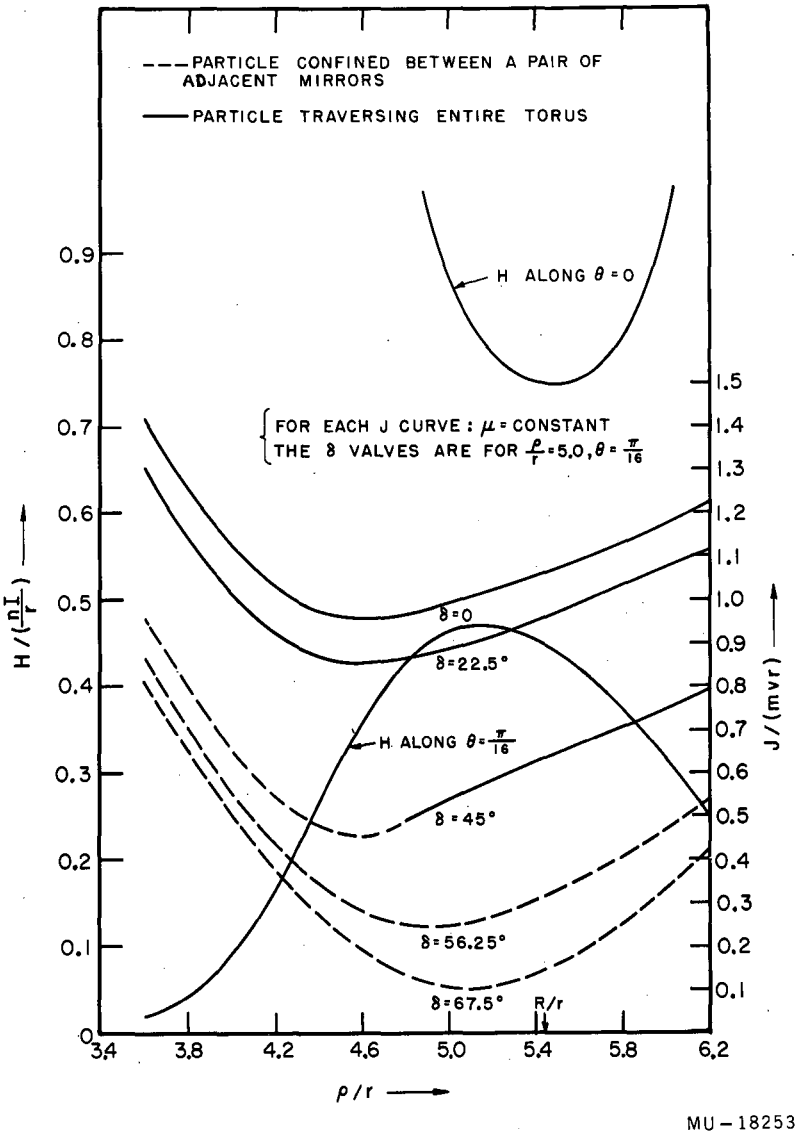

Fig. 10. Adiabatic invarients for a bumpy torus with N=16 and r/r=5.44.

If $v_{||}$ is nearly zero at a mirror, the longitudinal period is very long and J does not necessarily remain constant in time.[3] Such a particle has $v_{\perp} = v$ = constant and therefore follows a curve for which H = constant in the plane of the coil (i.e., at $\theta = 0$). It is planned to investigate this case in more detail.

Scattering can change the value of μ suddenly so that a vertical transition occurs from one of the μ = constant curves to another at a nearly constant ρ. After the transition the particle is constrained to the new precessional surface associated with the new values of μ and J until another scattering occurs. Since the J-vs-ρ curves do not all have the same shape and since their minima do not all occur at a single value of ρ, scattering can result in a new type of diffusion, that is, the particles can diffuse onto precessional surfaces of larger and larger diameter. (This happens even for very small orbit diameters.) The rate of this diffusion is being investigated.

It is also planned to investigate different values of N and R/r. Increasing N and R/r proportionally should enable one to approach the degenerate case of a linear series of mirror machines and hence reduce the effect of this new type of diffusion.

ION-SOURCE DEVELOPMENT

John A. Fasolo

During the period covered in this report, development work on the Von Ardenne type source, Model III, has continued.

A check of the beam-current-metering circuit in use at the time the work covered in the previous report was performed disclosed that only half of the beam current was being measured by the beam-current meter. Values of current cited in the preceding report should therefore be multiplied by 2.

With a 0.032-in. magnetic lens gap, a number of modifications of the anode and extractor geometries were made. The maximum beam current for a 2.0-amp arc was of the order of 40 ma in every case. The effect of varying the lens gap was then studied. The gap was varied by taking successive slices off the pole tip of the Z electrode. The results obtained were as follows.

Lens Gap (in.)	Z-Electrode Pole Tip Diam. (in.)	Z-Electrode Bore Length (in.)	Arc Current (amp)	Beam Current (ma)
0.032	0.250	0.812	2.0	40
0.064	0.317	0.780	2.0	56
0.096	0.352	0.748	2.0	61
0.128	0.390	0.716	2.0	74
0.160	0.426	0.684	2.0	84
0.192	0.464	0.662	2.0	90

In each case the diameter of the aperture in the tungsten anode insert was 0.047 in. and the extraction voltage was 60 kv.

Beam currents given in the above table were measured electrically. Calorimetric measurements give values about 10% higher.

A new Z electrode with a pole tip diameter of 0.345 in. is now in use. The lens gap is 0.160 in. With a 0.047-in.-diameter anode aperture and a 2.0-amp arc, beam currents of the order of 90 ma have been obtained.

The anode aperture diameter has been enlarged to 0.064 in. During a brief bake-in run, 60 ma of beam current was obtained with a 1.0-amp arc and an extraction voltage of 54 kv.

The source shown in Fig. 11 was put into operation in the early part of July. With a 2.0-amp arc and an extraction voltage of 60 kv, the largest currents obtained were of the order of 200 μamp. With the modification shown in Fig. 12, beam currents of the order of 50 ma have been obtained; however, operation at this level is not reliable. For unknown reasons, the maximum obtainable beam current may vary by a factor of 2 from one run to the next. Furthermore, at the higher current levels, the beam current frequently drops 30 to 40% below its initial value in a matter of seconds after the arc is turned on and then remains constant. When this occurs, there is no significant change in arc current; it is therefore not likely that the fall-off in beam current is due to pressure changes in the source as the result of outgassing of the various surfaces bombarded by ions and electrons.

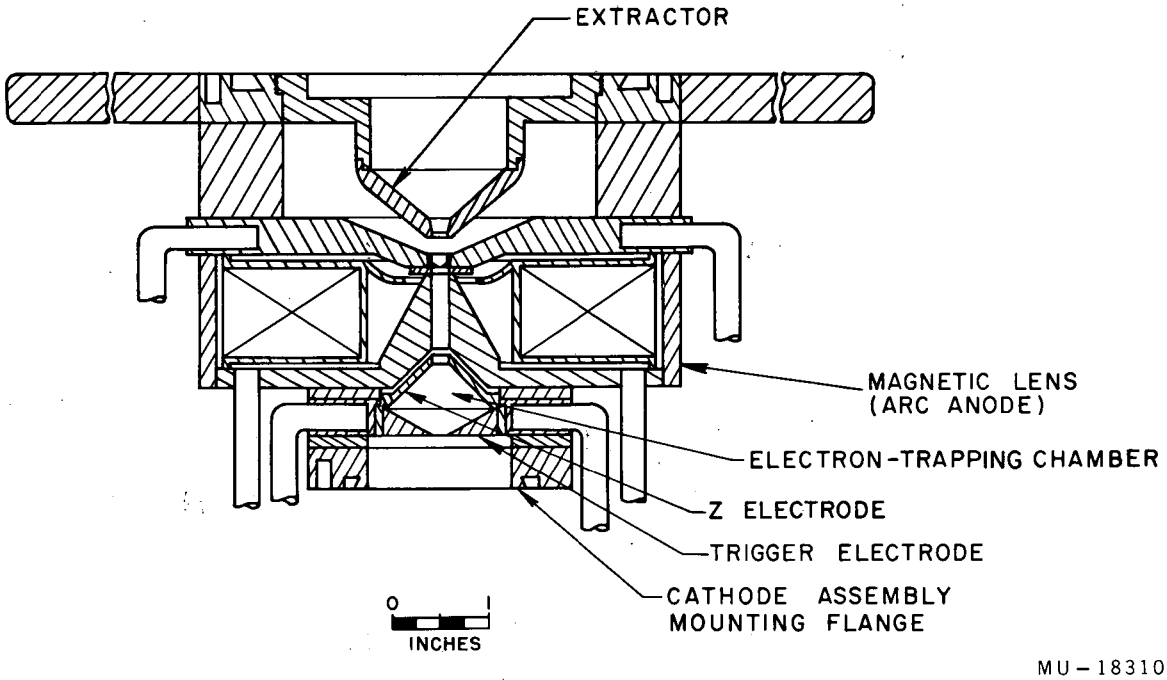

Fig. 11. Source I, Series C.

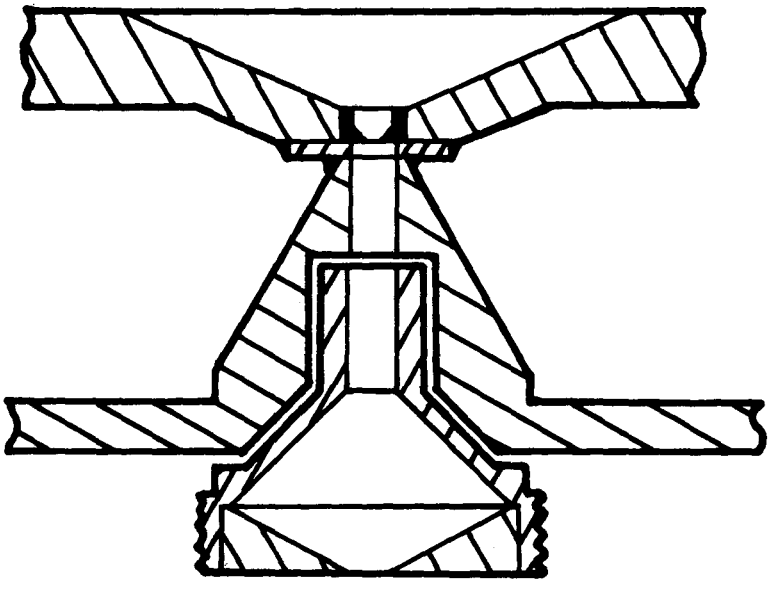

MU-18335

Fig. 12. Modified arc geometry, Source I, Series C.

III. ASTRON PROGRAM

DESCRIPTION AND IMPLICATIONS OF THE NEW INJECTION SYSTEM

Nicholas C. Christofilos

Introduction

In the preceding report a new injection method for the E-layer electrons was mentioned. The theory and the calculations required to evaluate this method have been developed during this quarter. The basic idea of this injection method is to allow the electrons to slide within a potential well while simultaneously losing energy to a suitable arrangement of passive circuits. Thus the electrons are trapped irreversibly within the potential well. The traveling-wave lines and pulsed coils required in the old injection system are no longer necessary. This new way of injection is described in the next section.

The only drawback of this system is that it can be effective only for high-energy electrons of 5 Mev or higher. However, this order of energy is required anyway, from plasma energy-balance considerations. Consequently this requirement does not impose a change of parameters for the contemplated Astron model.

In the dry-run experiments the intended goal of trapping one electron bunch has been achieved. At present confinement of the electrons for a few hundred microseconds has been observed. It is hoped in the next few weeks to extend this time to a few milliseconds. The best results have been accomplished by not energizing the mirror coil (which is near the injection tube). It turned out that the eddy currents induced in this coil by the field of the injected electrons generate enough mirror field to trap some of the injected electrons. This experiment is of extreme interest, as it is the first time that an electron beam of current high enough to modify the external field has been injected and trapped.

Simultaneously this experiment verified to a certain extent the theory of the postulated new injection system. The contention up to now was that particle beams would tend to leave the confining field because of resonances, instabilities, etc. In this experiment the opposite happened. The electrons managed to trap themselves with the help of magnetic fields generated by their own current. This first encouraging result indicates that the use of large currents can change drastically the behavior of electron beams, as has always been postulated in the Astron concept. The experimental results are described in more detail by W. A. S. Lamb in this report.

The self-consistent solution of field distribution of the E-layer has been further advanced by Lewi Tonks's studies (described in a subsequent section).

The function of the E layer is described as well as the effect of interaction of each injected bunch with the E-layer electrons. The parameters of the 5-Mev Astron model have been more or less crystallized, and construction of this model is to proceed in two steps:

(a) Completion of the model together with a 2-Mev, 200-amp electron accelerator;

(b) Extension of the accelerator up to 5 Mev.

Experiments to be undertaken with the 5-Mev model are described. These experiments include high-temperature plasma studies which can be conducted even before the field-reversal phase is reached.

Plasma-study experiments are described, which are possible even if the trapping of only one bunch of electrons is achieved. At the 2-Mev phase the performance of the new injection system is considered marginal. Hence the purpose of this step is to test the 2-Mev accelerator and to carry out some high-temperature-plasma experiments.

A. New Astron Injection System

A new injection system for the Astron has been conceived and studied in the past few months. It is extremely simple, for no active pulsed circuits are required nor partial neutralization of the injected electron bunch, as in the old injection arrangement.

The basic requirement of the injection system in the Astron is the injection of electron bunches in the E-layer region:

(a) In an irreversible way.

(b) Without seriously disturbing the electrons already injected.

(c) In a manner such that the presence of the E layer will not disturb each electron bunch during the injection phase.

In order to inhibit the already injected electrons from returning to the injector tube or from leaving the E-layer region we must trap the injected electrons within a potential well. Since under normal operating conditions the electrostatic field of the layer is neutralized by positive ions it is obvious that the confining potential well must be created by a proper magnetic field configuration. Such a configuration is a mirror field, as originally proposed for this purpose. In order to avoid any active circuits and traveling-wave lines we must inject the electrons at the top of the potential well and thereafter allow them to slide "downhill" towards the region where they are to be trapped. During that motion the presence of a friction force is required to absorb the momentum gain during their fall into the potential well. Thus, the electron bunch arrives at the bottom of the hill with very small axial momentum.

This required friction force is realized by forcing the electrons to pass near resistive loops in which an emf is induced by the moving magnetic field of the electron bunch. The induced emf generates currents in the resistive loops, resulting in energy losses, which in turn absorb axial kinetic energy from the bunch. The forces thus created tend to slow down the "fall" of the bunch into the potential well. The energy loss per electron is linearly proportional to the total current of the electron bunch. It appears that a

circulating current (in the electron bunch) of the order of a few thousand amperes is required in order to obtain the desired results. The electron-gun current necessary to meet this requirement is 100 to 200 amp for 0.1 to 0.3 μsec, which is not much higher than the 50 amp already achieved. Hence it is reasonable to postulate that the higher current required for the new injection system is attainable. The actual arrangement of the passive circuits or resistive loops is shown in Fig. 13.

An annular space is defined between two metal coaxial cylinders, Nos. 10 and 12, of radius R_1 and R_2 respectively. The resistive loops, 11, of radius R_s are placed in this annular space so that each lies in a plane normal to the axis of symmetry of the two cylinders. The resistive loops consist of high-frequency resistors (coated glass) with a thickness of resistive material which is much less than the skin depth corresponding to the frequency of the generated emf.

The electron gyration radius (R_e) is one-half the sum of the radii of the loops and the inner cylinder. In this way the radial distance from the outer cylinder, 12, to the resistive loops is equal to the distance from the loops to the electron bunch and from the inner cylinder to the electron bunch. The vector potential of the magnetic field of the bunch has been solved in the linear approximation; i.e., by assuming the electron bunch to be a straight electron beam and the two cylinders to be planes. A solution in the cylindrical configuration has been obtained in the form

$$A_\theta = \sum_n c_n C_1(nkr) \cos(nkz), \qquad (1)$$

where $C_1(kr) = [c_2 I_1(nkr) + c_3 K_1(nkr)]$ and I_1, K_1 are the modified Bessel functions. However, no numerical calculations have been done thus far. In this solution, it has been assumed that the bunches appear periodically and that the distances between bunches are much larger than the radial dimensions of the system.

The linear approximation leads to the conclusion (see Appendix) that the ratio μ of the current induced in the loops to the current in the electron bunch is

$$\mu = \frac{60}{\pi L c} \left(\frac{\omega_0}{a^2 + \omega_0^2} \right), \qquad (2)$$

where L is the inductance per cm length of the loop, ω_0 is the frequency of the magnetic field of the moving bunch as it appears to the standing loop, and $a = R/L$ (of the loops). The induced current in turn generates a magnetic field. The radial component of this field interacting with the electron current opposes the motion of the bunch along the z direction (z is the coordinate parallel to the axis of symmetry). The inductance of the loops per cm length is $3 \cdot 10^{-9}$ h, approximately. The maximum losses occur for $\omega L = R$. Hence

$$\mu \approx 0.1.$$

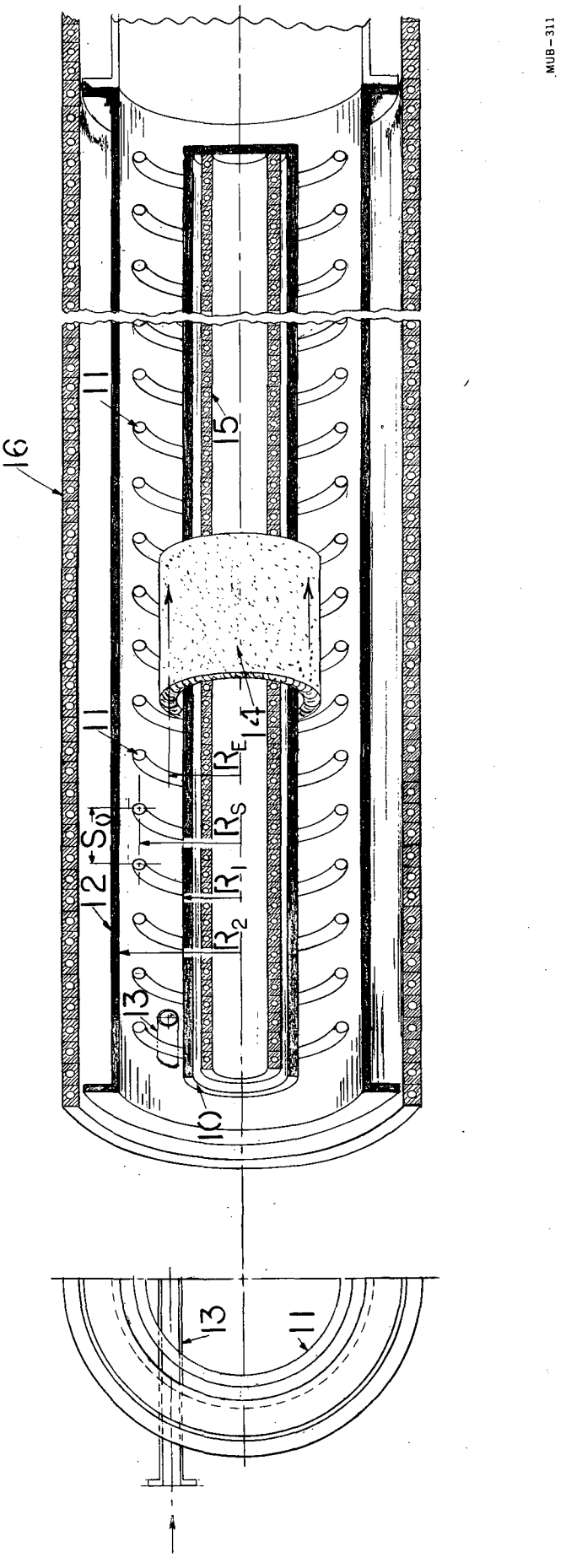

Fig. 13. Astron injection system.

The electron energy loss must be equal to the energy loss in the loops, since the electrons are the only source of energy. However, the electron energy loss has been calculated also by integrating the force opposing the motion of the electron bunch in the z direction. The two calculations gave, as expected, the same results.

The slowing-down or friction force can be expressed in terms of a radial magnetic field (B_s) which interacts with the electron current I and yields a force $B_s \times I$. The value of this field has been calculated for a specific resistor arrangement as shown in Fig. 13. (See Appendix). The result is

$$B_s = \frac{I}{360} \quad \text{gauss}, \tag{3}$$

where I is the current in the electron bunch. This expression is correct provided that the length of the bunch does not exceed the radial distance between the two confining cylinders. For a longer bunch the value of the current entering in Eq. (3) would be only the current confined in the first 30 cm of the electron bunch.

The resistor-loop system is placed within a mirror field. The slope of the mirror field (which is the slope of the potential well) is equal and opposite to the friction field B_s. In this way the electron bunch moves downhill without undergoing any increase of axial momentum. However, the flux linked to the bunch is reduced by an amount

$$\delta\Phi = 2\pi r \int B_s dz. \tag{4}$$

This change results in an energy loss of the electrons, as one can easily calculate, considering the invariance of the canonical azimuthal momentum of the electrons.

Because of the approximations made, the values derived above should be considered approximate; a factor-of-two variation from the calculated values is quite possible. The solution of the problem in cylindrical coordinates, now under preparation, will yield more accurate values. Consequently, allowing for an error of a factor of 2, we estimate that with a loop assembly (60 loops) 20 ft in length, 20% of the electron energy will be absorbed. Thus, the magnetic potential well has such a depth that the electrons injected into the E-layer region must acquire 25% additional energy in order to come out again, so that the depth of the potential well is considered adequate to ensure the trapping of the electrons. A necessary condition for the effective performance of the injection system is that the axial defocusing force at the head of the beam (due to the self-field of the bunch) must be smaller than the slowing-down force. Otherwise the bunch would tend to expand in the z direction, with the result that the effective current of the bunch would be diminished very fast and the slowing down would not be accomplished. Since both the defocusing force (due to the self-field) and the friction force are proportional to the current of the bunch, the ratio of these forces is independent of the current. However, the defocusing force is proportional to $(1 - \beta^2)$ or γ^{-2}, thus decreasing fast as the electron energy increases. The approximate value of the defocusing field $\bar{B}$ (where $\bar{B} = E_z - \beta B_r$) is

$$\bar{B} = \frac{I}{30\gamma^2} \quad . \tag{5}$$

This field must be smaller than B_s. Hence

$$\gamma > 3.5$$

or

$$E > 1.25 \text{ Mev.}$$

Considering, however, that the value of B_s is accurate only within a factor of 2, we derive

$$E > 1.8 \text{ Mev.}$$

Consequently, 2 Mev is the minimum energy required for marginal performance of the injection system. However, in this case the allowed depth of the potential well is very small so that only one or two bunches can be injected and trapped. At 5 Mev, on the other hand, the self-defocusing force is only 10% of the friction force and the system should operate very well.

We shall now follow the electrons through the injection process to illustrate the performance of the system. The electrons are to be injected through the injector tube 13 (Fig. 13) in approximately the azimuthal direction. A small amount of axial (z-direction) velocity is to be provided so that the injected beam will miss the injector after one turn. Thus, the beam will follow a helical path of a pitch angle θ_0. The top of the mirror field is at a distance s from the injector tube, so that no acceleration will be applied to the electrons from the static field as they travel this distance s. Owing to the presence of the resistive loops, however, the head of the beam will be retarded, and by the time the tail end of the beam is injected the axial velocity of the head of the beam will have been reduced considerably. Thus, the axial length of the bunch can be reduced to 30 or 40 cm. Thereafter, the bunch (14 in Fig. 13) will enter the mirror field and the slowing-down process will start. The bunch will move slowly through the resistive loops, losing energy. In order to maintain the bunch at constant radius, while the flux linked with the bunch changes as it moves through the mirror field, this field must fulfill the betatron conditions; i. e., the change of flux through the bunch must be twice the product of the change of the guiding field times the enclosed area. Coil arrangements 15 and 16 in Fig. 13 to produce this field have been described elsewhere.[1]

[1] N. Christofilos, Astron Electron Injection, UCRL-5617-T, June 1959.

B. Formation of the E Layer; Interaction of the Injected Bunches with the E Layer

The electron bunch upon entering the E-layer region is freed of the constraints imposed by the presence of the resistive loops. Hence it is spread along the E-layer region (length approximately 600 cm) confined between the two mirror fields. The energy stored in the electromagnetic field of the bunch practically vanishes as the length of the bunch increases to 15 or 20 times its initial length. This energy is not lost, of course, but is transformed to electron kinetic energy. The stored energy in the electromagnetic field in a bunch of 30 cm length and a current of 6000 amp is 300 kev per electron in the bunch. (See Appendix.) Thus, the electrons of the first bunch injected into the E-layer region gain about 300 kev as they spread in this region.

The second incoming bunch loses its electromagnetic stored energy in the same way. But now this energy is shared with the previously injected bunch, thus the energy gain is now 150 kev per electron. As the process continues the electrons which are already injected gain more and more energy. However, the energy gain increases logarithmically as the injection continues, since upon injection of the Nth bunch the energy gain per electron is

$$\delta\bar{\Phi} = 300 \cdot \frac{\delta N}{N}_i \quad \text{kev.} \tag{6}$$

Hence the total energy gain per electron the Nth bunch after injection of N_1 additional bunches is

$$\bar{\Phi} = 300 \ \ell n \left(\frac{N_1 + N}{N} \right) \quad \text{kev.} \tag{7}$$

The depth of the potential well for 5-Mev electrons is to be 1 Mev. Then

$$\ell n \left(\frac{N_1 + N}{N} \right) < 3.3. \tag{8}$$

After injection of 30 bunches we observe that the first is lost. After injection of 120 bunches the energy gains of some of the bunches are:

N	$\bar{\Phi}$ (kev)
1	1430
3	1100
5	950
10	750
20	590
30	410
40	330
60	210
80	120
100	60

We observe that only the first five are lost, while the energy gain of 20 others is more than 50% of the depth of the potential well. Hence, it appears that even more bunches can be injected without appreciable loss.

Therefore, we can inject now enough electrons to obtain field reversal without relying upon scattering losses to force the electrons to move in phase space. Consequently, our injection system is much more flexible than the old one and many more electrons can be injected than required for field reversal. In conclusion we can say that the interaction of the incoming bunches with the already injected electrons no longer presents a serious problem.

We shall now examine the interaction of the magnetic field of the E-layer electrons with the incoming bunches before they enter the E-layer region. The magnetic field of the layer is like the field of a solenoid; therefore, it would attract the incoming pulses by creating a deeper potential well. This is not desirable, as the dynamic value of the slowing-down field cannot change during the build-up of the layer. Consequently it is not desirable for the mirror field to be modified by the self-field of the E layer in the injection region. This effect can be avoided by providing coils which will create a field in the injection region equal and opposite that of the E-layer field. This combination would restrict the magnetic field due to the E-layer electrons within the E-layer region. Thus an electron in the E layer moving from the end to the center of the E-layer region must cross all the flux created by the E-layer current. This is very desirable in order to maintain the E-layer radius constant during the build-up phase. Initially, we inject the electrons at a radius equal to the Larmor radius. Consequently the vacuum field is

$$B_0 R_e = \frac{p_0 c}{e} , \tag{9}$$

where p_0 is the total mechanical momentum of the electrons and R_e the desired injection radius. However, the electrons are not moving in perfect circles of radius R_e because of the presence of random radial momentum. Hence the electrons are spread radially in a region of finite thickness. The average value of the guiding magnetic field is then the sum of the vacuum field plus one-half the self-field. Since the self-field is in the opposite direction to that of the vacuum field we find that the average field ($\bar{B}$) is

$$\bar{B} = B_0 - \frac{1}{2} B_e . \tag{10}$$

The flux created by the E layer is

$$\Phi = \pi B_e R_e^2 . \tag{11}$$

As the electrons move back and forth from the ends to the center of the E-layer region they cross this flux, undergoing a change in azimuthal mechanical momentum,

$$\delta p_\theta = \frac{e}{2c} B_e R_e . \tag{12}$$

Consequently, the azimuthal mechanical momentum becomes

$$p_\theta = \frac{e}{c} \left(B_0 - \frac{1}{2} B_e\right) R_e . \tag{13}$$

The gyration radius is

$$R = \frac{c}{e} p_\theta / \bar{B} . \tag{14}$$

Equations (10), (13), and (14) yield

$$R = R_e . \tag{15}$$

We observe that by confining all the E-layer flux within the E-layer region we can maintain constant radius of the layer without requiring the change of the main guiding vacuum field.

The quantity referred to as g_2 in Dr. Tonks's calculations is the ratio of the injection radius to the Larmor radius in the vacuum field. From the above equation we find

$$g_2 = \frac{p_0}{p_\theta} , \tag{16}$$

or

$$g_2 = \frac{1}{\left(1 - \frac{B_e}{2B_0}\right)} . \tag{17}$$

At the point of just reversing the field $B_e = B_0$ and $g_2 = 2$, as it is in one of the cases in Dr. Tonks's solutions. In conclusion we observe that the flux of the E layer (which crosses the layer at both ends) ensures the gradual change of g_2 from the value unity (initial injection value) up to the required value of 2 for field reversal. The above calculations are of course the thin-layer approximation. More accurate results for a thick-layer case can be obtained from the more elaborate solutions Dr. Tonks has obtained.

C. Parameters of the Astron Model (5-Mev Electrons); Possible Experiments

The new injection system, described in Section B above, is relatively simple. However, it is required that the self-field forces of the electron bunch be much smaller than the slowing-down forces generated in the passive circuits. As is shown in Section B, this condition can be met only by electrons of energy high enough in the relativistic range, for only in that range does the difference between magnetic and electric forces, which is proportional to $(1-\beta^2)$, become very small. For electrons of 5 Mev the quantity $(1-\beta^2)$ is 0.01. Any experiments intended to test the Astron concept, both in establishing the E layer and confining a plasma, must be carried out with electrons in this energy range in order to be significant.

Calculations of the plasma density as a function of the E-layer electron energy indicate that this is about the energy required to establish a high-temperature plasma of pressure comparable to the magnetic field pressure (high-β-plasma). Since in the final Astron version the ratio of the plasma pressure to the magnetic field pressure approaches unity, it is obvious that only under these conditions would it be possible to prove conclusively the feasibility of the Astron concept. However, this is the final step of the Astron model, requiring at first injection and trapping of an adequate number of electrons in order to reverse the magnetic field and create the magnetic bottle. The parameters of the electron injector in the planned model are

Energy	5 Mev
Injection current	200 amp
Duration of injection	0.15 μsec
Pulses per second	30 to 60
Average current	0.9 to 1.8 ma
Number of pulses required to establish E layer	100
Maximum plasma density allowed for continuous operation (approximately)	$2\times10^{12}/cm^3$

Although proof of the Astron concept requires injection and trapping of a large number of electrons (almost 100 pulses) in order to reverse the field, this is by no means necessary to establish a high-temperature plasma. Such a plasma of temperature of about 10 kev, but of very low density, can be established even by trapping one electron bunch. Although this way of operation is not consistent with the ultimate goal of the Astron experimental program, this possibility would allow us to do very interesting experiments in plasma physics in a range of temperature not yet attained in any other experiment in the Sherwood program. This aspect of the Astron program was known from the very first description of the Astron in 1953. However, it was never emphasized, as it is not too pertinent in the final operation. Since much emphasis has been given recently to plasma physics per se as prerequisite for the solution of the controlled-fusion problem and practically nothing is known experimentally about high-temperature plasmas, (above 5 kev, for example) it appears of extreme interest to conduct such interim experiments with the Astron model.

The plasma in the Astron device before the field reversal occurs consists of the high-energy E-layer electrons and high-temperature ions produced by acceleration in the potential well formed by the E layer before it is fully space-charge neutralized. The time required for space neutralization of each injected bunch depends on the density of the residual neutral gas. We assume that a vacuum of 10^{-8} mm is attainable. This is a density of 6×10^{8} air atoms/cm^3. The degree η of neutralization, as a function of time, is

$$\eta = (n_D + 8n_a)\,\sigma\,c\,t, \qquad (18)$$

where n_D is the deuteron density, n_a the air density, t the time, and $\sigma=10^{-19}\,cm^2$, the ionization cross section. Assuming $n_D = 5.10^9/cm^3$, we

find

$$\eta = 30\ t. \tag{19}$$

The created plasma consists of 50% D ions and 50% air ions, approximately.

The repetition time or time between injection of electron bunches is 16×10^{-3} sec (for 60-pps operation). Then in the time between two consecutive pulses the neutralization proceeds up to 50%. In this fashion a potential well is always maintained and more ions are trapped as more pulses are injected. The geometric parameters of the E-layer are

Average radius	27 cm
Length	600 cm
Thickness	10 cm
(outer radius	32 cm)
(inner radius	22 cm)

The number of electrons per unit length of the E layer after injection of one bunch is (for $\gamma = 10$),

$$N = \frac{\gamma}{100\ r_e} = 3.5 \times 10^{11}. \tag{20}$$

The electric field at the outer radius (32 cm) is

$$E = 3\ \text{kv/cm}. \tag{21}$$

An ion born at the E layer is attracted inwards towards the field-free space enclosed by the E layer, oscillating in and out thereafter. An ion born at the outer radius of the E layer acquires an energy of 15 kev, approximately, before any neutralization occurs. After the bunch is 50% neutralized this potential gain is reduced to 7.5 kev. The potential difference between the E layer and the wall (the wall radius is 50 cm) is

$$\Phi = E\ r_0\ \ell n \left(\frac{r_D}{r_0}\right) = 45\ \text{kev}. \tag{22}$$

This potential fluctuates from 45 to 22 kv during the process of neutralization between consecutive bunches. Thus, the ions of higher energy (15 kev) initially produced at the outer radius of the E layer are still confined in the potential well.

The E-layer electron density is approximately

$$n_e = 2 \times 10^8\ N_b, \tag{23}$$

where N_b is the number of bunches injected. The ions are spread in a volume about twice the E-layer volume. Hence, the ion density is

$$n_i = 10^8\ N_b. \tag{24}$$

During this process the high-energy ions are undergoing losses by charge exchange. The charge-exchange cross section in the range of 5 to 50 kev is approximately $\sigma_{10} = 4\times10^{-16}$ cm^2/atom. However, half the time the charge exchange occurs within the E-layer field and the new ion is again accelerated. Consequently, only one-half the ions undergoing charge exchange lose their energy. Hence, the effective cross section becomes

$$\sigma_{10} = 2\times10^{-16} \text{ cm}^2/\text{atom}.$$

The time constant, T, for charge exchange is

$$T = (\sigma v n)^{-1} = 10 \text{ milliseconds}, \tag{25}$$

where $n = 5\times10^9$ and $v = 10^8$ cm/sec. Because of this effect only a part of the ions remain at high energy. The rate of change of the high-energy ions, $\bar{n}_i$, is

$$\frac{d\bar{n}_i}{dt} = 30\,(n_e/2) - \frac{\bar{n}_i}{T} \quad . \tag{26}$$

Upon integrating this equation and substituting the numerical values, we obtain

$$n_i = 3\times10^7\,(1-e^{-t/T}). \tag{27}$$

From Eqs. (24) and (27) we observe that the high-energy ions are about 30% of the total. The average energy of these ions is 10 kev, approximately.

Equation (27) is correct for the case in which we inject only one electron bunch. As soon as we inject more bunches the percentage of high-energy ions initially decreases because they interact for a longer time with the residual neutrals. However, as the density of the E layer is building up, less neutrals are required for a given rate of ion production. Furthermore, the density of the residual air atoms is decreasing fast during this process. The rate of ion production by ionizing air molecules is

$$\frac{dn_{ia}}{dt} = (8\sigma n_e c)n, \tag{28}$$

where

$$n = n_0 - \frac{F_i}{F_0}\, n_{ia}, \tag{28a}$$

n_0 is the initial air density, n_i is the ion density, and F_i and F_0 the volume occupied by the ions and the neutral atoms respectively; this ratio is approximately one-third.

If the electrons are injected at a rate of 60 pps the E-layer electron density is

$$n_e = 2\times10^8 \cdot 60t. \tag{29}$$

Equations (28) - (29) yield, upon integration,

$$n = n_0 e^{-t^2/T^2}, \tag{30}$$

where

$$T \approx 0.14 \text{ sec.}$$

After a few tenths of a second the air density is reduced below $10^8/cm^3$ and the contribution to charge exchange becomes negligible. We shall calculate now the required deuteron density and thereafter estimate the rate of charge exchange. The rate of ion production must be equal to the rate of increase of the E-layer density namely,

$$(\sigma c n_e)n = \frac{dn_e}{dt}. \tag{31}$$

From Eqs. (29) and (31) we obtain

$$n = 3\times10^8/t. \tag{32}$$

The rate of change of the high-energy ions now becomes

$$\frac{d\bar{n}_i}{dt} = 1.2 \cdot 10^{10} \epsilon - \frac{6\bar{n}_i}{t}. \tag{33}$$

Upon integration Eq. (33) yields

$$\bar{n}_i = 1.7 \cdot 10^9 \epsilon \cdot t. \tag{34}$$

The total number of ions is

$$n_i = 1.2 \cdot 10^{10} \epsilon \cdot t. \tag{35}$$

Hence

$$\bar{n}_i/n_i = 0.14, \tag{36}$$

where ϵ is the ratio of the volume occupied by the E layer to the volume occupied by the ions. The value of ϵ is approximately one-half at the beginning of the electron injection and approaches unity as soon as a large number of bunches are injected. In the above results the presence of the air atoms has been neglected. Hence they are correct for $t > 0.5$ sec.

As soon as we interrupt the injection of the electrons the neutralization proceeds to 100%, and all the high-energy ions are replaced by much lower-energy ions, and gradually the potential well vanishes. This experiment can be performed with one bunch initially; then more and more bunches can be

injected up to the number required for field reversal. In this interim experiment the behavior of the plasma can be studied by analyzing the energy distribution and measuring the density by probes biased in different potentials. The density of this plasma ranges from 10^8 up to 10^{10}, depending on the number of bunches injected. This is rather low in comparison with what is required in fusion reactors. However, since no plasma has been achieved at this high temperature thus far at any density, it is useful at least to investigate the behavior starting at low densities such as 10^8 and progressively increasing the density attainable (discussed in more detail hereafter), which is approximately 2×10^{11} at a temperature of a few tenths kev. At this point, I would like to clarify an obvious question; namely, What is the purpose of studying a plasma in which the ions are held to the electrons through an electrostatic field? The answer to this is that in any plasma in which there are two kind of ions, the rate of diffusion of the ions tends to be much higher than the plasma electrons (because of ion-ion diffusion). Consequently, the plasma is polarized and an electric field is developed which reduces the ion-diffusion rate while the electron-diffusion rate is enhanced to twice the initial value. The net result is that in the equation for the electron diffusion, the total pressure gradient (electron and ion) enters, which means that the electron Hall current interacting with the magnetic field compensates the plasma pressure gradient, i.e., the magnetic confinement of the plasma is effected through the plasma electrons. The plasma ions are held to the electrons by means of the aforementioned electrostatic field. Thus, the case to be investigated with the incomplete E layer is of extreme interest, inasmuch as instabilities cannot be developed in the low-density plasma (10^8 to 10^9) because the Debye wave length is comparable to or larger than the dimensions of the plasma. Consequently, even plasma oscillations cannot be developed. At higher density we would have a unique opportunity to observe the transition phenomenon from stable to unstable state and study this phenomenon in a way not attained thus far in other experiments.

The next step will be to inject enough electrons to establish the E layer up to the point where field reversal is possible. As soon as the pattern of closed magnetic lines is created plasma can be trapped under different conditions than in the case of the open magnetic lines. The difference is that plasma electrons can now be magnetically confined. Consequently, the plasma density can now rise to a level higher than the density of the E-layer electrons.

The plasma now undergoes losses by diffusion across the closed pattern of magnetic lines. The attainable density and temperature depend on the balance between energy loss by diffusion and energy gain transferred to the plasma from the E-layer electrons by Coulomb scattering. This calculation has been described in the Astron paper.[2] The diffusion loss is maximized (for a given plasma density) at a temperature U_0 which is a function of the E-layer electron energy and the degree of the field reversal. Let the field (B_w) outside the E layer be ten times stronger than the reversed field (B_i) just inside the E layer, i.e., 110% field reversal.

[2] N. C. Christofilos, Astron Thermonuclear Reactor, in Proc. Int'l Conf. on Peaceful Uses of Atomic Energy, 2d Geneva, 1958 (United Nations, New York, 1959), Vol. 32, p. 279-290.

The allowable plasma density and temperature of the maximum diffusion rate are respectively (see Reference 2, p. 283)

$$n_0 = \frac{\gamma^4}{r_e} \cdot \frac{\cos^2\delta}{16\pi r_1^2}, \tag{37}$$

$$U_0 = \frac{2.5 \cdot 10^6}{\gamma^2} \text{ ev}, \tag{38}$$

where γ is the E-layer electron energy expressed in rest-mass units, δ is the angle between the mechanical azimuthal to total momentum of the E-layer electrons, r_e is the classical electron radius, and r_i is the average radius of the E layer. The angle δ is 60° approximately.

For the parameters

$$\gamma = 10, \qquad r_i = 27,$$

$$\cos\delta = 0.5, \qquad B_w = 630 \text{ gauss},$$

the above equations yield

$$n_0 = 2.5 \times 10^{11}, \qquad U_0 = 25 \text{ kev},$$

$$p = 2\, n_0\, eu = 2 \cdot 10^4 \text{ dynes/cm}^2.$$

The required external magnetic field is

$$B_0 = (8\pi p + B_w^2)^{1/2} = 950 \text{ gauss}.$$

The ratio is

$$\beta = \frac{8\pi p}{B_0^2} = 0.55. \tag{39}$$

This value of β is high enough for study of the plasma behavior. It should be noted that after the creation of the pattern of closed magnetic lines it is not necessary to proceed in the formation of such a high-β plasma. At first a low-density, low-β, but high-temperature plasma will be created. The density of this plasma will not exceed the value obtained before establishing the complete E layer, i.e., 10^{10} approximately. The plasma density can be controlled by adjusting the flow of neutral gas which replaces the diffused plasma. Hence, the plasma behavior will be studied in the entire range from 10^{10} up to a few times 10^{11}.

Thus, it will be possible to observe the conditions under which instabilities set in if such instabilities do occur.

In conclusion, I would like to observe that with the Astron model as it is now conceived we would be able to explore a range of plasma density extending over three orders of magnitude, thus acquiring extremely valuable information on plasma behavior. This is one goal of the Astron experiment. The main purpose, however, is to evaluate the Astron concept as a possible solution of the controlled-fusion problem.

D. Possible Experiments with the 2-Mev Astron Model

As is mentioned above, the construction of the 5-Mev Astron model is to proceed in two steps:

(1) Completion of the electron accelerator up to 2 Mev electron energy, including modification of the present electron gun to yield 200 amp and completion of the other Astron components: E-layer tank, coils, passive circuit injection system. After testing the performance of the electron beam at 2 Mev, as well as the injection system, we shall proceed to the next step.

(2) Completion of a 3-Mev extension of the accelerator. In the interim (about 12 months would be required for the fabrication and installation of the additional 3-Mev extension) a sequence of interesting experiments is contemplated.

(a) Testing the injection system. The slowing-down forces will be measured experimentally and the allowed depth of the mirror-field potential well will be determined. The number of electron bunches that can be trapped depends on the depth of this potential well. Since with 2-Mev electrons the performance of the injection system is marginal, the trapping of one electron bunch only can be guaranteed. If more are trapped the electron lifetime and stability will be studied. However, if it were not possible to trap more than one electron bunch at a time, even so we could perform an interesting plasma experiment.

(b) Plasma studies. For this purpose the length of the E layer will be restricted to length 150 cm. The electron current in one bunch is 4000 amp, approximately, or 25 amp/cm of length of the E layer. A vacuum of 10^{-8} mm Hg is postulated, and in addition a deuterium atom density of 5×10^{9} will be maintained in the E-layer region.

The electric field at the surface of the E layer is

$$E_0 = 10 \text{ kv/cm}.$$

The potential difference between the vessel wall and the E layer and the potential well within the E layer are respectively

$$\Phi = 150 \text{ kv},$$

$$\Phi_e = 50 \text{ kv}.$$

The electron density is

$$n_e = 5 \times 10^8.$$

The high-energy ion density after 10 msec will be, from Eqs. (26), (27),

$$\bar{n}_i = 5 \cdot 10^7/\text{cm}^3,$$

while the total ion density is

$$n_i = 1.1 \cdot 10^8/\text{cm}^3.$$

The average electron energy at this time will be approximately 5 kev. This is of course a very thin plasma, but since no such hot plasma has yet been attained, it would be of interest to start with some density even though quite small. Because the density will be very low, the Debye wave length will be larger than the plasma container, so that the plasma should be free of instabilities. By proper probes the energy distribution can be studied and the density measured. Furthermore, by replacing the deuterium gas by a 50-50 D-T mixture, a detectable yield of neutrons ($\sim 10^4$/pulse) can probably be produced as an additional diagnostic indication.

The above experiments are characteristic of the potential of the Astron facility. It is likely that other experiments will be devised as soon as the facility is ready for operation.

Appendix

Calculation of the Friction (Slowing-Down) Force

The arrangement of the resistive loops for this function is shown in Fig. 13. The calculations of the induced emf, currents, and resulting magnetic fields have been done in the plane approximation; i. e., we assume that the electron bunch is a straight beam along the y direction located at x = 0; the two cylinders 10 and 12 are (two planes) located on the planes x = -b and x = 2b; respectively. The resistive loops are straight conductors along the y direction located on a plane x = b. Finally we assume that the electron current is along the y direction and that the electron beam moves (parallel to itself) along the z direction with a velocity $v_z \ll c$.

Then the vector potential of an electron beam (of circular cross section of radius "a" and current I) in a coordinate system at rest assumed the form

$$A_y = \frac{I}{10} \ell n \left[\frac{\sin^2 k_1(x+2b) + \sinh^2(k_1 z - \omega t)}{\sin^2 k_1 x + \sinh^2(k_1 z - \omega t)} \right], \qquad \text{(A1)}$$

(This solution is valid as long as $v_z/c \ll 1$),

$$\omega = k_1 v_z, \qquad k_1 = \pi/2d,$$

where d is the distance between the cylinders 10 and 12; then b = d/3 and the vector potential for x = b (the plane where the resistive elements are located) becomes

$$A_y(b) = \frac{I}{10} \ln \left[\frac{\cos^2 h\,(k_1 z - \omega t)}{.25 + \sin h^2 (k_1 z - \omega t)} \right] . \tag{A1a}$$

The components we are interested in are

$$E_y = \frac{1}{c} \dot{A}_y, \tag{A2}$$

$$B_x = - \frac{\partial A_y}{\partial z} . \tag{A3}$$

From Eq. (A1) we obtain

$$\frac{1}{c} \dot{A}_y = - \frac{v_z}{c} \frac{\partial A_y}{\partial z} \tag{A4}$$

or

$$E_y = - \frac{v_z}{c} B_x, \tag{A5}$$

and

$$B_x = \frac{I}{5} \left(\frac{\pi}{2d} \right) \left[\frac{\sin h\,(k_1 z - \omega t) \cos h\,(k_1 - \omega t)}{.25 + \sin h^2 (k_1 z - \omega t)} - \tan h\,(k_1 z - \omega t) \right] . \tag{A6}$$

The above solution has been computed numerically for $k_1 z = -\pi$ and $0 < \omega t < 2\pi$ and is shown in Fig. 14. Then the function is approximated with a sinusoidal function (valid in the interval $0 < \omega_0 t < 2\pi$), namely,

$$B_x = \frac{I}{5d} \sin (\omega_0 t), \tag{A7}$$

where $\omega_0 = 2\omega$

For $\omega_0 t < 0$,

$\omega_0 t > 2\pi$,

$B_x = 0$,

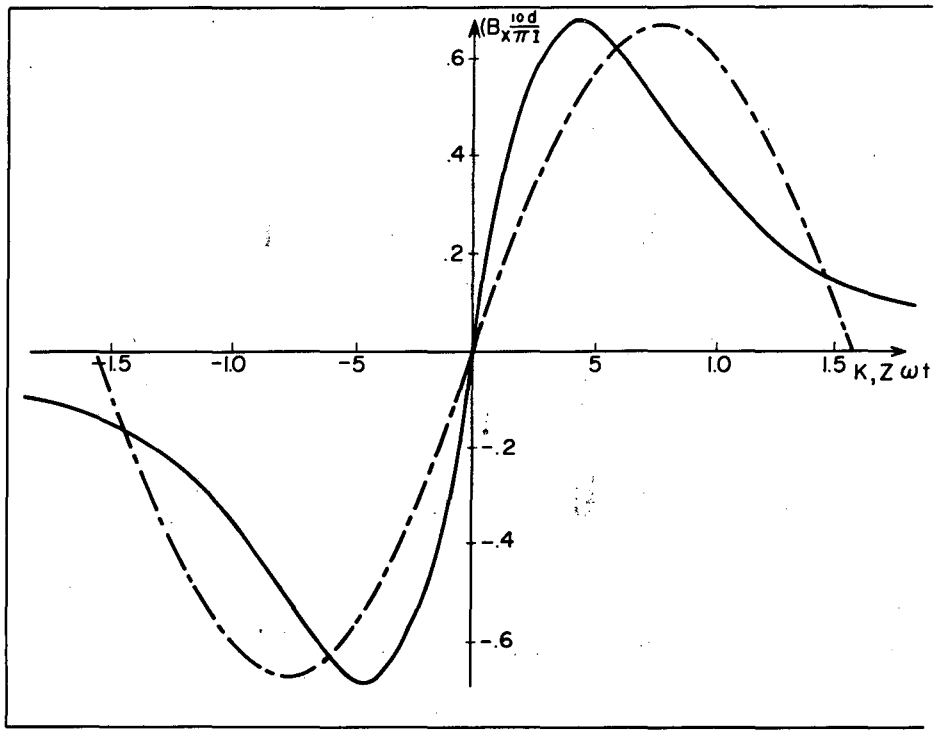

MU-18360

Fig. 14. Solution of Eq. (A6).

The next step is to derive the current on the resistive loop due to the field E_y. The current can be determined from the equation

$$\frac{dJ}{dt} + \frac{R}{L} J = \frac{E_y}{L} . \tag{A8}$$

Substituting E_y from the above equations, we obtain

$$\frac{dJ}{dt} + J = \omega_0 J_0 \sin(\omega_0 t), \tag{A8a}$$

where

$$a = \frac{R}{L} \sec^{-1}, \quad J_0 = \frac{60 I}{\omega_0 L d} \cdot \frac{v_z}{c} \text{ amp.} \tag{A9}$$

Substituting $\omega_0 = 2 k_1 v_z/c$, we have

$$J_0 = \frac{60}{\pi} \cdot \frac{I}{Lc} \text{ amp,} \tag{A10}$$

where R and L are the resistance (in ohms) and the inductance (in henries), respectively, per cm of length of the resistive elements. Equation (A8a) yields

$$J = \frac{J_0}{(a/\omega_0)^2 + 1} \left[\cos \omega_0 t - e^{-at} - \frac{a}{\omega} \sin \omega_0 t \right] \tag{A11}$$

for

$$+ 0 < \omega t < 2\pi.$$

For $\omega t > 2\pi$,

$$J = \frac{J_0}{(a/\omega)^2 + 1} (1 - e^{-2\pi a/\omega}) e^{(2\pi a/\omega - at)}. \tag{A12}$$

The energy loss in the resistor is

$$W = \frac{R}{\omega} \int_0^{2\pi} J^2 \, d(\omega t) + R \int_{t = \frac{2\pi}{\omega}}^{\infty} J^2 \, dt. \tag{A13}$$

The first and second integrals yield, respectively,

$$W_1 = \pi L J_0^2 \left[\frac{a/\omega}{(a/\omega)^2 + 1} + \frac{1}{2\pi} \frac{1}{[(a/\omega)^2 + 1]^2} (1 - e^{-\frac{4\pi a}{\omega}}) \right], \tag{A14}$$

$$W_2 = \frac{LJ_0^2}{2} \frac{1}{[(a/\omega)^2 + 1]^2} (1 - e^{\frac{-2\pi a}{\omega}})^2 . \quad \text{(A15)}$$

The losses are maximized for $a/\omega = 1$. Then

$$W = \frac{\pi}{2} L J_0^2 \left[1 + \frac{1}{2\pi} (1 + e^{-4\pi} - e^{-2\pi})\right] . \quad \text{(A16)}$$

Since the second term in the brackets is small, we can write

$$W_1 \approx \frac{\pi}{2} L J_0^2 . \quad \text{(A17)}$$

This energy loss is subtracted from the kinetic energy of the electrons. The equations of motion for the electrons are

$$\dot{p}_y = - e \left[E'_y + \frac{v_z}{c} B'_x\right] , \quad \text{(A18)}$$

$$\dot{p}_z = + e \frac{v_y}{c} B'_x , \quad \text{(A19)}$$

where E'_y and B'_x are the field components generated by the current in the resistors at the location of the electron beam. This current is traveling (relative to the electrons) towards the negative y direction. The relative positions of electron beam to the resistors are symmetric with respect to the planes $x = -b$, $x = d - b$. Hence, similar expressions can be obtained for the B'_x field as obtained for the field of the beam on the resistive elements. From Eq. (A5) we observe

$$E'_y + \frac{v_z}{c} B'_x = 0. \quad \text{(A20)}$$

Thus, all the energy dissipated in the resistors is at the expense of the axial momentum of the electrons.

The value of B'_x is

$$B'_x = \frac{J}{5d} \sin \omega t, \quad \text{(A21)}$$

where

$$J = \frac{J_0}{(a/\omega)^2 + 1} \left[\cos \omega t - e^{-at} - \frac{a}{\omega} \sin \omega t\right] . \quad \text{(A22)}$$

The total energy lost per cm of length of the beam is

$$W_b = N \gamma v_z \int \dot{p}_{z'} \tag{A23}$$

where

$$N = 2 \cdot 10^8 \, I \text{ electrons/cm}, \tag{A23a}$$

and I is expressed in amperes.

By performing the integration for $0 < \omega t < 2\pi$, we find exactly the same losses as given by Eq. (A14), as expected. We are interested in the average value of B'_x, or

$$\langle B'_x \rangle = \frac{1}{2\pi} \int_0^{2\pi} B'_x \, d(\omega t). \tag{A24}$$

The integration yields

$$\langle B'_x \rangle \approx \frac{J_0}{10d} \left[\frac{a/\omega}{(a/\omega)^2 + 1} \right] . \tag{A24a}$$

Upon substituting $a/\omega = 1$, and the value of J_0, we find that Eq. (24a) becomes

$$\langle B'_x \rangle = + \frac{I}{20\pi d} \left(\frac{120}{L \cdot c} \right) \text{ gauss}. \tag{A25}$$

This value is averaged along a length

$$\ell_x = v_z \frac{2\pi}{\omega_0} , \tag{A26}$$

or

$$\ell_x = 2d. \tag{A26a}$$

The inductance L can be calculated from the vector potential, namely

$$L = \frac{.10^{-8} A_y}{I} , \tag{A27}$$

or

$$c \cdot L = 60 \, \ell n \left[\frac{\sin (\pi a'/2d)}{\sin \frac{\pi}{3}} \right] , \tag{A27a}$$

where a' is the radius of the resistive conductor.

For $b/a' = 6$,

$$c\,L = 138,$$

and

$$L = 4.6 \cdot 10^{-9} \text{ henries/cm.}$$

Then

$$\left\langle B'_x \right\rangle = \frac{I}{72\,d} \quad , \tag{A28}$$

$$R = \frac{430}{d}\left(\frac{v_z}{c}\right) \text{ ohms/cm.} \tag{A29}$$

For $d = 30$ cm, $v_z/c = 0.1$, $R = 1.44$ ohm/cm.

Thus far these calculations have been done for one loop of resistors. We shall now extend these calculations for N_0 resistive loops evenly distributed along a cylinder of length L_0. The distance between adjacent resistors is L_0/N_0. This distance must not be too small, otherwise the mutual inductance between adjacent resistors should be taken into consideration in the calculation of the resistor current. For $L_0/N_0 > 10$ cm this effect is very small. The average value of B_x now becomes

$$\left\langle B_x \right\rangle = \frac{N_0 I}{36\,L_0} \quad . \tag{A30}$$

For $L_0/N_0 = 10$, Eq. (A30) becomes

$$B_x = \frac{I}{360} \quad . \tag{A31}$$

In deriving this equation we have set $a = \omega_0$, implying that ω_0 is a constant. This will be possible only if the value of B_x resulting from the dynamic action of the passive circuits is compensated by a static component equal and opposite to the dynamic value as given by Eq. (A31). This is accomplished by injecting the electrons at the top of a mirror field. This mirror field is designed to provide a constant slope, approximately, along the region where the resistors are located (see Fig. 13); thus the flux enclosed by the electron bunch is continuously decreasing as the electrons move through the resistor region. Then the vector potential of the static field will be reduced by $B_x \cdot L_0$ or

$$\delta A_\theta = \frac{I\,L_0}{360} \quad . \tag{A32}$$

This change of vector potential in turn results in a change of the azimuthal momentum of the electrons, since

$$\delta A_\theta = \frac{c}{e} \delta p_\theta . \tag{A32a}$$

In this way, finally, the energy loss is at the expense of the total momentum of the electrons. This happens because by imposition of the static field the azimuthal momentum is continuously transformed to axial momentum, which in turn is absorbed by the resistor action.

From Eqs. (A32) and (A33) we obtain

$$L_0 = \frac{360}{I} \gamma V_0 \left(\frac{\delta p_\theta}{p_\theta} \right) \text{ cm}, \tag{A33}$$

or, substituting $V_0 = 1700$ esu,

$$L_0 = \frac{6.1 \cdot 10^5}{I} \gamma \left(\frac{\delta p_\theta}{p_\theta} \right) \text{ cm}. \tag{A34}$$

A reduction by 20% of the total momentum is considered adequate to secure confinement of the E-layer electrons. Then for $\gamma = 10$, $I = 7500$, $L_0 = 163$ cm. It should be recalled at this point that the above calculations have been done for the plane approximation. However, since the field of a circular loop is less than the field of a straight wire (with the same current), we should increase the length L_0 by a factor of 2 to 3. Hence in the first experimental arrangement an L_0 of 500 cm is advisable.

It will be of interest to examine the pure slowing-down process, i.e., the case in which no static field exists to compensate for the decelerating dynamic field. In this case ω is variable and the average value of B_x is

$$B_x = \frac{I}{360} \frac{2 a/\omega_0}{(a/\omega_0)^2 + 1} . \tag{A35}$$

Let us assume that $a/\omega_0 = 1$ upon entering the slowing-down region and β_0 the initial ratio v_z/c. Then, from Eqs. (A19) and (A35) we obtain

$$\left[\left(\frac{\beta_0}{\beta} \right)^2 + 1 \right] \frac{d W_z}{dt} = - \frac{ecI}{360} \beta_0 , \tag{A36}$$

where W_z is the instantaneous value of the axial kinetic energy. Equation (A36) upon integration yields

$$\frac{t}{T} = \ell n \left(\frac{W_0}{W_z} \right) + \left(1 - \frac{W_z}{W_0} \right) , \tag{A37}$$

where W_0 is the initial axial energy and

$$T = \frac{180\ \gamma\ v_0}{I\ c}\ \beta_0 \tag{A38}$$

or

$$T = 10^{-5}\ \frac{\gamma}{I}\ \beta_0 \text{ sec.} \tag{A39}$$

For the numerical example $\gamma = 10$, $I = 7500$,

$$T = 1.33 \cdot 10^{-2}\ \beta_0 \ \mu\text{sec.} \tag{A40}$$

We may find also the length ℓ_1 required to absorb an initial axial velocity β_0. The result is

$$\ell_1 = \frac{8.10^5\ \gamma}{I}\ \beta_0{}^2 \text{ cm,} \tag{A41}$$

or for $\gamma = 10$, $I = 7500$,

$$\ell_1 = 1066\ \beta_0{}^2 \text{ cm.} \tag{A42}$$

In the injection region, before the compression occurs the beam current I_0 is 250 amp and $\beta_0 = 0.06$. Then $\ell_1 = 115$ cm. This result applies to other injection parameters provided that γ/I_0 remains constant. Since the axial velocity is reduced e times every 115 cm, we observe that the length of the injected bunch will be reduced, too, since the reduction of the axial velocity reduces the pitch of the helical paths of the injected electrons. More specifically, the length of the electron bunch is reduced by a factor of ten, as desired, after it has traveled 260 cm beyond the injection tube.

Calculation of the Stored Energy in the Electromagnetic Field of the Electron Bunch

We assume that "n" circular beams of radius "a" placed side by side constitute the electron bunch. The current in each beam is I/n, where I is the total current in the bunch. The axis of the n beams is at $z = a(2m-1)$. The value of the vector potential at $z = 0$ can be evaluated as the sum of the vector potential at the point of all the n beams; namely, from Eq. (A1) and for

$$d/a = 10,$$

we obtain

$$A_y(0) = \frac{I}{10n} \sum_{m=1}^{m=n} \ell n\left(1 + \frac{.75}{\sinh^2[.16(2m-1)]}\right); \tag{A43}$$

For n = 5, $A_y(0) = 0.12$ I.

In a similar way we can calculate the vector potential at z = an (i.e., at the center of the bunch). The result is $A_y(an) = 0.21$ I. The average value of the vector potential per electron of the bunch is

$$\bar{A}_y = 0.165 \text{ I.}$$

The electrostatic potential (expressed in esu) is equal numerically to the vector potential. Hence

$$\Phi = 50 \text{ I volts;}$$

For I = 6000 amp, $\Phi = 300$ kv.

ASTRON E-LAYER CALCULATIONS

Lewi Tonks*

The continuing attack on the self-consistent analysis of the E layer has reached another milestone. At this stage the analysis of a model E layer in which all the electrons have the same kinetic energy but vary in canonical angular momentum has been completed. The work has been written up as UCRL-5643 under the title "The Self-consistent Field and Motion of Electrons which have a Range in Canonical Angular Momentum in a Uniform Magnetic Field". Only a remaining touch or two need to be made on the manuscript. In formulating this report a considerably clearer understanding of the exact mathematical method appropriate to this kind of problem has been arrived at.

The extension of the analytical method used in the simpler model of the E layer, in which no momentum spread was present, to cover a range of angular momentum among monoenergetic electrons reveals some modification in form and characteristics of the self-consistent configurations. Field reversal is still possible even with the maximum possible range in momentum. Two configurations for a given layer strength, one with unreversed and one with reversed field, are still present. In addition, the same ratio of internal to external field--reversed or unreversed--can be consistent with two different layer strengths. Undoubtedly stability considerations enter strongly.

The next milestone will be the analysis of the more realistic problem in which electrons of one energy and one canonical angular momentum are injected into an Astron and then slowed down under the dynamical friction of the plasma. The code for this (on the 704) has continued, through a considerable part of the present period, to present us with new bugs. Now, however, the code seems to be clean and we have run through more than 30 separate cases. Since this is a three-parameter problem, a considerably larger number of cases will be necessary for covering the interesting ranges

*Consultant to LRL from General Electric Co. Vallecitos Atomic Laboratory, Pleasanton, California.

and understanding what is going on. It is contemplated that the total number will be something like 100. Strong field reversal continues to be evident. Unfortunately, the possibility of having two entirely different configurations--one with reversed, the other with unreversed field but both requiring the same electron supply--has still not been clearly eliminated. In cases in which field does not reverse it is still possible (as it was in the simplest model of the E layer) for the internal magnetic field to exceed the vacuum field outside. In some cases of reversal, it is possible for the reversed field to exceed the external vacuum field in magnitude. A recent modification to the code has been for the purpose of finding out to what extent the electron layer undergoes shear, in that electrons with different energies and different angular momenta circulate around the axis with different average angular velocity. This can be important for stability of the layer. A write-up of the theoretical part of this problem is about three-quarters complete.

The more general problem, which includes scattering of the electrons, has been set aside for the present in order to allow complete attention to the slowing-down problem. The present indication is that although it is solvable in principle, the complications are so formidable that only an approximate method of analysis will be practical.

ASTRON dc TEST

W. A. S. Lamb

During this period some minor modifications of the accelerating column of the electron gun have resulted in a marked increase in reliability and resulted in much longer periods of operation between shutdowns to clean insulators.

A redesign of the accelerating column has been completed which was aimed at increased operating voltage and increased current. The principal features of the new design are improvements in the supporting insulators (see Fig. 15).

The main solenoid of the dc test machine was rewound to a diameter corresponding to the outside diameter of the flanges that fasten the vacuum system together. This removed a perturbation in the uniform field which was responsible for the loss of substantial fractions of the beam about 18 to 20 inch downstream from the inflection apparatus.

Measurements of the beam current on probes, with no compensation for space-charge forces, showed that nearly all the beam could be demonstrated at the far end of the solenoid 10 ft downstream from the inflection apparatus. Specifically, out of 30 amp measured at the first 1/4 turn from the inflector, 28 amp was observed at the 10-ft point. The beam bunch expanded in the axial direction to about 12 in. long after about 10 turns around the solenoid, or about 40 in. downstream, and then stayed about the same to the maximum distance, namely, 120 in. downstream.

A mirror winding was then installed at the downstream end of the solenoid (Coil B). This mirror winding was energized and no beam could be observed on the probe, which was placed immediately behind the mirror.

A probe was placed immediately upstream from the inflection apparatus in order to measure the reflected beam that missed the inflection tube. With the B coil energized a signal was observed on this upstream probe corresponding to the beam that had made a round trip down the solenoid and back. This signal was about 0.2 μsec later than the injected pulse.

At a beam energy of 600 kev the velocity of the electrons is 2.66×10^{10} cm/sec and the mean radius of the electron orbit is 30 cm, so that

$$s = vt = 2.66\times10^{10}\times2\times10^{-7}$$

$$= 5.3\times 10^{+3} \text{ cm in } 0.2 \text{ μsec},$$

$$\frac{s}{2\pi\rho} = \frac{5.3\times10^{+3}}{2\pi \times 30} = 28 \text{ turns/round trip},$$

and the average pitch is

$$\frac{600 \text{ cm}}{28 \text{ turns}} \simeq 21 \text{ cm/turn},$$

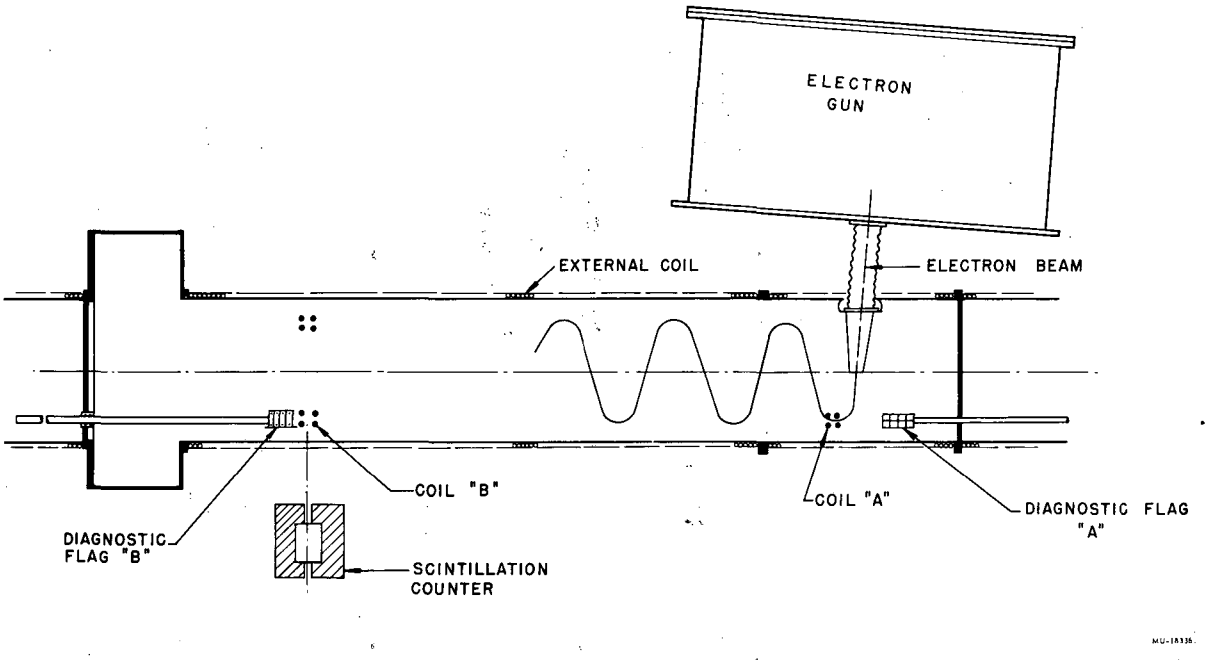

Fig. 15. Astron dc test experimental arrangement.

which corresponds to the geometry. Further, the axial velocity is

$$\frac{600 \text{ cm}}{2\times10^{-7} \text{ sec}} = 3\times10^{9} \text{ cm/sec},$$

which corresponds to an axial energy of about 3 kev. The mirror ratio required to reflect electrons is then given by

$$R_m = W/W_{\perp} \cong \frac{600}{597} \cong 1.005.$$

The experimental value of the current required to reflect the electron beam corresponds to this value.

The next series of experiments (still in progress) was an attempt to trap a single pulse of beam. A coil was placed (Coil A) just downstream from the inflector, and this was energized by a very-fast-rising pulse of current in order to trap the beam which is returning upon reflection from the downstream coil (Coil B).

The beam was monitored by means of a scintillator counter placed at B coil. B coil was energized and then canceled by means of a fast pulse with a time delay from the time of injection at the disposal of the experimenter. An estimate of the fraction of the beam trapped could be obtained by comparing the amplitude of the x-ray signal when the B coil was not energized or was canceled with the amplitude of the x-ray signal after a delay of 0.5 μsec, for example.

These measurements, which are still in progress, have indicated that beam is trapped for up to 300 μsec, and enable one to set a lower limit on the time for the trapped beam to reach its half value at about 100 μsec. The fraction of beam trapped is estimated at between 10% and 30% of the beam injected.

A significant observation during these measurements was the discovery that the beam was trapped even though the fast-rising coil at the injection end (Coil A) was not energized. Observation of the current across a shunt demonstrated the induction of currents in the coil by the beam which were sufficient to trap the beam. Currents of 10 amp circulating in the coil were observed, and this is sufficient to trap a significant fraction of the beam. This observation is a manifestation of the currents induced by these high-current beams which are to be used in the new injection system.

The brief account above represents very preliminary results, and many more experiments are planned to explore the properties of the trapped beam.

Concluding Remarks

The experimental philosophy in the measurements described above was to make a rapid series of survey experiments to develop information on the requirements of components of the Astron machine and on the associated

apparatus necessary to perform such measurements. The results are quite incomplete and for the most part rather qualitative. In spite of this, however, one can conclude some things about the original aims of the dc experiment.

In particular one can say that the simple beam-inflection system, though not optimum, is adequate, and that with relatively crude techniques one can trap substantial fractions of the beam for periods of time that suffice for establishing an electron layer with the injection systems now contemplated.

IV. LIVERMORE PINCH PROGRAM

Dale H. Birdsall, Stirling A. Colgate, and Harold P. Furth

LINEAR HARD-CORE PINCH

Tubular pinches have been studied in which either H_z or H_θ or both have a zero inside the plasma. The observation has been confirmed that a zero in H_z is not a strong instability-inducing factor. Azimuthal current densities as high as 1.5 ka/cm^2 have been reached at the zero in H_z, without causing noticeable instability, whereas 0.4 ka/cm^2 was found quite sufficient to cause instability in the "inverse stabilized pinch." In pinches involving a zero in H_θ, marked instabilities are observed, comparable to those in the "inverse stabilized pinch" or conventional "stabilized pinch" for similar current densities.

The theory (mentioned in the preceding report) that high axial rather than high azimuthal current density is responsible for small-scale instabilities therefore is still supported by experiment. This result is consistent with hydromagnetic stability theory, but may equally well be related to electrostatic rather than hydromagnetic considerations. The azimuthal component of the current density circulates in the plasma, but the axial component must flow out of and into electrodes, thus raising the possibility of electrode-sheath or arc-spot modulation of the current, with consequent generation and propagation of various current-flow instabilities. Such phenomena are familiar from classical studies on low-current-discharge tubes.

In order to study the effect of electrodes--especially the cathode--more closely, a special electrode has been built, consisting of a molybdenum diaphragm that can be heated to a light orange. Surface conditions will presumably be widely different depending on whether the molybdenum is hot or cold, and the effect on instability level will be studied.

Another approach to the problem has been to insert an axially oriented probe through one electrode, extending all the way to the other, with spaced magnetic pick-up loops in between. The object has been to look for anode-cathode asymmetries, and these have indeed been found. In the conventional stabilized pinch, it is found that the current-carrying front is markedly sharper near the cathode, and that high-frequency, low-amplitude magnetic disturbances are present there. Near the anode, high-frequency disturbances are mostly absent, but low-frequency large-amplitude disturbances are evident. A possible interpretation is that the high current density near the cathode leads to current-flow-type instabilities, the low-frequency component of which is selectively amplified as one proceeds downstream. The above results have been observed for a wide variety of current levels, densities, and pinch ratios, and are invariant under reversal of tube voltage or of H_z.

If the same experiment is done on the "inverse stabilized pinch," the results are more inconclusive. In most cases it appears, in fact, that the current front is more sharply defined near the anode. Definite conclusions on this point, as well as a more detailed examination of anode-cathode asymmetries in general, will await construction of an improved linear hard-core tube, designed for this purpose.

A study has been made of the rate at which magnetic fields inter-diffuse in various configurations. No dramatic extension in diffusion time has been observed in what are apparently the most stable pinches. The plasma resistivity in all cases seems to correspond to about 10 ev electron temperature, as usual (such a temperature is expected in linear geometry regardless of stability). One interesting phenomenon that has been investigated relates to the processes by which the conventional "stabilized pinch" manages to keep H_z field entrapped for as long as it does (several-hundred-microsecond containment has been achieved by various laboratories in 12-in. tubes). As has been pointed out by several theoreticians, as long as an axial driving voltage is applied to the "stabilized pinch" there is a constant diffusion of H_θ flux toward the pinch axis, which acts convectively on the plasma and also on the H_z field, which is coupled to the plasma. Thus it would be possible to maintain a nonvacuum field H_z distribution on a steady-state basis, if the steady-state distribution were hydromagnetically stable--which it is not entirely. At any rate, one concludes that the entrapment of H_z observed in conventional "stabilized pinch" experiments is only partly due to transient phenomena that depend on high plasma conductivity (i. e. skin effect), and is partly due to the "steady state" radial inward convection of H_z by H_θ field. To measure this effect, we have done two stabilized pinch experiments in the hard-core tube, one with the center rod disconnected, so that the tube acts like a conventional tube, and one with the center rod shorted to both electrodes. In the former case H_θ can diffuse continuously inward, remaining at a low value near the glass insulating tube of the center rod. In the latter case, a current springs up on the center rod, and H_θ field accumulates, rising to a high value in the vicinity of the rod, and approaching the $1/r$ vacuum field distribution throughout the tube. With the center rod connected, the configuration is considerably more stable, but the H_z field diffuses outward more rapidly than with the center rod disconnected. Thus the difference between pure diffusion of H_z and diffusion plus convection can be demonstrated and measured directly for the stabilized pinch. Similar experiments can be performed for more general configurations. We have been particularly interested in examining pinches in which H_z of H_θ passes through zero inside the plasma, to see whether or not there is a large accumulation of the nonzero field component at these points, or whether local regions of high plasma pressure result. Experiments to date have indicated that there is some accumulation of the nonzero field component, but not nearly enough to balance magnetic pressure. These studies are still in progress.

The dynamic tubular pinch has been duplicated in our tube, and results similar to the Berkeley results are obtained. In the beginning, there is a period of dynamic oscillations, free from instabilities (about 10 μsec). Near current maximum, instability signals appear that are very similar to those observed for the other unstable configuration we have studied. At instability time, an erratic H_z signal is observed. A study of anode-cathode asymmetry was made, but no marked asymmetry was observed. Addition of a small initial H_z diminished the dynamic behavior and slightly hastened the onset of instabilities. (Addition of H_z to the tubular dynamic pinch reduces it to the configuration with a zero in H_θ and nonzero H_z, which was mentioned earlier).

The linear hard-core experiment is being temporarily discontinued to facilitate construction of a longer tube with various added probe ports. Gamma pinch bank will be used meanwhile to complete the sodium pinch study. A hard-core sodium pinch experiment has been built, to test whether complete hydromagnetic stability exists, as predicted theoretically.

THE LEVITRON

A small prototype Levitron with square cross section (2 by 2 in.) has been used to confirm the Levitron theory (see preceding report). A 60-cycle current of 2.5 ka gives essentially complete steady-state levitation. Alternatively, pulsed levitation can be achieved by using a capacitor bank and monitoring the core position with fast signals induced on the core and received on magnetic probes at the wall. , A similar Levitron with 3-by-3-in. cross section, a 3/4-in. copper core, and a glass and Micalex vacuum liner has been completed. The core levitates at about 6 ka (rms). This device is currently being put into pinch operation and levitation with all required H_θ and H_z fields has been attained.

Parts for the large (12-in.) Levitron are being accumulated and a stainless steel liner has been ordered. Alternative liner designs, based on metal plating on plastic, are under study. Completion of the unit is estimated for the end of this year.

ELECTRON BEAM EXPERIMENT

The electron gun has been improved by installation of a 6-in. vacuum chamber with increased pumping speed, and various conducting shields to grade the potential. As a result, satisfactory performance can now be achieved consistently up to 300 kv. The pinch transmission experiment will be resumed as soon as the Beta pinch bank (currently used with the small Levitron) becomes available.

PLASMA ACCELERATOR EXPERIMENTS

The first stage of the pinch-type accelerator has operated successfully. The driving bank has been increased to four 14-μf 20-kv capacitors, which are fired in series-parallel through four spark gaps, using the method of ultraviolet cross-illumination.

A new rail-type accelerator has been invented and is being evaluated theoretically. The basic idea is to draw a current pulse between two rails, and across an orthogonal magnetic field (linear version of the Homopolar). The plasma reaches an equilibrium velocity $v = (E/H)c$ of 5×10^6 to 10^7 cm/sec, along the rails. The magnetic field is so arranged as to drop suddenly in magnitude as one proceeds along the rails beyond a certain point.

As the plasma slug crosses this point, the front of the plasma is accelerated to a higher equilibrium velocity, corresponding to the diminution of H in the expression $v \doteq (E/H)c$. This acceleration is accomplished by a surge current that flows out of the bulk of the plasma slug and decelerates it in the process. Thus the working principle is seen to be essentially that of using a moving plasma as a low-inductance high-dielectric-constant capacitive energy source. This principle has been discussed at length elsewhere, in connection with the Homopolar.

MATRIX MARX BAND

Three capacitor files have been connected in parallel and fired successfully in unison, at 10 kv (150 kv total). The present firing system therefore appears to be entirely sound. On the other hand, troubles due to capacitor failure have been encountered. Individual capacitors have been tested and indeed found somewhat short of specified performance. The main trouble, however, is thought to be the special stress imposed on capacitors by operating many in series. Under these conditions, any loss of capacity of a given unit leads to higher voltage across the unit, and higher current concentration. Thus any slightly deteriorated capacitor becomes quickly worse. To compensate for this inherent danger in a series-connected capacitor bank, parallel cross-connections may be introduced in each row of the Marx bank, rather than merely in the two end rows (as is the case now), provided satisfactory gap firing can still be achieved.

V. BERKELEY PINCH PROGRAM

SHEET PINCH STUDIES

Oscar A. Anderson

Introduction

The pinch program at Berkeley is presently exploiting some near-stable plasma configurations which are distinguished by their simple magnetic field patterns, i. e., sheet pinches with transverse fields.[1] This exploitation has followed two somewhat separate paths: (a) a high-temperature program, intended to produce plasmas in the hundreds-of-volts region, and (b) a program designed to investigate the formation and ensuing behavior of the sheet pinches per se. The latter project tended to become isolated because the diagnostic techniques originally required a reduction to the tens-of-volts level. At the conclusion of this section there is a discussion of the plans to integrate these programs more fully while attempting to set up in addition a small plasma physics project. Here the sheet-pinch configuration would be used for easily making certain fundamental plasma measurements which are otherwise rather difficult.

The 4-Inch Tubular Pinch (Triax)

Most of the low-level diagnostics and much of the high-level work have been done in the past with Triax tubes measuring 4 in. o. d. by 1.5 in. i. d. by 24 in. Because of the many advantages of the new 10-in. tubes they will henceforth be employed for both types of work; the old tubes will mainly be held in reserve for special measurements. Accordingly, during the last quarter the preheating studies previously reported were temporarily discontinued in anticipation of transferring them to the larger tube. The 4-inch Triax was used instead for an investigation of edge effects in sheet pinches. Normally the tubular pinch has no edges, only ends, but by insertion of a longitudinal barrier the Triax was converted into a sort of curled-up ribbon pinch. Thus there was hope for an easy, direct comparison of the dynamic behavior in the two cases. Enough voltage wave forms were obtained to indicate that the difference is small over most of the tube, at least for the first few microseconds, the period of primary interest. However, a serious difficulty hindered completion of the experiment: the inner insulator of the Triax was invariably cracked after a few shots. It was interesting that the crack always occurred on the side opposite the barrier. Apparently the local reduction of pressure allowed the insulator to be pushed toward the barrier, and thus to be broken on contact with the hard core.

---

[1] O. A. Anderson, W. R. Baker, J. Ise, Jr., W. B. Kunkel, R. V. Pyle, and J. M. Stone, International Conference on the Peaceful Uses of Atomic Energy, 2d, Geneva, 1958 (United Nations, New York 1959) Paper No. 2349, Vol. 32, p. 150.

Switches

A small version of the Baker switch[2, 3] has been built for use with the preheating banks. The de-ionization time will be measured and compared with that of ignitrons and spark gaps. The switch that performs best in this application will be used to complete the current-cutoff experiments described in the last report. Although this measurement has not yet been made, the small switch has already produced some useful results. Solid stainless-steel voltage-dividing plates were used in the design, the replaceable brass inserts normally surrounding the discharge apertures being eliminated. It was found that the switch in this form was almost impossible to trigger. When brass inserts were installed throughout, except around the trigger pin, the performance was hardly any better. Finally with brass surrounding the trigger normal performance was obtained. It is concluded that probably either emission of zinc vapor or secondary electron emission is responsible for good breakdown. Other materials will be tried to verify which is the case.

The new switches for the 200-μf bank have been designed and are under construction. The new design utilizes solid insulation molded to fill all the region formerly pressurized with air. This should eliminate the previous breakdown problems while simultaneously providing the benefit of lower inductance since the insulation space was reduced. The material to be used is Silastic, a room-temperature-vulcanizing silicone rubber. For dc dielectric strength it seems about as good as any plastic except Mylar. Samples have been molded and tested here at 400 v/mil (over 0.2 in.), which substantiates the manufacturer's claim.

The 10-Inch Triax--Preliminary Operation

Since the switches for the large bank were further delayed, it was decided to drop the radiation experiments that had been occupying the old 100-μf bank and employ it for some preliminary measurements with the 10-inch Triax. It should be noted that with this setup, operating at 1.5×10^6 amp, the magnetic fields are about the same as in the old low-level magnetic-probe measurements. These, it will be recalled, were distinguished by the high degree of reproducibility of the discharge and the large number of oscillations of the initial shock wave back and forth through the plasma.[1] In the present experiment, when it is operated without preheating current (as with the "well-behaved" Triax), a similar voltage pattern is shown except for some small unexplained variations in oscillation amplitude. The spectrum was briefly studied and showed strong deuterium lines, with faint impurities. When the D_β line was observed with a photomultiplier, the intensity was seen to maximize reproducibility at the time of the first bounce, and again much later (during the second half-cycle of current). The amount of visible light indicates a low temperature, as expected.

---

[2] William R. Baker, in Controlled Thermonuclear Research Quarterly Report, UCRL-8682, March 1959, p. 54.

[3] William R. Baker, High-Voltage, Low-Inductance Switch for Megampere Pulse Currents, (UCRL-8414 Rev. Dec. 9, 1958), Rev. Sci. Inst. (to be published).

The tube has also been operated with a preheating pulse of 5×10^4 amp preceding the main discharge. Here the results were somewhat unexpected. At all the pressures investigated so far the voltage and photomultiplier signals show that the ensuing pinch is poorly formed and erratic. This was noticed previously with the 4-inch Triax when the main bank was fired during the preheat pulse,[4] but here the adverse effect is still observed when up to 1 msec intervenes. It is not possible to compare these directly with the previous results, which were obtained with a stronger magnetic field, lower pressure, and walls of silica rather than alumina. This situation is temporary because the high magnetic field will be attained when the 200-μf system is completed. A spark-type pre-ionizer currently being added should permit low-pressure operation, and high-purity alumina insulators are being prepared for the small Triax to allow a direct comparison of wall effects.

Ribbon Pinch

The Kerr-cell measurements with the $1/2\times2$-in. flat sheet pinch[4] were completed shortly after the preceding report was written. It was observed that the time for the ribbon width to become one-half the tube width was about five times the pinch time in the narrow direction. Unfortunately the last suitable piece of quartz tubing was inadvertently broken during a reassembly operation and magnetic probe measurements were not made. At any rate, the ribbon geometry seems sufficiently interesting for further study; hence a 1.5×8-in. version is under design.

Future Plans

In addition to the various specific plans for the next quarter that have already been mentioned, the over-all plans for the Berkeley pinch program warrant some discussion. In the introduction it was mentioned that there are two main lines of investigation here and that these may in the future be brought together. This is possible because the diagnostic program, which heretofore has been isolated from the high-energy research, may be extended by new techniques into the high-temperature realm; this will benefit both programs. The main problem in the high-temperature effort at present is to determine where the energy goes as the power level is increased, and why it goes where it does. The answers will most likely come from high-powered diagnostic techniques which arise from the second part of the program. Conversely, as the high-energy work becomes more successful the measurements made of the machine dynamics and so forth will become more interesting. (These might even become simpler in some respects; for example, the skin effect should be sharper and the magnetic boundary easier to define.) The techniques that make all this possible are only now becoming feasible. Larger magnetic (and acoustic) probes will survive higher-energy discharges, and only the new large machine can allow good resolution to be maintained. As another example, streak-camera studies have previously been impracticable with the Triax because, although its topology requires an end view, the length-to-diameter ratio was too large. This is not serious with the new tubes because only the diameter, not the length, was increased.

---

[4] Oscar A. Anderson, in Controlled Thermonuclear Research Quarterly Report, UCRL-8775, June 10, 1959, p. 49.

Finally, there is in the future a possible third line of research, namely the matter of utilizing the sheet pinch principle for plasma physics. It is true that many of the measurements made so far have been of interest only in direct relation to the Triax device. However, there may be certain investigations of general interest for which the sheet pinch is uniquely suited. For instance, investigations of propagation and reflection of microwaves through hot plasmas are difficult because of the complicated magnetic fields usually present. But the sheet pinch, especially the flat version, has the simplest possible confining field. This same property lends itself to experimental investigation of both sound-wave and Alfvén-wave propagation. An added attraction is that the calculations as well as the measurements are simplified. It is even possible that some problems can be readily studied theoretically in this geometry (and compared with experiment) which would be formidable in other devices.

HOMOPOLAR III DIAGNOSTIC STUDIES

Alexander Bratenahl and Klaus Halbach*

The Homopolar III probe signal studies have been continued with interesting results. When the outside electrode is an anode, the current density during the steady-state phase shows a remarkable band structure--rather equally spaced arcs run around the machine at the drift velocity of the plasma. They extend 2 cm in the direction of motion and some 50 cm perpendicular to this direction, i.e., along field lines. When the outside electrode is a cathode an entirely different effect is observed. Three components of the current can be distinguished: a steady component, probably ion current; very short, high spikes, probably cathode spots; and finally fairly regular pulses resembling the anode bands. The latter remain a complete mystery at present. None of the pulses appears to move more than a centimeter, if at all.

Further study of the outside anode condition was made with several new techniques. A double Langmuir probe placed very close to the outside gave a hint of an E_θ field that reverses sign as a band passes by. Although this is consistent with conditions making possible radial current spokes, the data are probably untrustworthy for the simple reason that any probe thrust into the plasma flow causes a serious and possibly not so local disturbance to the flow.

A pyrex rod was inserted through a hole in two of the current-measuring probes (current buttons). As the rod is thrust further into the plasma an increasing steady current is observed on the current button. This current is superimposed on the band structure, which remains essentially unchanged. This effect is strong at 30° to the equator, but at 60° is almost negligible by comparison. Since the initial charging-current pulse also shows this distribution, one may conclude almost certainly that practically all the plasma is confined in the equatorial region extending perhaps some 45° above and below the equator. This is a happy result if true (it should be confirmed by microwave transmission), as this at least follows from the basic design concept of the toroidal geometry. A simple calculation shows that indeed centrifugal forces alone could assemble a plasma disc in a time very short compared with the initial charging-current pulse. It seems possible, if not quite likely, that most of the drag in this machine occurs on the outside electrode rather than the axial insulator as in the disc homopolar. The boundary condition in this case is quite different, and one is led to suspect that Nature may be solving the radial boundary condition by breaking up the plasma into spokes, as in a paddle wheel.

In order to see how far inward (toward the cathode) the bands remain well-defined, a hollow ceramic tube closed at the outside end with a short quartz rod was inserted through a current button and viewed with a photomultiplier. Superimposed on the general light of the discharge, light flashes were clearly seen in coincidence with the passage of current bands over the

---

*Visitor from University of Freiburg, Freiburg, Switzerland.

current probe. The correlation persists with the tube thrust 2/3 of the way into the cathode; however, it is possible that the light is entering the sides of the translucent tube. An aluminum foil liner has been added to the tube and the experiment will be repeated.

Inserting a rod at 30° produces a steady current not only on its current probe but also a reduced contribution on the 60° current button, i. e., a current sheet approximately along a field line results. The current sheet should lie along a line at an angle to the direction of flow determined by a parameter depending upon the Alfvén speed, flow speed, and sound speed. It may be possible to deduce the temperature of the plasma from a study of this angle. A probe system has been constructed to explore the current sheet in greater detail.

VISCOUS EFFECTS IN HIGHLY IONIZED ROTATING PLASMAS[1]

Wulf B. Kunkel and Alan W. DeSilva

Of interest in the Homopolar program is the effect of viscosity on a rotating plasma. The walls of any of the rotating-plasma machines must hinder plasma flow adjacent to them, and it is desirable to determine the extent of this effect. Under the simplifying assumptions of steady-state laminar fluid flow and uniform viscosity, two extreme cases may be treated analytically. In the first, the flat-disc approximation, the flow is considered to be controlled by axial shear alone. If zero slip is assumed to exist at the insulating surfaces that confine the plasma axially, the current is shown to flow in a thin boundary layer, the thickness of which is of the order $\delta = (1/B)(\sqrt{\mu/\sigma})$. Consequently, the electrical resistance of the plasma appears many times that in the absence of the magnetic field. It also follows that the speed of rotation of the plasma in this case should be inversely proportional to the distance from the axis. These conclusions are partially supported by experimental evidence.

In the second case treated analytically, the long-cylinder approximation, only radial shear is considered important. In this case the current density is independent of the axial position. Here the apparent resistance is even higher because now all the current has to pass through regions of rapidly spinning plasma in whose frame of reference the electric field is very low. It is therefore practically impossible to construct a simple rotating-plasma machine whose volume resistance is lower than the resistance along the end plates. The obvious solution is to remove the plasma from the vicinity of the insulators. This is attempted in Homopolar III by placing the insulating surfaces parallel to the axis of the machine and utilizing centrifugal force to throw the plasma away from them. Another scheme which is now under

[1] A detailed report, W. R. Baker, A. Bratenahl, A. W. DeSilva, and W. B. Kunkel, Viscous Effects in Highly Ionized Rotating Plasmas (UCRL-8861, Aug. 1959), was presented at the IV International Conference on Ionization Phenomena in Gases, Uppsala, Sweden, August 1959.

consideration is to construct a long machine with insulators at the extreme ends. Initially a high vacuum is established and the radial electric field applied. The gas is then introduced near the center of the machine, and breakdown and rotation should occur before the gas ever reaches the insulating ends.

PIEZOELECTRIC PROBES

Alan W. DeSilva

In connection with the work with Homopolar II it was thought desirable to probe the rotating plasma disc directly to attempt to determine the radial and the z dependences of velocity. The piezoelectric ceramics now available seemed to offer a way to accomplish this. Attempts were made to mount a small disc of barium titanate (Brush Ceramic "A") at the end of a quartz tube to be inserted directly into the plasma stream. The results were not good, because of some persistent reflections. The scheme found most workable was to use an acoustic transmission line of fused quartz to transmit the pressure pulse to the outside of the machine. The quartz rod is supported tangentially to the rotating plasma disc, and a pressure pulse roughly proportional to ρv^2 is communicated to the rod. At a point outside the discharge region the ceramic element is inserted into the line and forms a part of the line. Contacts to the ceramic are made by painting the connecting ends of the line with silver conducting paint, and the electrical signal travels by means of a coaxial line to an oscilloscope. The acoustic line is long enough that reflections do not arrive back at the element until the phenomena of interest are past. With the rod inserted in the manner described, the plasma strikes the end moving parallel to the axis of the rod. However, back of the end, plasma hitting the side of the rod causes a shear wave to be generated. The element will respond to such a wave, so a quartz tube is placed around the rod in the discharge region to shield it from this force (see Fig. 16). Pressure rise times of about 3 μsec have been observed with the Homopolar machine. John S. Weir, working with a test pulser, has observed rise times of about 0.2 μsec, using a 0.5-mm-thick ceramic element.

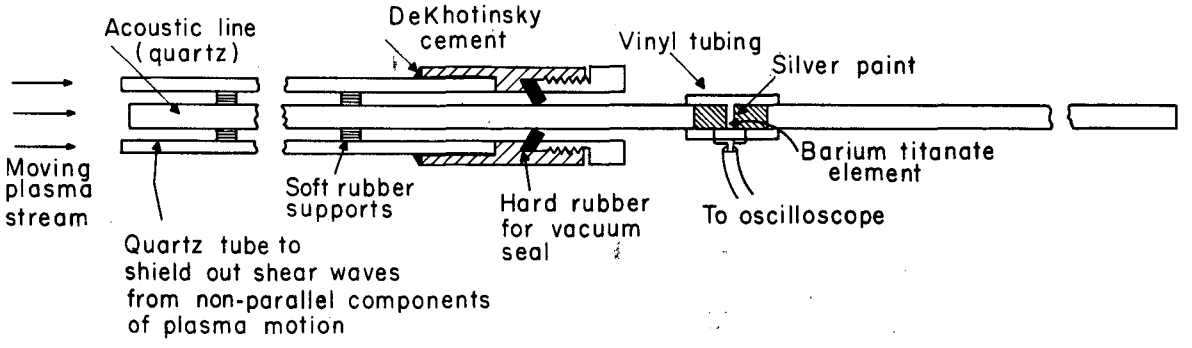

Fig. 16. Accoustic transmission line used for detection of transient pressures.

VI. THEORETICAL RESEARCH

SCATTERING LOSS RATE IN MIRROR GEOMETRY

David J. Berkowitz

Previous calculations[1, 2] using a direct numerical integration of the Fokker-Planck equation have yielded the loss rate of ions due to ion-ion interactions in a mirror geometry, but have assumed for ease in calculation that the mirror could be suitably approximated by a spatially homogeneous square-well system. Qualitatively, however, one expects that the loss rate for a mirror system that contains spatial variation will be markedly different. It is of interest to develop a method to obtain numerical values for the loss rate in a physical model which more closely approximates actual mirror spatial variation. Accordingly, the formulation of the problem has now been extended to include the effect of the spatial variation, by using the assumptions of adiabatic constancy of the magnetic moment and the integral invariant of the charged-particle motion in the magnetic field. Physically, the process consists of suitably time-averaging the scattering effects along a trajectory. A two-pronged series of numerical calculations is being carried out which bears on this general problem and which can be summarized as follows:

1. JUDY I, JUDY II, and JUDY III

The mirror system may be approximated by a series of stepwise increases in the magnetic field. In the limit of infinitely many such steps the mirror system is described smoothly. The loss rate in this composite system can be calculated by assuming that the asymptotic speed distribution has been reached and that the scatterers are isotropically distributed. Justification for this latter assumption for ion-ion scattering in a simple square-well model has been discussed elsewhere.[3, 4] For a Lorentz gas (i.e., a linear problem) the assumption is quite good. The angular effects of scattering in each region may be deduced by a modal expansion into Legendre functions appropriate for the boundary conditions--that is, the mirror ratio--of each region. The necessary Legendre functions do not exist in the literature. Accordingly, a machine calculation on the IBM 704, JUDY I, has been completed for the calculation of the solution to the Legendre equation for non-integral values of the index subject to the condition of symmetry at x = 0 and

---

[1] John E. Roberts, End Losses from Pyrotrons, UCRL-5132, Feb. 1958 p. 382.

[2] Marlene Carr and John E. Roberts, End Losses from Mirror Machines, UCRL-5651, Sept. 1959.

[3] A. Garren, R. J. Riddell, L. Smith, G. Bing, L. R. Henrich, T. G. Northrop and J. E. Roberts, in International Conference on the Peaceful Uses of Atomic Energy, 2d, Geneva, 1958, Paper No. 383, Vol. 31, p. 65.

[4] Judd, MacDonald, and Rosenbluth, End Leakage Losses from the Mirror Machine, WASH-289, June 1955, p. 158.

carried over the range from x = 0.00 to 0.99. The values of n for which the solutions have been calculated run from 0 to 36 according to the pattern

$$(x^2 - 1)\frac{d^2F_n}{dx^2} + \frac{dF_n}{dx} - n(n+1)F_n = 0, \qquad (1)$$

with increments as follows:

n	Δn
0 - 1	0.0625
1 - 10	0.1250
10 - 36	0.2500

This procedure for modal expansion of the scattering terms in each magnetic field region then allows spatial integration over the entire mirror system. The results permit the rather convenient expression of the angular behavior in velocity space as

$$\frac{dA_j}{dt} = \sum_k a_{jk} A_k + \sum_k \sum_p b_{jkp} A_k A_p, \qquad (2)$$

where A_j is the amplitude of the normalized Legendre function (symmetric) corresponding to the jth decay mode in a mirror system whose over-all loss cone cosine is

$$\mu_c = 1 - \sqrt{\frac{B(z = 0)}{B(z = z_{max})}}.$$

(In JUDY II and III the system is arbitrarily truncated at six modes.) The first term on the right-hand side is an approximation to scattering effects which are linear, such as would be encountered theoretically in a Lorentz gas, or, in practice, in an experiment such as the Gibson-Lauer experiment.[5] The second term on the right-hand side is an approximation to the nonlinear ion-ion interactions, such as would be encountered in a mirror system such as the Felix experiment. This term represents a suitable generalization of Reference 4 for a spatially inhomogeneous system. It is especially interesting that the terms a_{jk} and b_{jkp} are functions only of the spatial variation in the mirror. These may be called the geometric matrices for the mirror system. A code, JUDY II, is completed, and

[5] Gordon Gibson and Eugene J. Lauer, Containment Time of Mev Positrons in a Magnetic Mirror Machine, UCRL-5529-T (Abstract), March 1959.

calculations are in progress for the determination of the geometric matrices of the mirror system of the Gibson-Lauer experiment and of the mirror system described by

$$B = B_0 \left(1 - a \cos \frac{2z\pi}{a}\right), \tag{3}$$

where

$$\frac{B_m}{B_0} = \text{mirror ratio} = \frac{1 + a}{1 - a}$$

for mirror ratios of 1.5 and 3.

Having the geometric matrices of these mirror experiments, one can now calculate the time-dependent behavior of the angular distributions. A code, JUDY III, numerically integrates Eq. (2), using inputs from JUDY II, and a parametric study of mirror shapes is planned.

By means of these codes it is hoped that a suitable and reasonably accurate approximate description may be arrived at for mirror scattering loss rates. This series has the advantage of simplicity and requires little machine time.

2. JUDY IV

In a parallel approach the exact numerical computation of the ion-ion scattering effects as given by the Fokker-Planck equation is being made. Such a calculation uses in part the Alice code,[1, 2] applying Eq. (31) of Reference 6 in a slightly modified form. This modification, which is in the nature of a numerical approximation, reduces the machine time by a factor of approximately 10. Spatial magnetic field variation, revised boundary and stability conditions, source, and burnout have also been introduced. This code series is known as JUDY IV. The computations involving JUDY IV still, however, require a good bit of machine time, and the purpose of JUDY IV is to arrive at exact numerical solutions of the problem providing inputs for the engineering approach taken in the series JUDY I, II, and III. JUDY IV, in addition, includes features that make it applicable to variations of the mirror-containment system.

3. Modal Equations

A totally separate approach to the solution of the Fokker-Planck equation is under way as well. Calculations have been made to reduce the two-component Fokker-Planck equation to a set of coupled equations in speed under the assumption that the scatterers are isotropically distributed. These represent in fact a specialization of coupled equations given by Judd et al.[6] and an extension of the method of Garren et al.,[3] and are being programmed by John Killeen for application to mirror and other programs.

---

[6] Judd, MacDonald, and Rosenbluth, Fokker-Planck Equation for an Inverse-Square Force, Phys. Rev. 107, (1957).

THE SLOWING DOWN OF FAST IONS IN A PLASMA

Warren Heckrotte and John Killeen

The theory of the build-up of a plasma by means of high-energy injection into a mirror machine has been studied by a number of individuals. These treatments usually neglect the energy loss of the trapped ions during the build-up due to their interaction with the electrons of the plasma and of the arc used to dissociate the injected molecular ions. The results of the generalization of the build-up equations to include the effect of energy loss to the arc are given elsewhere in this report; it was found that this energy loss dominated the build-up to a considerable extent. Since the arc electrons are not, as a group, heated up by this process, it was felt that the energy loss to the plasma electrons could be neglected at this stage of the calculations. We now propose to extend the calculations to study the effect of the energy loss to the plasma electrons. A theoretical description of the interaction of the ions and electrons between themselves is given by the Fokker-Planck equation. The scheme by which these equations are solved numerically is given below. Out of a full treatment of this problem would come the electron and ion energy distributions, and the time to achieve steady-state conditions.

Initially we propose the simpler problem of the interaction of an isotropic distribution of ions and electrons, the electrons initially having an energy of about 10 ev and the ions having an energy of about 100 kev. The problem can be further simplified initially by neglecting the energy loss of the ions until the electrons have picked up a mean energy of 1 or 2 kev. With this electron distribution as an initial electron distribution, the slowing down of the ions can then be followed.

Richard F. Post has conjectured that the rate of energy loss of the ions to the electrons will be lower than the usually stated value because of the action in which the very-low-energy electrons are scattered by ions to higher energies faster than they diffuse downward in energy to fill this hole in the distribution. Although very simple estimates suggest there is little or no effect here, more detailed--but still approximate--calculations by Post suggest that the ion energy loss rate will be decreased by a factor of 2 to 4. Whether or not this is so should come directly out of our calculations. Furthermore, to the extent that we can initially neglect the ion energy loss, the effect of large energy transfers to individual electrons by ions--neglected in the Fokker-Planck formulation--can be included easily in the numerical treatment.

DION - A plasma Fokker-Planck Equation Code

In studying such problems as the energy loss of hot ions in a magnetic mirror machine, the most suitable mathematical description is by means of the Fokker-Planck equations for the ions and electrons of the plasma. This is because the dominant mechanism for energy transfer between particles is by long-range Coulomb interactions. The Fokker-Planck equations for the distribution functions of ions and electrons where the two-body force is an inverse-square law has been derived.[1]

[1] M. N. Rosenbluth, W. M. MacDonald, and D. L. Judd, Phys. Rev. 107, 1 (1957).

Some numerical solutions to the Fokker-Planck equation for one species of particle have been obtained.[2] Recently an IBM 704 code for the solution of the two coupled equations for ions and electrons has been completed by Oak Ridge theoretical group.[3] In this treatment the differential equations are solved by solving a set of explicit difference equations. They also use two grid sizes in the energy variable. In replacing partial differential equations by explicit difference equations a severe restriction is imposed on the size of the time step that can be used.[4] To avoid this difficulty the code to be described employs an implicit difference scheme. A variable energy mesh size is also used.

Consider the equation for the ion-distribution function,

$$\frac{\partial f_+}{\partial t} = A_1(f_+, f_-, x, t)\frac{\partial^2 f_+}{\partial x^2} + B_1(f_+, f_-, x, t)\frac{\partial f_+}{\partial x} + C_1(f_+, f_-, x, t);$$

$$0 \leqslant x < \infty, \quad t \geqslant 0.$$

A similar equation can be written for the electron distribution function f_-. In this equation x is the energy variable and t is the time.

Consider the x - t mesh shown below.

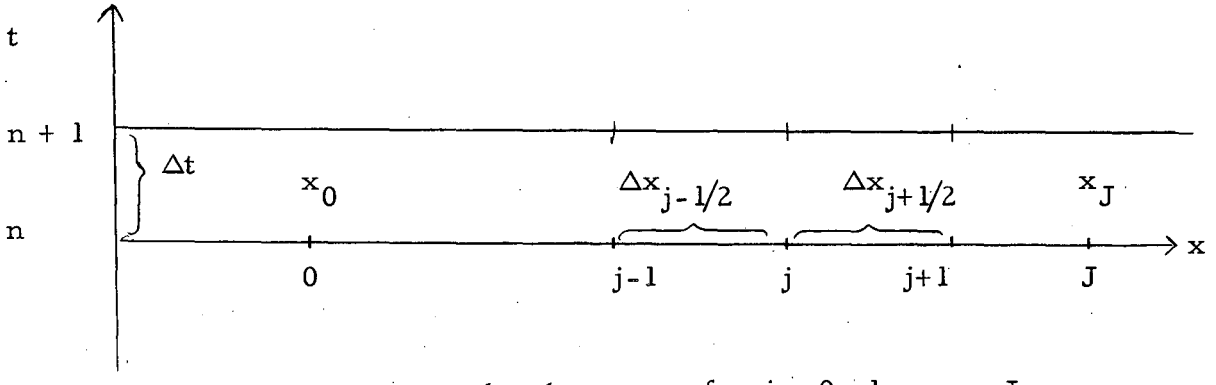

$$x_0 \leqslant x \leqslant x_J, \qquad \text{for } j = 0, 1, \ldots, J.$$

Let $\Delta x_j = \frac{1}{2}(\Delta x_{j-1/2} + \Delta x_{j+1/2})$.

---

[2] W. M. MacDonald, M. N. Rosenbluth, and W. Chuck, Phys. Rev. 107, 350 (1957); J. E. Roberts et al., International Conference on the Peaceful Uses of Atomic Energy, 2d, Geneva, 1958, A/Conf. 15/P 383 (United Nations, New York, 1959).

[3] T. K. Fowler, F. M. Rankin, and A. Simon, Boundary Conditions and Conservation Properties of FOPP, a Plasma Fokker-Planck Code, ORNL 59-2-75.

[4] R. D. Richtmyer, Difference Methods for Initial Value Problems (Interscience Publishing Co., New York, 1957).

We define

$$(\delta^2 f)_j^n = \frac{\Delta x_{j-1/2} f_{j+1}^n - 2\Delta x_j f_j^n + \Delta x_{j+1/2} f_{j-1}^n}{\Delta x_{j+1/2} \Delta x_{j-1/2} \Delta x_j} ,$$

$$(\delta f)_j^n = \frac{f_{j+1}^n - f_{j-1}^n}{2\Delta x_j} ,$$

$$A_j^n = A(f_j^n, x_j, t_n), \text{ etc.}$$

The implicit difference equation to be solved is

$$\frac{f_j^{n+1} - f_j^n}{\Delta t} = \frac{1}{2} \left\{ A_j^{n+1} (\delta^2 f)_j^{n+1} + B_j^{n+1} (\delta f)_j^{n+1} + C_j^{n+1} \right.$$

$$\left. + A_j^n (\delta^2 f)_j^n + B_j^n (\delta f)_j^n + C_j^n \right\} .$$

In the case of two species of particles, then, there is another such equation which must be solved simultaneously. In solving an implicit difference equation the set f_j^{n+1}, $j = 0, 1, \ldots J$, must be solved all at once. If the A_j^{n+1}, etc. are extrapolated from the A_j^n, etc., then the system is a linear set of equations for f_j^{n+1}. After the f_j^{n+1} have been obtained in this manner the functions A_j^{n+1}, etc. can be re-evaluated in terms of the f_j^{n+1} and the linear equations solved again for a second iterate. In this manner an iterative solution can be obtained to the nonlinear difference equations.

The solution to the linear equations is obtained by the following method. Let

$$a_j^{n+1} = \frac{\Delta t}{2} \left[\frac{A_j^{n+1}}{\Delta x_{j+1/2} \Delta x_j} + \frac{B_j^{n+1}}{2\Delta x_j} \right] ,$$

$$\beta_j^{n+1} = \frac{\Delta t\, A_j^{n+1}}{\Delta x_{j+1/2}\, \Delta x_{j-1/2}} \quad ,$$

$$\gamma_j^{n+1} = \frac{\Delta t}{2}\left[\frac{A_j^{n+1}}{\Delta x_{j-1/2}\Delta x_j} - \frac{B_j^{n+1}}{2\Delta x_j}\right] \quad ,$$

$$\delta_j^{n+1} = \frac{\Delta t}{2}\left[C_j^n + C_j^{n+1}\right] \quad ,$$

$$\psi_j^n = -\alpha_j^n f_{j+1}^n - (1 - \beta_j^n) f_j^n - \gamma_j^n f_{j-1}^n - \delta_j^{n+1} \quad .$$

Then the difference equation becomes

$$\alpha_j^{n+1} f_{j+1}^{n+1} - (1 + \beta_j^{n+1}) f_j^{n+1} + \gamma_j^{n+1} f_{j-1}^{n+1} = \psi_j^n \quad ,$$

$$\text{for } j = 1, \ldots, J - 1.$$

This system of equations must be solved for f_j^{n+1}.

Let

$$f_{j-1}^{n+1} = e_{j-1}^{n+1} f_j^{n+1} + d_{j-1}^{n+1} \quad ; \qquad (1)$$

then the difference equation becomes

$$\alpha_j^{n+1} f_{j+1}^{n+1} - (1 + \beta_j^{n+1}) f_j^{n+1} + \gamma_j^{n+1} e_{j-1}^{n+1} f_j^{n+1} + \gamma_j^{n+1} d_{j-1}^{n+1} = \psi_j^n$$

or

$$f_j^{n+1} = \frac{a_j^{n+1} f_{j+1}^{n+1} + \gamma_j^{n+1} d_{j-1}^{n+1} - \psi_j^n}{1 + \beta_j^{n+1} - \gamma_j^{n+1} e_{j-1}^{n+1}}$$

Hence

$$\left.\begin{aligned} e_j^{n+1} &= \frac{a_j^{n+1}}{1 + \beta_j^{n+1} - \gamma_j^{n+1} e_{j-1}^{n+1}} \\ d_j^{n+1} &= \frac{\gamma_j^{n+1} d_{j-1}^{n+1} - \psi_j^n}{1 + \beta_j^{n+1} - \gamma_j^{n+1} e_{j-1}^{n+1}} \end{aligned}\right\}, \quad \text{for } j = 1, \ldots, J-1. \tag{2}$$

The computation procedure is to compute e_0^{n+1}, d_0^{n+1} from the boundary condition x_0, then compute the

e_j^{n+1}, d_j^{n+1} by using Eq. (2), which is a recursion formula.

The value f_J^{n+1} is obtained from the boundary condition at x_J. The remaining f_j^{n+1} are then computed on a backward sweep by using the recursion formula (1).

If we take as boundary conditions

$$\left.\frac{\partial f}{\partial x}\right|_{x=x_0} = 0 \qquad \text{and } f(x_J, t) = 0,$$

then

$$e_0^{n+1} = 1, \; d_0^{n+1} = 0 \text{ and } f_J^{n+1} = 0.$$

We can apply the code described to many physical situations in plasmas.

SHIELDING AGAINST MAGNETIC RADIATION LOSS FROM A HOT PLASMA

James Paul Wesley

A paper of this title has been issued as UCRL-5606, June 1959; the abstract is as follows:

Classical electromagnetic theory indicates that a conducting metallic shield can reduce the magnetic radiation loss from a hot plasma (centrally located) undergoing D-D burn to less than 1%, or by two orders of magnitude.

VII. BASIC EXPERIMENTAL RESEARCH

EXPERIMENTS WITH PARTIALLY IONIZED GASES

T. K. Allen,* M. C. Horton, George A. Paulikas, Robert V. Pyle, and Ferd Voelker

Several experiments that involve partially ionized gases are being worked on, partly for their intrinsic interest and partly to aid in the evaluation of phenomena occurring in the devices that produce warm, fully ionized plasmas. Two of these experiments are as follows.

Diffusion of Plasma Across a Magnetic Field

The recent paper by Lehnert[1] has again raised the problem of enhanced diffusion of plasma across a magnetic field. This is a problem close to the hearts of Sherwood physicists, and in its present form provides an opportunity to measure plasma phenomena that is not ordinarily available in a pinch program.

The controversy started with observations by Bohm et al.[2] that the experimental spreading of the plasma around an arc column implied a diffusion constant more than two orders of magnitude larger than that predicted by ambipolar diffusion theory for a plasma in a magnetic field, namely

$$D_{\perp amb} \approx 2D_{-\perp} = 2\frac{D_-^0}{1+(\omega_-\tau_-)^2} ,$$

where D_-^0 is the diffusion constant for electrons in the absence of a magnetic field. Bohm suggested that the electric fields associated with plasma oscillations enhanced the diffusion rate. This conclusion was criticized by Simon,[3] who calculated that in a typical arc experiment the diffusion should not be ambipolar although the diffusion coefficient is still proportional to $1/B^2$. The ions and electrons can diffuse at their own intrinsic rates because the space charge can be neutralized by currents flowing along magnetic field lines to conducting end plates. Simon's calculated diffusion rates, without plasma oscillations, are in agreement with experimental results of Neidigh[4] and also those of Bohm. Simon pointed out that ambipolar diffusion should be restored if the discharge had sufficient length in the direction of the magnetic field or if the end plates were insulators--adding, however,

---

*Visiting Lawrence Radiation Laboratory from AERE, Harwell.

[1] B. Lehnert, United Nations International Conference on the Peaceful Uses of Atomic Energy, 2d, Geneva, 1958 (United Nations, New York, 1959), A/Conf. 15/P/146, Vol. 32, 349.

[2] D. Bohm, E. H. S. Burhop, H. S. W. Massey, and R. M. Williams in The Characteristics of Electrical Discharges in Magnetic Fields ed by A. Guthrie and R. K. Wakerling (McGraw-Hill Book Company, New York, 1949).

[3] A. Simon, Phys. Rev. 98, 317 (1955).

[4] Albert Simon and R. V. D. Neidigh, Diffusion of Ions in a Plasma Across a Magnetic Field, ORNL-1890, July 1955.

that perfect insulators do not exist. For a positive column, and in low values of magnetic field, there are definite relations between such parameters as rate of ion production, wall losses, diffusion coefficient and longitudinal electric field. Bickerton and von Engel[5] showed that the variation of these parameters with magnetic field was compatible with theory.

Lehnert extended this work to higher values of magnetic field and showed that at fields higher than a few thousand gauss the longitudinal electric fields showed a marked increase and that there was an associated increase in intensity of electric noise (5000 cps and 10,000 cps). His conclusion was that the diffusion coefficient followed the value given by binary collision theory up to an initial magnetic field, but at higher fields the particle losses were more characteristic of "drain" diffusion.

The Berkeley experiment is similar to Lehnert's except that the tubes are somewhat shorter. The observations are more extensive in that several gases are used, the noise is observed over a greater frequency spectrum, the light output is monitored with photomultipliers, and a number of electrode configurations are used.

The geometry is shown in Fig. 17. Seven electric probes permit measurements of the axial electric field gradient with electrostatic voltmeters. Noise emitted by the discharge is measured at several positions along the tube as a function of B. Capacitive and inductive pickups are used, the signal being detected by a USN URM-6B receiver (14 to 250 kc). Photomultipliers view the discharge at points inside and outside the magnetic field, which has a maximum value of 3200 gauss with the power supply currently available. Bare filaments and indirectly heated cathodes have been used and the gas flows through the system continuously. Discharge currents from 50 to 500 ma have been used.

Figure 18 shows the behavior of a 19-mm (i. d.) tube containing He at 330μ pressure. At a magnetic field strength of about 920 gauss the slope of the curve for E vs B changes sign, and the amplitude of the noise detected by a capacitive pickup probe along the outside of the tube from cathode to anode increases at the cathode end of the magnet and remains approximately constant up to the anode. Qualitatively the various gases behave in the same way, but it is found that the change in noise amplitude at the critical magnetic field is strongly dependent on the pressure and nature of the gas. This change is large when the positive column is normally uniform and small in a normally striated column. In either case there is a noticeable change in striation pattern. The results are not appreciably affected by an order-of-magnitude change in current. The strength of the magnetic field, B_c, at which the behavior of the discharge changes is plotted as a function of pressure in Fig. 19 for the electric field measurements and in Fig. 20 for the electrical noise measurements. Lehnert's points are included for comparison. Preliminary data have been obtained in a 55-mm tube (i. d.) with similar results.

[5] R. J. Bickerton and A. von Engel, Proc. Phys. Soc. B69, 468 (1956).

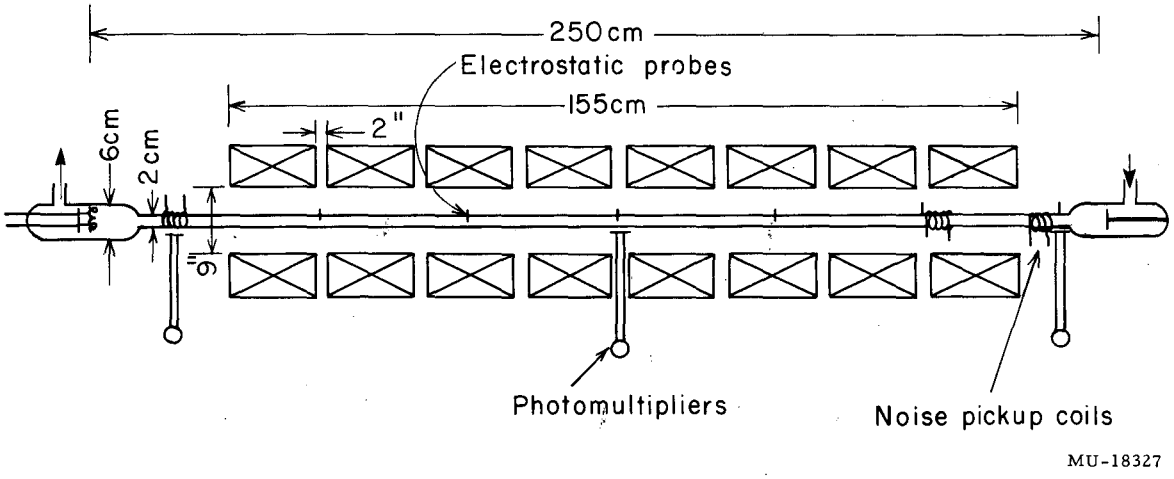

Fig. 17. Apparatus for diffusion experiment.

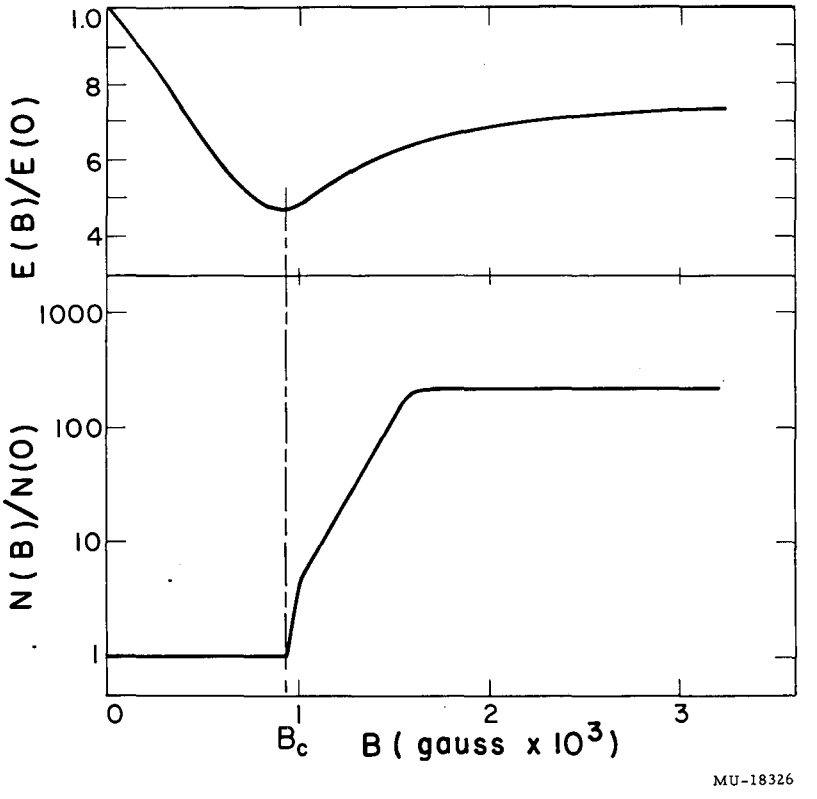

Fig. 18. Electric field and 125-kc noise voltage vs B for 330 μ He.

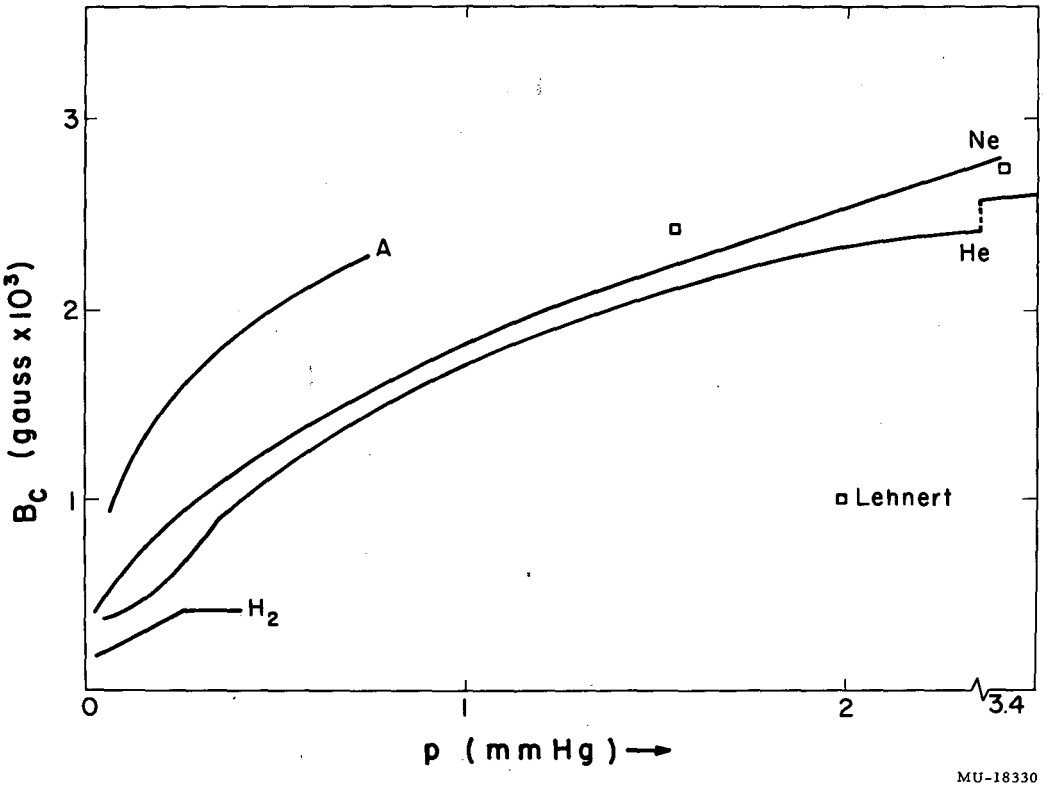

Fig. 19. B_c of electric field vs pressure, for various gases.

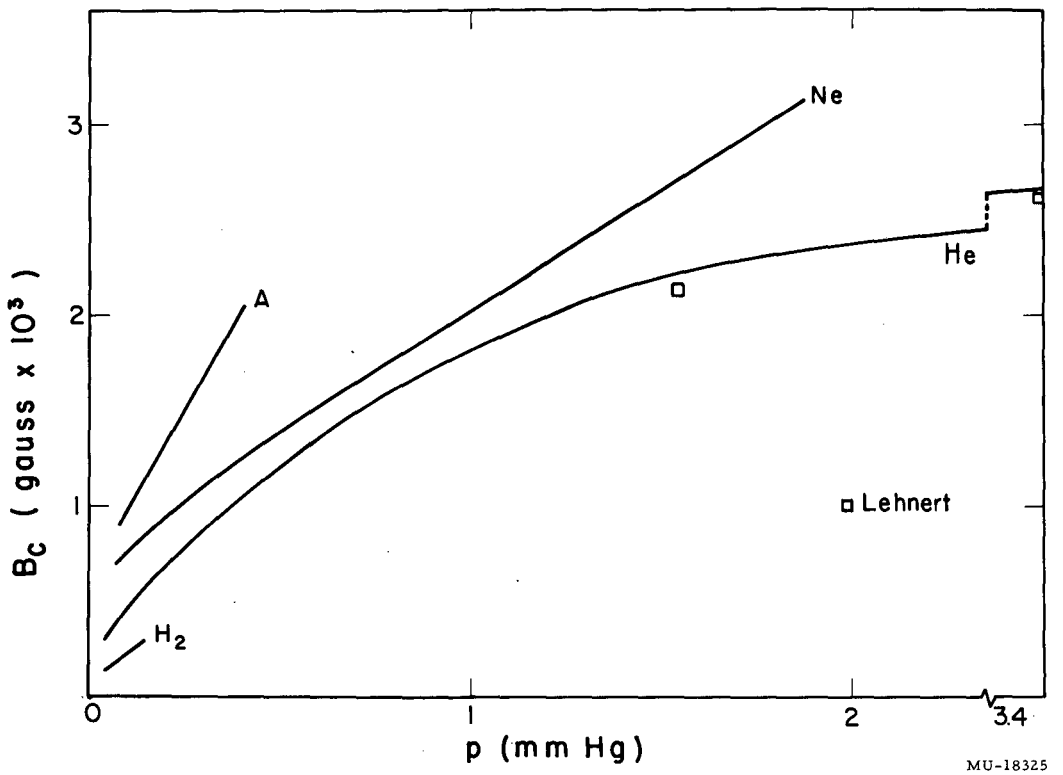

Fig. 20. B_c of 125-kc noise vs pressure, for various gases.

The results of Lehnert have thus been verified and extended, although no mechanism for the enhanced plasma losses has been discovered yet. The association with striations, of the moving variety, is significant although the lack of a complete theory of plasma economics in the presence of striation makes it difficult to decide what part the striations play in the observed effects. Other mechanisms may be responsible for the enhanced diffusion, real or apparent--e. g., noise generated at the transverse magnetic field region where the tube enters the magnet.

Present experiments include placing the electrodes inside the magnet, changing their shape so that the magnetic field lines cut them in different ways inside the magnet, measuring the electric field gradient when the gas current is modulated by externally generated noise, probing the electron density and radial electric field distributions, and attempting to observe the propagation of noise down the tube. It is also hoped the use of a subsidiary discharge at the anode will reduce or remove the normal anode oscillations, which certainly tend to confuse the picture, if not otherwise affect the measurements.

No claim is made by us that similar phenomena occur in more fully ionized gases.

Microwave Diagnostics

PIG Discharge Measurements

Microwaves with wave lengths of 1 cm and 8 mm have been propagated through a high-density plasma produced in a cylindrical PIG discharge tube with a maximum axial magnetic field of 2 kilogauss. In an attempt to provide a fairly clean experimental situation, the circular anodes have been replaced by discs having 1×2.5-in. rectangular apertures to produce a plasma with approximately plane faces (Fig. 21). Probe measurements are presently in progress to determine the rate at which the plasma diffuses beyond the region defined by the geometry of the anodes. With the microwave E field parallel to the static B field, the phase-shift presentation appears to be reasonable with cutoff easily reached in the noble gases. When the E field is perpendicular to the static B field an apparent stop band is observed at low densities, the transmission resuming at higher densities. No such stop band is predicted for the cyclotron frequencies existing in this device, and it will probably turn out to be instrumental rather than real. This experience at least demonstrates the desirability of having rather simple plasma devices available to aid in checking diagnostic techniques. Lester J. Hadley and J. Warren Stearns have participated in this experiment.

Microwave Diagnostics Equipment

The 8-mm microwave diagnostics equipment currently in use was designed on the same principle of operation as that of Wharton.[1] The object of the system is the measurement of phase shift occurring in a plasma. The

[1] C. B. Wharton, Microwave Diagnostics for Controlled Fusion Research, UCRL-4836 (Rev), Sept. 1957.

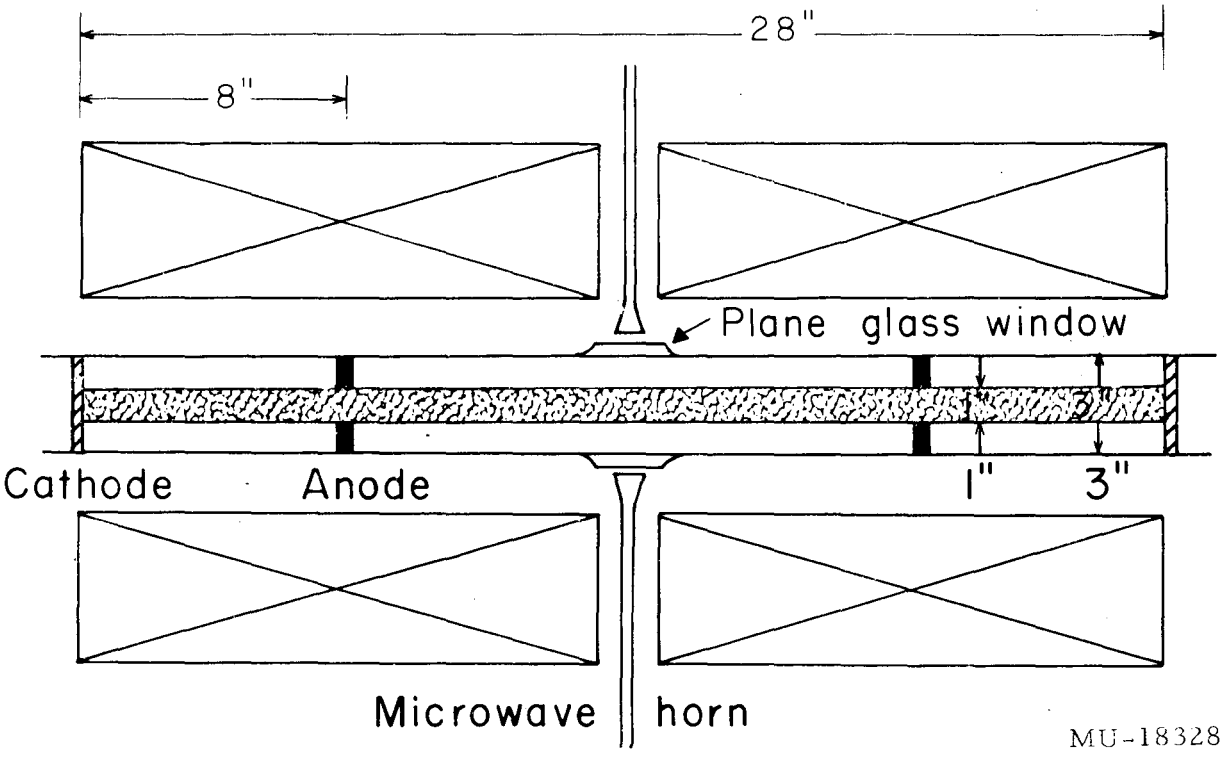

Fig. 21. PIG discharge apparatus.

8-mm source is a klystron whose repeller is sawtooth-swept at a 20-kc rate through about 50 Mc frequency change. The source power out of the klystron is split into two separate waveguide arms and then brought together in a magic-T balanced detector. One of the two arms contains approximately 1000 wavelengths of delay plus the plasma phase shift, whereas the other arm contains only about 30 wavelengths. Thus an interference, or beat frequency corresponding to the difference in the klystron frequency due to the delay time difference is produced in the detector. This beat frequency is approximately 40 kc and carries the same plasma phase shift as the original 8 mm wave. Presentation is made on an oscilloscope as a series of "interference" fringes for a pulsed plasma arc.[1]

The problem with this type of system arises from the fact that the klystron repeller must be swept over most of its mode in order to achieve a high enough beat frequency. This means (1) that the power output and (2) the beat frequency vary considerably with each saw-tooth period. Also, any unbalance in the dual crystal detector will allow the mode shape to produce a non-zero base line for the beat frequency. The result of all these variations is to produce "fringes" on the oscilloscope of varying width and to allow the amplitude of some "fringes" within the saw-tooth period to decrease. A system without this disturbing feature would constitute an improvement.

One system which has been used at lower carrier frequencies requires no klystron repeller modulation. However, it is necessary to produce a single sideband modulation (i. e., a frequency shift) of the klystron carrier frequency, and this is difficult to achieve at 8 mm. Some tests were performed on a two-crystal single sideband modulator using a 30 mc shift frequency; however, the leak-through power at the carrier and image frequencies is only about 4 db below the desired shifted frequency, and further discrimination would render the system extremely sensitive to frequency changes. Therefore this method has been abandoned, at least temporaily, for lack of a practical method of achieving single sideband modulation at 8 mm.

Another system was devised using a phase-locked servo loop. The klystron repeller voltage is varied to produce a frequency change, and the frequency change produces an interesting phase shift in the thousand-wavelength path difference of the microwave interferometer. Thus an error voltage is produced which is amplified, integrated, and reapplied to the repeller to nullify the error voltage. The repeller voltage can be calibrated as a direct measure of phase shift for any "average" carrier frequency. This system is very similar to the one currently in use; however, it is capable of eliminating the aforementioned malfeatures, since it is now possible to servo in amplitude the klystron grid. The presentation will be different, and can be given as a single curve for phase shift --and(or) amplitude--versus time on a scope, recorder, or meter. Phase-shift accuracy should be much better than in the current system. One problem arises from the number of wave lengths (N) of delay required to allow the number of 2π fringe shifts ($\Delta\phi/2\pi$) expected in some of the diagnostic applications. For $\Delta\phi/2\pi = 5$, which is the order of fringes required for plasma cutoff in the present "little pig" experiments, and for a total repeller frequency variation within the mode of 33 Mc ($f/\Delta f = 10^3$), the number of wave lengths of delay required is

$$N = \left(\frac{\Delta\phi}{2\pi}\right)\left(\frac{f}{\Delta f}\right) = 5\times10^3,$$

which is a delay length of about 59 meters. However, some relief may be offered in the fact that a direct phase shift in klystron output results when the repeller voltage is changed.

A transistorized differential integrating amplifier is now being tested for use in this system. When it is completed, tests will be made using the present 40-ft delay line to establish the amount of phase shift that can be compensated with this system. A 30-cm amplitude modulation may also be used in the plasma arm of the interferometer to eliminate the dc amplification required in the unmodulated system. The conversion efficiency of a single-crystal amplitude modulator at 30 Mc was established as -4 db. A 30-Mc IF amplifier has been ordered for use with this system. It is expected that the dc system can be tested within 2 weeks.

A transistorized differential integrating amplifier is now being tested for use in this system. When it is completed, tests will be made using the present 40-ft delay line to establish the amount of phase shift that can be compensated with this system. A 30-cm amplitude modulation may also be used in the plasma arm of the interferometer to eliminate the dc amplification required in the unmodulated system. The conversion efficiency of a single-crystal amplitude modulator at 30 Mc was established as -4 db. A 30-Mc IF amplifier has been ordered for use with this system. It is expected that the dc system can be tested within 2 weeks.

Microwave Components

A polarization rotator is being developed, using the TE mode in a circular guide. This is for use in diagnostics so that linear polarization may be readily rotated by simple rotating a section of circular guide without having to disconnect and physically rotate the plane of rectangular waveguide. A rectangular-to-circular guide section has been fabricated and is presently being matched. A matched termination for the circular guide has been built. There remains to be designed the 90-deg and 180-deg differential phase shifters and the mechanics of the rotating section.

Preliminary Microwave Transmission Tests Made on Triax Geometry

RG-96/U 8-mm rectangular waveguide was soldered into the outer brass cylinder (i. d. = 110 mm) of the Triax discharge tube to make preliminary tests on microwave transmission and reflection. The results are only qualitative, but give an indication of the type of tests that may be practical with this discharge geometry.

The polarization of the waveguides is parallel to the cylinder axis, and two of the guides are located diametrically opposite on the cylinder. The third guide is in the same plane as the other two and is oriented at an angle of about 10 deg to one of them (170 deg to the other). A center rod of 38 mm o. d. (the same as is used for the center conductor of the Triax) was inserted, and transmission between the diametrically opposite guides was checked.

The transmitted signal strength was reduced by a factor of 1/2 when the center conductor was inserted, showing that there is considerable diffraction around it. Inserting intermediate-diameter brass and dielectric tubes (between center and outer conductor) produced both phase and amplitude variations that were highly dependent upon position, indicating a high degree of multiple reflections. The reflection from the center conductor back into the waveguide oriented at 10 deg to the input guide was next checked and found to be quite high, but highly sensitive to the exact position of the center conductor. The same was true of the intermediate-diameter brass and dielectric tubes. A phase shift is always directly associated with a small motion of the tubes toward the waveguide openings. Bench work is continuing in the hope that plasma cutoff density measurements and time-resolved determinations of the radial position of the current sheath in the Triax will prove feasible.

HYDROMAGNETIC WAVE STUDIES

John M. Wilcox, Forrest I. Boley,* and Alan W. DeSilva

Hydromagnetic wave properties such as velocity, attenuation, impedance, and energy transfer have been measured in a cylindrical plasma. Our experimental results have been compared with theoretical discussions of Alfvén-wave propagation under similar conditions given by Newcomb[1] and by Lehnert.[2] Our analysis is given in terms of only the lowest-order mode.

The geometry of the apparatus used in these experiments is shown in Fig. 22. A 5-3/4-in. (i.d.) 34-in.-long copper cylinder is placed in a uniform axial magnetic field of the order of 10 kilogauss. At each end of the cylinder is a pyrex insulator in which is mounted a coaxial electrode 2-in.-in diameter and 2 in. long. After evacuation to approximately 0.6 μ Hg, hydrogen gas is allowed to flow through the cylinder at a pressure of 100μ Hg (7.1×10^{15} protons/cm^3). The equilibrium pressure is monitored with a Pirani gage which is periodically calibrated by use of a McLeod gage. The voltage on each electrode is measured with a resistive divider, and the results are presented on a dual-trace oscilloscope.

Plasma Preparation

The gas is ionized by discharging a 45-μf "slow" condenser bank between the two center electrodes. The resulting current and voltage wave forms are displayed in Fig. 23. The (inductive) impedance of the external circuit is larger than the impedance of the tube, so that while the condenser bank is charged to 10 kv, only 2 kv appears across the tube. The ionization mechanism is not well understood, and has not been studied in this experiment. After the plasma has been formed by the slow bank, a 0.2-μf fast

*Summer visitor from Wesleyan University, Middletown, Conn.

[1] W. A. Newcomb, Magnetohydrodynamics (Stanford University Press, Stanford, 1957), p. 109.

[2] B. Lehnert, Plasma Physics on Cosmical and Laboratory Scale. Nuovo cimento (to be published).

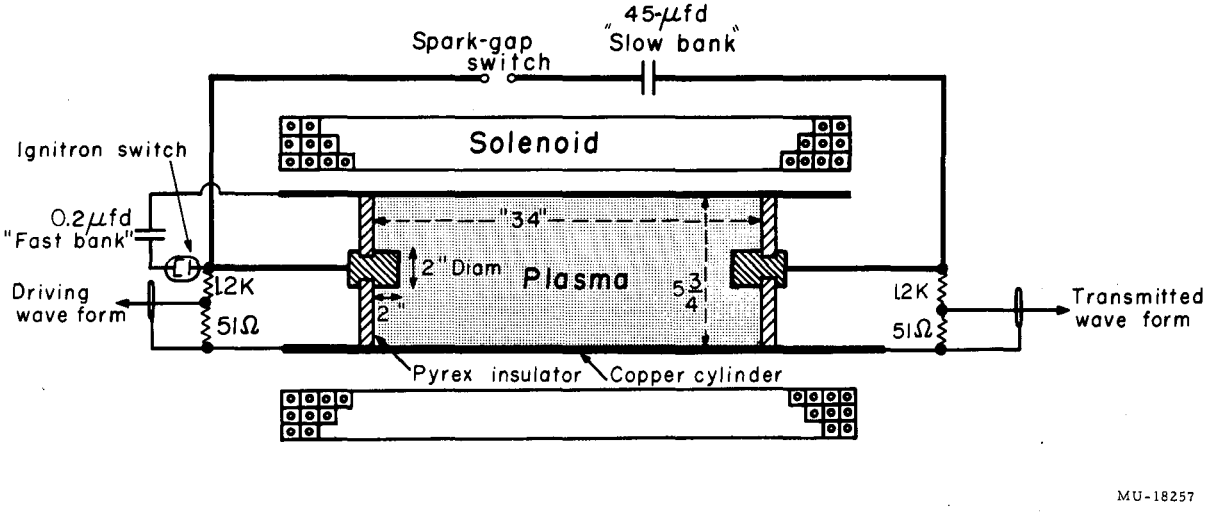

Fig. 22. Experimental geometry.

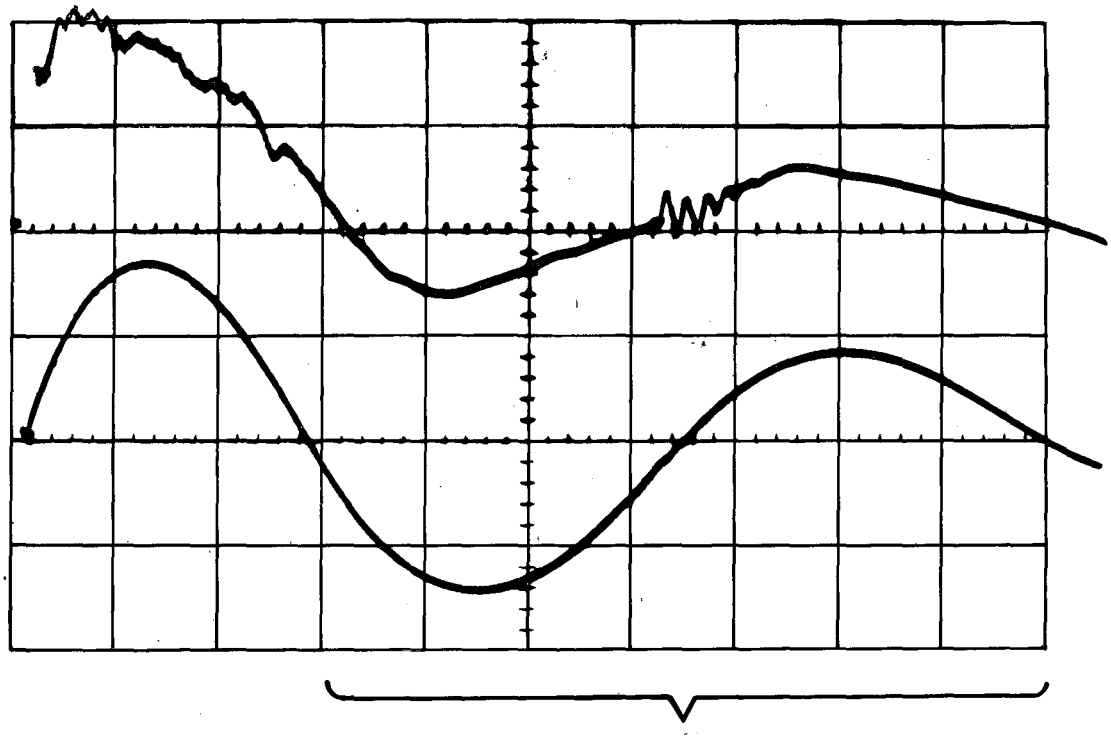

MU-18302

Fig. 23. Slow-bank voltage and current. Horizontal scale 10 μsec per large division. Top trace is voltage between the center electrodes at 1000 v per large division. Bottom trace is current at 40 ka per large division.

condenser bank is discharged between one electrode and the outer cylinder. This voltage creates a radial electric field at one end of the plasma which induces the hydromagnetic wave. The resulting voltage wave forms on the sending and receiving electrodes are displayed in Fig. 24.

The wave has been propagated at various times after the slow bank has been fired, as indicated by the bracket on Fig. 23. The fast bank was fired at approximately 65 μsec for this figure. At the earliest times (before the bracket) the traces are hashy and the Alfvén wave cannot be distinguished. Over a range of 70 μsec the measured wave velocity is essentially constant, as shown in Fig. 25, which indicates that the density ρ in the equation for the Alfvén velocity,

$$v_A = B_0/\sqrt{4\pi\rho} \quad , \tag{1}$$

is not changing during this time. The measured wave velocity is shown in Fig. 26 as a function of the fast-bank voltage. Since the velocity is constant over the range from 4 to 16 kv the density ρ in Eq. (1) is not changing due to ionization or other effects of the fast-bank voltage. As the slow-bank voltage is increased the measured wave velocity decreases. This is apparently caused by evolution from the tube walls. Since this effect has not been measured quantitatively, and since the percentage ionization has not been independently determined, the density ρ in Eq. (1) is computed from the observed wave velocity.

Velocity

The wave velocity was determined as a function of B_0 from dual-beam oscilloscope traces of driving and received voltage wave forms similar to those in Fig. 24. The resulting velocities are plotted in Fig. 27. The dependence of wave velocity on B_0 is very nearly that predicted from Eq. (1), although the dashed "best-fit" straight line extrapolates to a nonzero velocity intercept. The cause of this nonzero intercept is not known.

The plasma density can be evaluated from the measured wave velocity at a particular magnetic field. At B_0 = 10 kilogauss, $v_A = 2.8\times10^7$ cm/sec yields $\rho = 1.02\times10^{-8}$ g/cm^3, which is 6.1×10^{15} protons/cm^3.

Attenuation

The ratio of the received to driving wave voltage as measured between the center electrode and the outer cylinder is plotted as a function of magnetic field in Fig. 28. The solid curve is a plot of the function $e^{-\epsilon L}$, where ϵ is the theoretically determined attenuation factor and L is the length of the tube. The curve is normalized to fit the experimental data at 12 kilogauss. We may note that if the damping caused by ion-neutral collisions can be made negligibly small, the transverse conductivity can be calculated from the observed attenuation and thus the electron temperature can be determined from a theoretical discussion of conductivity such as that given by Spitzer.[3]

[3] L. Spitzer, Jr., Physics of Fully Ionized Gases (Interscience Publishers, Inc., New York, 1956).

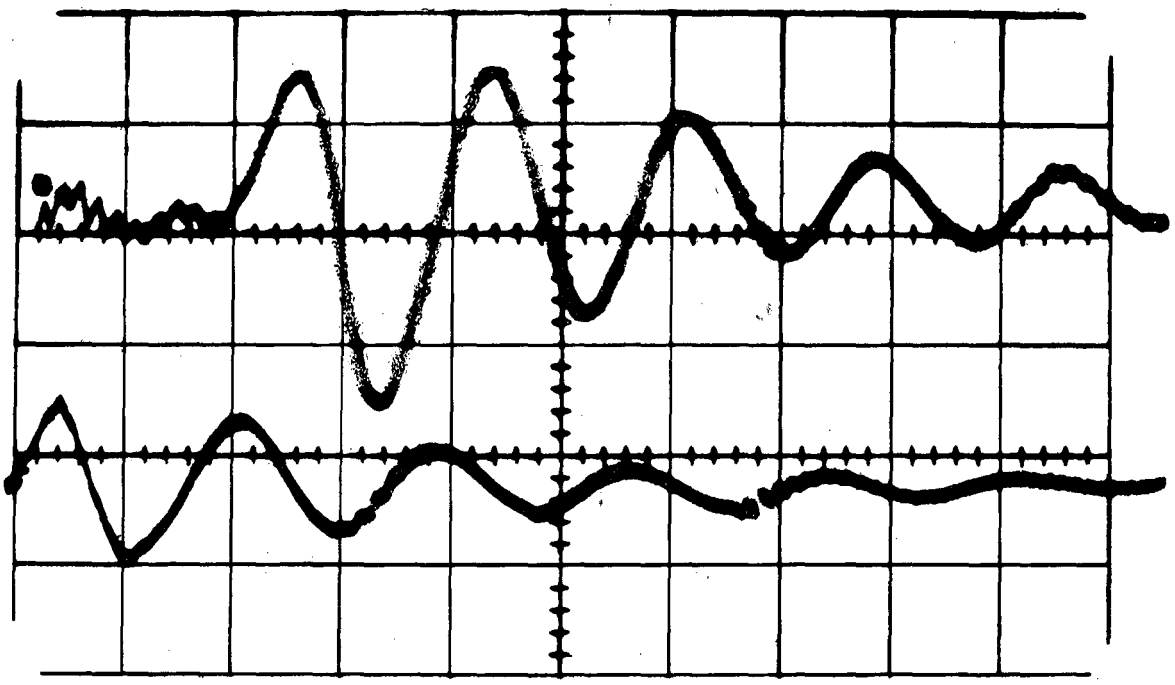

MU-13803

Fig. 24. Received and driving wave forms. Horizontal scale 1 μsec per large division. Top trace is received voltage and bottom trace is driving voltage. A filter is used to give a horizontal base line. A decay of about 2 μsec in the received signal can be seen.

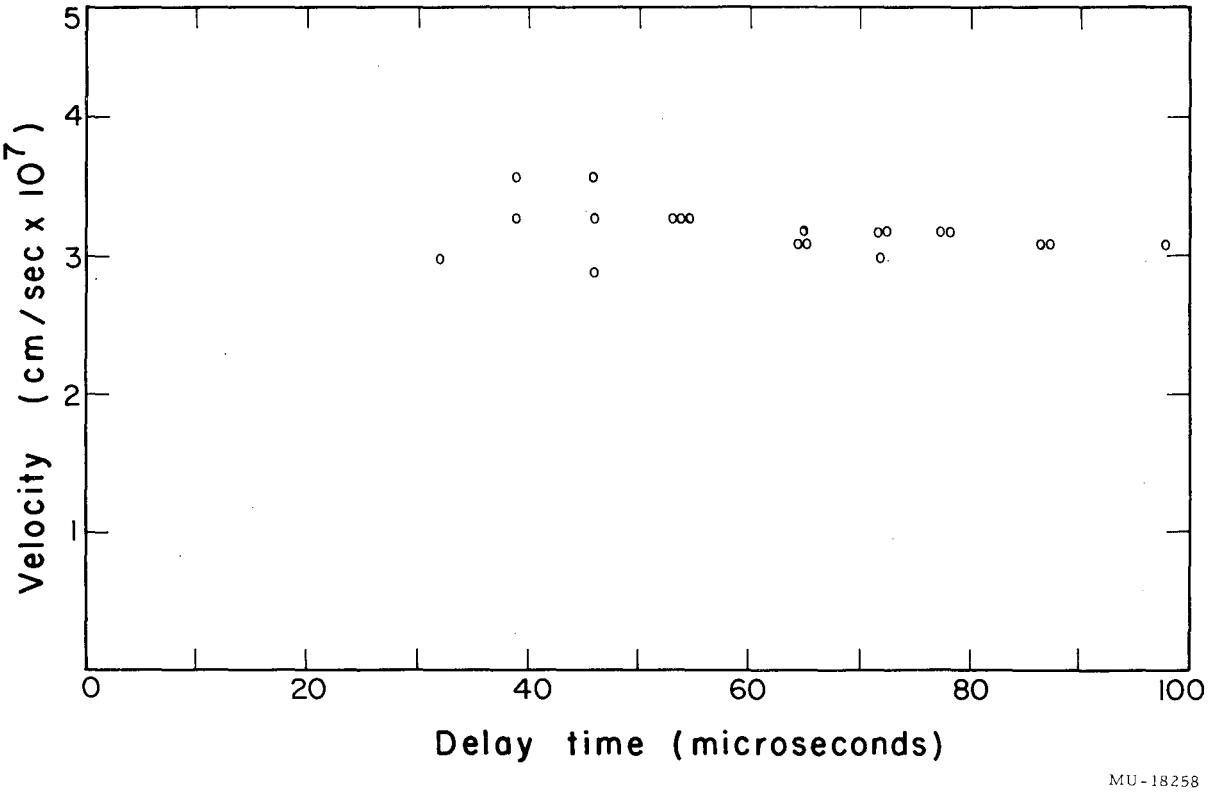

Fig. 25. Measured wave velocity vs time delay between firing of slow bank and fast bank.

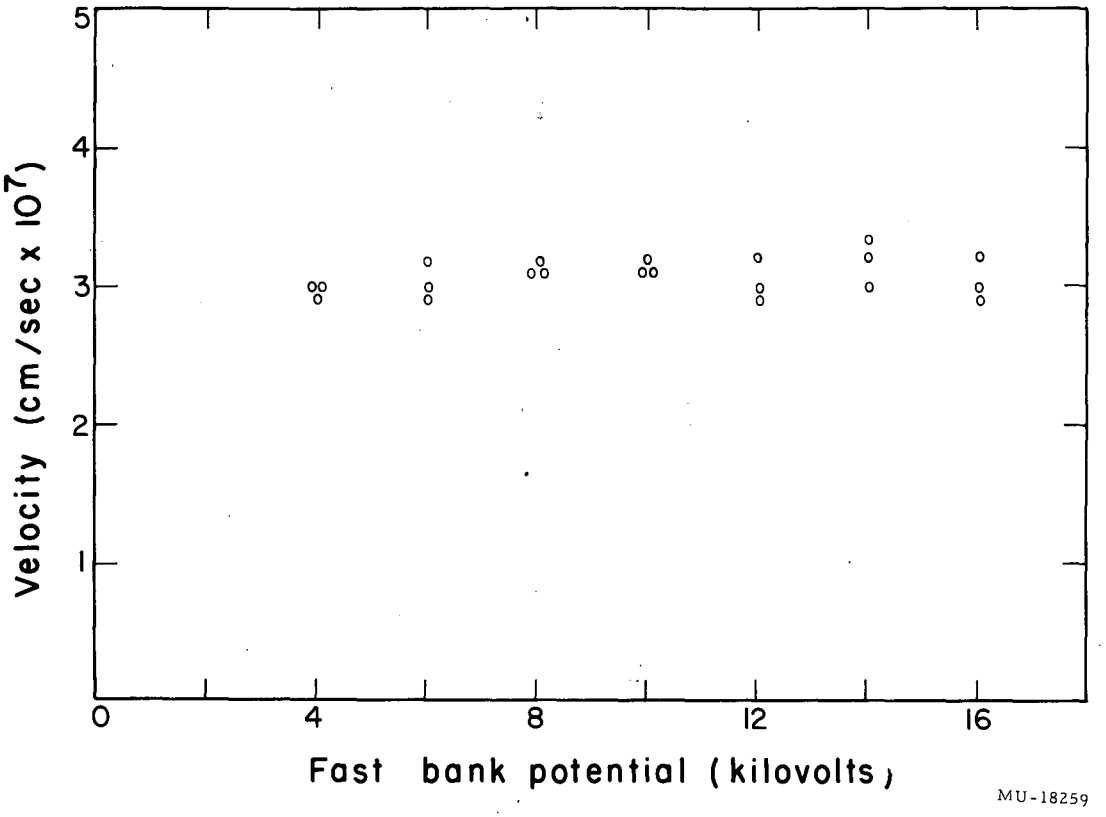

Fig. 26. Measured wave velocity vs fast-bank potential.

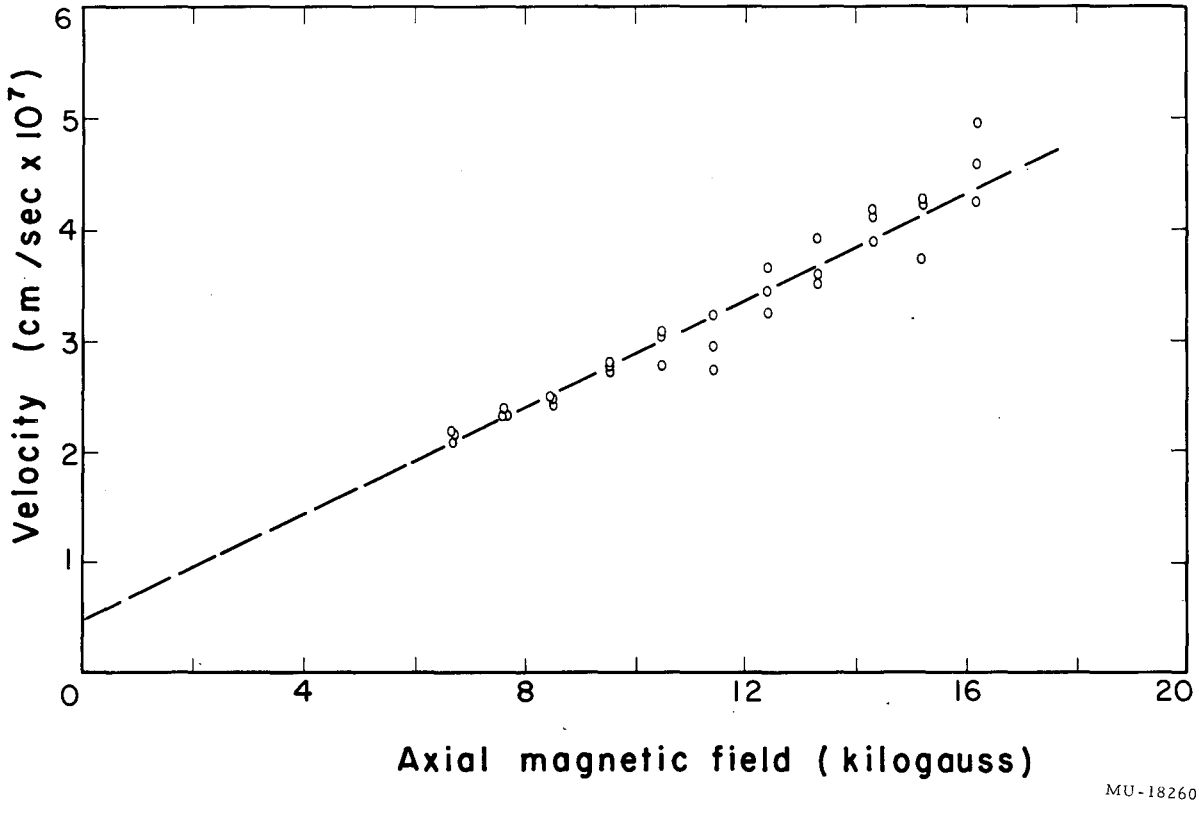

Fig. 27. Measured wave velocity vs axial magnetic field. Dashed line indicates linear dependence predicted by theory.

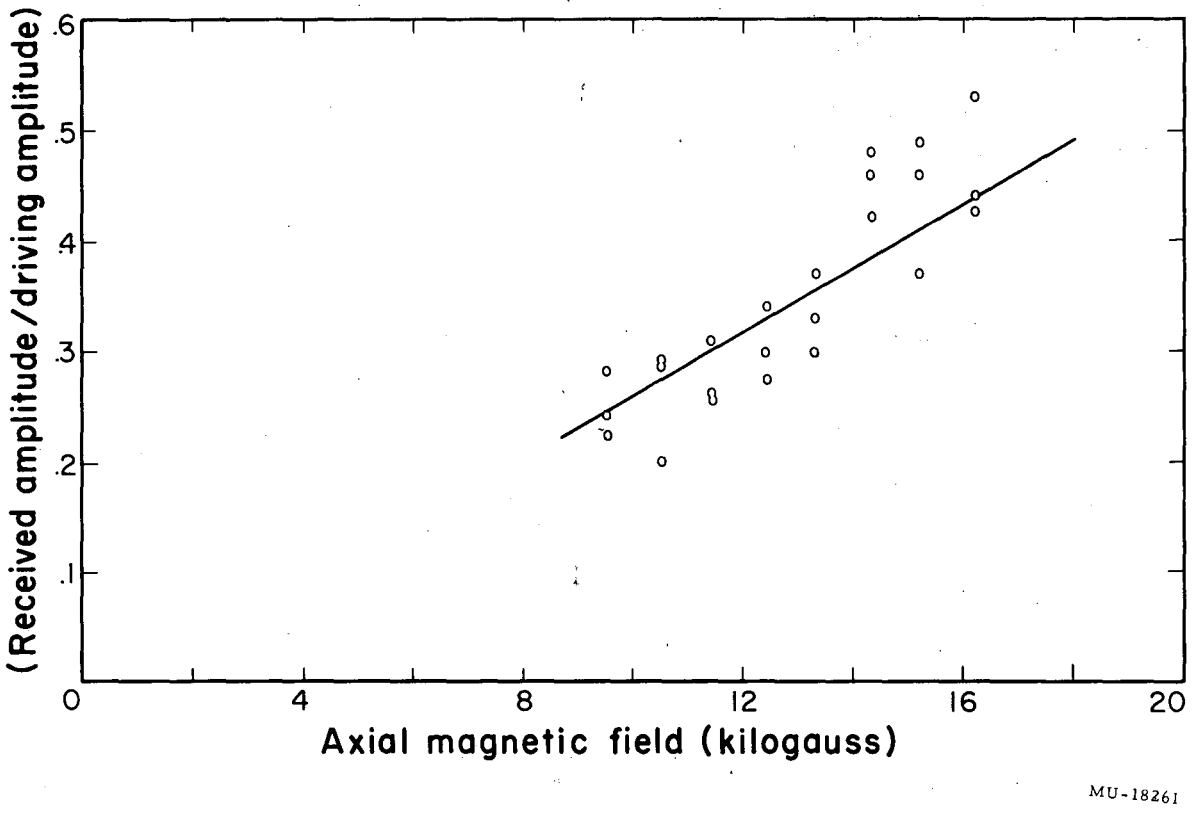

Fig. 28. Ratio of received amplitude to driving amplitude vs axial magnetic field. Solid curve is theoretical plot normalized at 12 kgauss.

A small change in temperature results in a large change in the ratio of the received to driving wave voltage.

Impedance

The impedance of the device was measured as a function of magnetic field from the driving current and voltage wave forms. This can be compared with the theoretical impedance of a coaxial wave guide of this size, using the plasma dielectric constant. At 13.3 kilogauss the measured impedance was found to be 0.085 ohm and the theoretical impedance was 0.080 ohm. However, the impedance was observed to be not as strongly dependent on B_0 as the linear relationship predicted theoretically.

Energy Transfer

The efficiency of the transfer of energy from the external oscillating circuit to the hydromagnetic wave has been measured. The energy delivered to the driving electrodes by the oscillating circuit has been obtained by numerical multiplication of the measured current and voltage wave forms. The second and third half-cycle have been chosen for this comparison. The energy content of the wave during this same interval has been measured with magnetic probes. For a wave traveling in the positive z direction Cowling[4] gives

$$\vec{b} = - \frac{B_0}{v_A} \vec{V} ,$$

where $\vec{b}$ is the magnetic field associated with the wave, $\vec{V}$ is the (transverse) plasma velocity, B_0 is the static axial magnetic field, and v_A is the Alfvén velocity. Then the magnetic energy $b^2/8\pi$ per unit volume equals the kinetic energy $1/2\ \rho V^2$ per unit volume. The magnetic field of the wave is measured with a probe located 1-3/4 in. beyond the end of the driving electrode, at a radial position $r = r_p$ midway between the coaxial electrodes. The largest magnetic field component associated with the wave is b_θ. We also observe the presence of b_r and b_z, but these are small compared with b_θ, so that b_r^2 and b_z^2 can be neglected in comparison with b_θ^2 for a first-order calculation.[5] Thus from the energy density $b_\theta^2/8\pi$ we calculate the energy which flows past the probe during the second and third half-cycles of the wave, add an equal amount of energy to represent the kinetic energy $1/2\ \rho V^2$, and compare the result with the energy input from the external oscillating circuit of the driving electrodes.

---

[4] T. G. Cowling, Magnetohydrodynamics (Interscience Publishers, Inc., New York, 1957), p. 36.

[5] Since b_z is in the same direction as the static axial field B_0, the energy density will be of the form $(B_0 + b_z)^2/8\pi = B_0^2/8\pi + b_z^2/8\pi + B_0 b_z/4\pi$. The first term is constant and the second is negligibly small, but the third term could be appreciable, since B_0 is large. However, it can be shown that the spatial integration of this term over the tube radius, at any value of z, is identically zero.

We measure with the magnetic probe the value of b_θ at $r = r_p$. The magnetic energy of the wave is calculated by integrating $b_\theta^2/8\pi$ over r and t at z = 0. The time integral is done as a summation employing the output wave forms of the magnetic probe. Energy input during the two half-cycles is found to be 9.5×10^6 ergs, while that in the wave for the same interval is 4.1×10^6 ergs, indicating the transfer of $43\pm10\%$ of the input energy to the wave.

The fate of the remaining energy is not presently known but may be in insulator or sheath losses, or possibly in a rapidly attenuated wave propagated in the negative z direction. In any event, the transfer of an appreciable fraction of the input energy into Alfvén wave energy is possible.[6]

The magnetic-probe measurement indicates that the field associated with the wave is about 100 gauss. Since the static field is 10,000 gauss, the wave field is about 1%, and therefore a small-amplitude theoretical treatment is valid.

A pulse line has been constructed to replace the pulse from the slow-condenser bank, which oscillates slowly with a unidirectional square-wave pulse. This will be tried out soon.

The next experimental geometry, called Hothouse II, is nearly completed. Although basically similar to the present geometry, it will have several improvements such as large pumping speed with diffusion pumps, access in the center of the magnet for probes and microwave horns, cooling of the liner surfaces, and a coaxial drive system for the wave energy input.

The attempt to fabricate quartz insulators with probe tubes attached has been a shattering failure.

---

[6] This efficiency is of particular importance for the "magnetic beach" plasma heating proposal of T. H. Stix. (Generation and Thermalization of Plasma Waves, in Proceedings of the International Conference on the Peaceful Uses of Atomic Energy, 2d, Geneva, 1958, Paper No. 361, Vol. 31, p. 125.) In this scheme a hydromagnetic wave is induced at one end of a magnetic-mirror geometry, and conditions are arranged so that the local ion-cyclotron frequency at the center of the mirror geometry is approximately equal to the wave frequency. Under these conditions Stix predicts that the wave energy will be absorbed and thermalized by the ions of the plasma, thus providing an attractive heating mechanism. The proposed plasma density is considerably smaller than in the present experiment.

ION-CYCLOTRON RESONANCE HEATING

Edmund S. Chambers

Experiments were continued using a hollow cylinder of plasma, formed by a reflex discharge, in a magnetic mirror. Energy was coupled to the plasma in the form of Alfvén (A) waves by applying a radial rf electric field across the plasma at one end of the mirror. These waves then transferred energy to ions at a point in the mirror where the static magnetic field, B_{st}, was adjusted for ion cyclotron resonance (ICR).

A tuned pickup coil was placed slightly to the driving side of the center of the machine with its axis parallel to the column of plasma. In this position ions gyrating about magnetic lines near the coil acted as magnetic dipoles linking flux with the coil. The coil voltage e_c depended on the mutual inductance M_n between each of the n orbits and the coil, and the orbit current, i_n, which would be the same for all ions in the same B_{st}. Thus

$$e_c = - n i_n \frac{d}{dt} \left(\sum_n M_n \right) .$$

This neglects the small electron orbits. Since $M_n \sim r^2$, where r is the gyration radius, and the ion energy is

$$E = \frac{1}{2} mv^2 = \frac{r^2 B^2 e^2}{2m} ,$$

then

$$\frac{dE}{dt} \sim e_c .$$

Thus the loop voltage can be interpreted as the rate of energy transfer from the A wave to the ions. This transfer is what I believe Stix[1] would call cyclotron damping. If the propagation of the A wave is considered analogous to a transmission line, the cyclotron damping corresponds to an energy transfer from the propagated electric wave to ions in a region of ICR. This is almost equivalent to the driving electrodes' being at the ICR point, yet has the advantage that the applied electric field is brought in through the plasma itself and hence should be considerably less subject to self-shielding by the plasma.

The coil voltage, e_c, was a maximum when B_{st} was adjusted for ICR at the center of the machine. There was another maximum or sharp break in the curve for e_c vs B_{st} where the ICR point was at the end of the driving end bore tube, where the machine diameter increased from 5-3/4 to 8 in. The outer diameter of the plasma was 2-3/4 in. (i.d. 2-1/8 in.). Deuterium neutral pressure, P, was 0.2 micron and the discharge current, i_a, was 1 amp at a discharge voltage, e_a, of about 500 v. There was a weak discharge all around the cylinder but most of the current was carried from a hot spot

[1] T. H. Stix, Phys. Fluids 1, 308 (1958).

about 0.r in. in diameter. Both maxima occurred at regions in which the axial gradient of B_{st} was relatively small, where a large number of ions would be in about the same magnetic field. The amplitude of the maxima varied approximately with the first power of the rf voltage. As B_{st} was increased above the ICR value at the center, e_c dropped off fairly steeply. This indicated that a wave could then propagate all the way through to the passive end of the machine. To check this a similar coil was placed at the passive end of the machine. As expected, the voltage in this end coil increased as the center coil decreased, as described above. Also the end-coil response was low at the points where the center coil had its maxima.

There were two obviously undesirable features in the above experiments. As mentioned above, only a small part of the self-heated cathodes became hot enough to carry a substantial part of the discharge current. The effect was that the A wave was more like a two-wire transmission line than a coaxial one. This should not interfere with the energy transfer via the A wave, but would result in a transverse (θ) polarization of the accelerated ions with respect to their electrons. Cathodes of different materials and thicknesses were tried. Discharge current was increased to 8 amp. A 60-cps electric field was superposed on the rf to cause a sustained azimuthal drift. None of these things increased the size of the hot spot substantially. A hot-filament cathode is now being developed.

The other complication, recently discovered, is that the driving voltage had a large second-harmonic component on it and under some conditions a third harmonic. A simpler π output-matching network is now being installed to eliminate the harmonics.

Several perplexing results have been obtained. The impedance at the radial gap across which the rf was applied was obtained by measuring the voltage with and without the plasma. As the coupling reactance was known, the gap impedance was calculated by solving three equations in three unknowns. With rf 68 v (peak), P = 0.2 μ, i_a = 1.0 amp, e_a = 500 v, a value of 5.5 ohms was obtained. This agreed well with a calculated reactance, assuming that the system could be represented by a hydromagnetic capacitor.[2] However, the experiment showed only a slight increase in impedance with 1/P, instead of linear; and practically no change with B_{st}, whereas a $1/B^2$ dependence was expected. The power dissipated, as measured by the change of input power to the amplifier, was 60 watts, which would correspond to an equivalent series resistance of 0.4 ohm. A more straightforward way of measuring load current and power is being planned.

A 300-v pulse was applied across the driving-end radial gap. A double-beam oscilloscope was used to look at this pulse and at one from a

---

[2] O. A. Anderson, W. R. Baker, A. Bratenahl, H. P. Furth, J. Ise, W. B. Kunkel and J. M. Stone, Study and Use of Rotating Plasma, International Conference on the Peaceful Uses of Atomic Energy, 2d, Geneva, 1958 (United Nations, New York, 1959) Paper No. 373, Vol. 32, p. 155.

similar type of gap at the passive end, 75 cm away. With a low plasma density ($i_a \sim 0.02$ amp) the two pulses arrived at about the same time, while with $i_a = 1.25$ amp there was a lag of about 0.04 μsec. This would indicate 1% ionization. However, when B_{st} was increased 45%, there was some increase in amplitude, but no detected change in wave velocity. It should depend linearly on B_{st}.

DISSOCIATION OF D_2^+

Gordon Gibson,* Willard C. Jordan,† Eugene J. Lauer, Robert L. Leber, Cornelius H. Woods, and J. Ralph Ullman

The experiment proposed to measure the dissociation of D_2^+ relative to the ionization of neutral deuterium in a deuterium arc has progressed to the stage of initial operation of part of the apparatus. Specifically, a stable arc has been operated in a solenoidal magnetic field, using an atmospheric leak as the gas supply. The arc is of the reflex variety, with currents of 10 to 20 amp and cathode voltages of approximately 300 v each. Adjustments of the collimator geometry and other arc parameters are in progress. Unfortunately, the two solenoid coils associated with the arc each have shorted layers, and at different radii, so that they produce a magnetic field not having a plane of symmetry, and having only 75% of the design value of intensity. However, they are adequate for initial experimentation, and a duplicate set of coils is being fabricated for use in the dissociation measurement.

The necessary power supplies and controls have been installed at the location where the equipment is being assembled, and work is in progress to provide power in the Cockcroft-Walton pit, where the experiment will be performed.

*Consultant from Westinghouse Corporation, Atomic Power Division, Pittsburgh, Pennsylvania.

†Consultant from Bendix Aviation Corporation, Research Laboratories Division, Detroit, Michigan.

VIII. ENGINEERING AND TECHNOLOGICAL DEVELOPMENT

ULTRAHIGH-VACUUM DEVELOPMENT

Norman Milleron and Leonard L. Levenson

Of the three areas of investigation,

(a) "black hole" pumping and beam catching,

(b) clean pumping with diffusion pumps, and

(c) complementary techniques, only (b) and (c) have been pursued experimentally during this third quarter.

Clean Pumping with Diffusion Pumps

4-Inch-Diameter Angle Trap

Tests using a diffusion pump, Type 300 MCF, and Oct-oil "S" with 13x molecular sieves in the trap geometry previously described[1] yielded the following results:

1. The tungsten filament B-A gage made by C. E. C. gave a constant current response independent of shutter position. During three days with the shutter closed and three days with the shutter open, the ion gage read between 3.5 and 4.5×10^{-10} mm Hg regardless of the shutter position. Interpretation of oil-trapping efficiency by means of the shutter permits us to establish a pessimistic lower limit of 0.99 on the trapping efficiency of the wire mesh and 13x combination.

2. Electrical power failure does not seem to vitiate the oil-trapping ability of 13x provided the pump system has an automatically closing foreline valve. With the electric power off for 104 hours, and the pressure in the diffusion pump system consequently at $\sim 10^{-4}$ mm Hg, the 13x material retained its oil-trapping properties. This is shown by the recovery of $< 1 \times 10^{-9}$ mm Hg pressure within ~ 3/4 hour after the restoration of electric power to the diffusion pump.

3. The affinity of the 13x material for H_2O, CO_2, CO was qualitatively confirmed and small atmospheric leaks were precisely located by using these materials to probe for the leaks.

4. Copper "bead" gaskets on the high-temperature section, together with a fuse wire and a rubber gasket on the unbaked sections, were replaced by make-and-break welded seals. No appreciable difference in ion-gage response between the two gasket systems was seen; however, the make-and break welded seals are deemed to be more reliable. No statistics regarding the relative merits of gaskets have been accumulated.

---

[1] Norman Milleron and Leonard Levenson, in Controlled Thermonuclear Research Quarterly Report, UCRL-8775, June 1959, p. 80.

5. The time necessary to activate the 13x material seems to depend on the ability of the system to pump the large amount of water and other gases evolved. By weighing the contents of a liquid nitrogen foreline trap, the amounts of condensible gas evolved during activation could be estimated. Activation of ~ 275 g of 13x bead material produced ~ 21 g of condensibles, almost all of which was water.

Large Diffusion-Pump Test System

Backstreaming tests were made on a 10-in. NRC H-10-P oil diffusion pump. The pump mouth was covered by a plexiglas plate so that the amount of backstreaming could be estimated visually by observing the amount of oil condensed on the plexiglas surface as a function of time. It was observed that for an unbaffled H-10-P pump considerable backstreaming of oil occurs, so that the plexigals plate surface is dripping wet with oil after two or three hours of operation. Narcoil-40 was the pump fluid used.

Tests on the backstreaming rate of a 32-in. NRC H-32-P oil diffusion pump have just been started. Preliminary indications are that the backstreaming rate for the unbaffled 32-in. NRC pump is comparable to that of the 10-in. NRC pump.

Conductivity Measurements

The measurement of conductivities of various trap geometries is continuing. Preliminary results indicate that it will be difficult to obtain a trap conductance larger than 30% of the conductance of the orifice to which the trap is attached, even if all the trapping surfaces, including the wall surfaces, can effectively capture pump fluid vapor on one bounce.

Complementary Techniques

Gaskets

No development work on gaskets was attempted during this quarter.

Valves

Thus far, preliminary tests have been made only on the actuator, which is described in the last quarterly report.[1] It has been found that the actuator, which is a flat annular inflatable bellows, had a recoverable travel distance of only 0.020 in. when it was inflated against a flat spring. This travel distance is probably marginal for a valve which may have a gate as large as 4 ft in diameter, since this is the clearance of the slot through which the gate would have to be moved to open or close the valve. However, these tests are only preliminary; much larger travel distances may be obtained later with other bellows and other springs.

Another method of recovering the extended bellows has been proposed by Levenson. It involves the use of another bellows mounted in opposition to the closure bellows. To retract the closure bellows, the pressure in the

closure bellows is relieved and the opposite bellows is inflated. A mechanical linkage that can transmit motion from one bellows to the other will then collapse the closure bellows as the opposition bellows expands, and vice versa.

Milleron has proposed and demonstrated the use of an inflatable diaphragm which consists of two flat circular metal sheets welded face to face at their edges. When pneumatic pressure is applied to the enclosed volume between the sheets, the faces of the diaphragm are deformed and the thickness of the assembly increases, with the maximum thickness occurring at the center. This system could be used to transmit pneumatic pressure to a seal within a valve. This type of actuator may be more applicable to small valves than to large valves, for which the annular-type bellows may be more useful.

Bakable Liquid Metal Rotary Seal

Machining, vacuum brazing, and assembly have been nearly completed for a molybdenum, Ga-In-Sn seal.

CRYOGENIC PUMPING

Gordon Gibson,* Willard C. Jordan,† Eugene J. Lauer, and J. Ralph Ullman

Figure 20 of the preceding report[1] shows the apparatus of these tests. The purpose is to test the feasibility of protecting a plasma from the cold gas charge-exchange loss by using an inner vacuum chamber whose walls can be lined with absorbent and which can be baked out and then cooled to liquid helium temperature. The outer vacuum system could be constructed with conventional techniques and would only be required to produce a vacuum of about 10^{-6} mm Hg. The two regions would be connected by open holes or tubes for transmission of the injected ion or atom beam. It would be required that the pressure in the inner chamber be less than 10^{-8} mm Hg in spite of the gas entering from the higher-pressure outer chamber, escaping plasma particles, etc.[2]

---

*Consultant from Westinghouse Corporation, Atomic Power Division, Pittsburgh, Pennsylvania.

†Consultant from Bendix Aviation Corporation, Research Laboratories Division, Detroit, Michigan.

[1] Gibson, Lauer, and Ullman, Liquid Helium Experiment, in Controlled Thermonuclear Research Quarterly Report, UCRL-8775, June 1959.

[2] G. Gibson, W. A. S. Lamb, and E. J. Lauer, Injection into Thermonuclear Machines Using Beams of Neutral Deuterium Atoms in the Range from 100 kev to 1 Mev, Phys. Rev. 114, 937 (1959).

Three tests of the pumping action have been run (see Figs. 29, 30, and 31). The absorbent was the same for the three runs; namely 886 grams of charcoal in a mesh basket 1-in. i.d., 3-in. o.d., and 20 in. long. The charcoal was supplied by Messrs. Satcliffe, Speakman and Company, Ltd., Leigh, Lancashire and was type 203B, of 1/4- to 3/8-in. mesh and impregnated by a copper nitrate process. Before each run the charcoal was outgassed at about 200°C.

In the first liquid helium run (Fig. 29), the helium transfer tube was defective and no thermometer was used. For these reasons it is not known whether liquid helium was actually collected in the apparatus or not. In spite of these difficulties, it was observed that the bottom ion gage remained at its base pressure of about 2×10^{-8} mm Hg for longer then 8 minutes even when hydrogen was allowed to leak into the top region at a steady rate which caused the top ion gage to increase from its base pressure of about 2.5×10^{-8} mm Hg to about 5×10^{-6} mm Hg.

On the second liquid helium run, hydrogen was allowed to leak in at a greater rate, which caused the top gage to increase to 1.3×10^{-5} mm Hg. Again the bottom ion gage remained at its base pressure for about 5 min. The bottom pressure increased slowly at first, and then rapidly at about 19 min to a fairly steady value of about 10^{-6} mm Hg. Following this, the bottom pressure remained at about 10^{-6} mm Hg even when the hydrogen leak was closed and the valve was opened to the diffusion pump. A carbon resistor thermometer was used on this run to measure the temperature inside the liquid helium chamber and therefore it is known that the chamber was maintained nearly full of liquid helium. The resistor calibration was checked by immersing the resistor in liquid helium.

Figure 31 shows the results of a run at liquid nitrogen temperature. The pressure difference is uninteresting at this temperature, as is expected.

The top and bottom nude Veeco ion gages and the VGIA ion gage at the input end of the leakage-rate metering tube were calibrated on neon gas against a McLeod gage. Then the sensitivity to hydrogen was determined by assuming that the ratio of sensitivities to hydrogen and to neon was 3:1, as was measured in the β-ray apparatus. The gages on the cryogenic pumping system could not be calibrated directly on hydrogen because the charcoal has a small persistent hydrogen-gettering action.

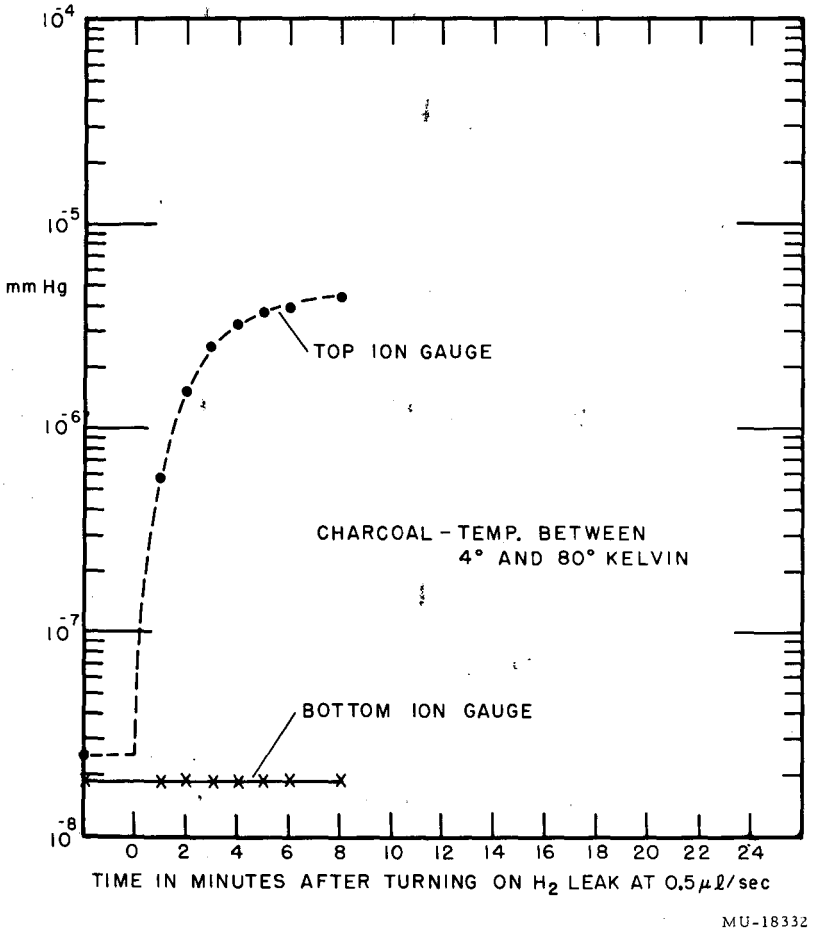

Fig. 29. Results of pumping test - first run.

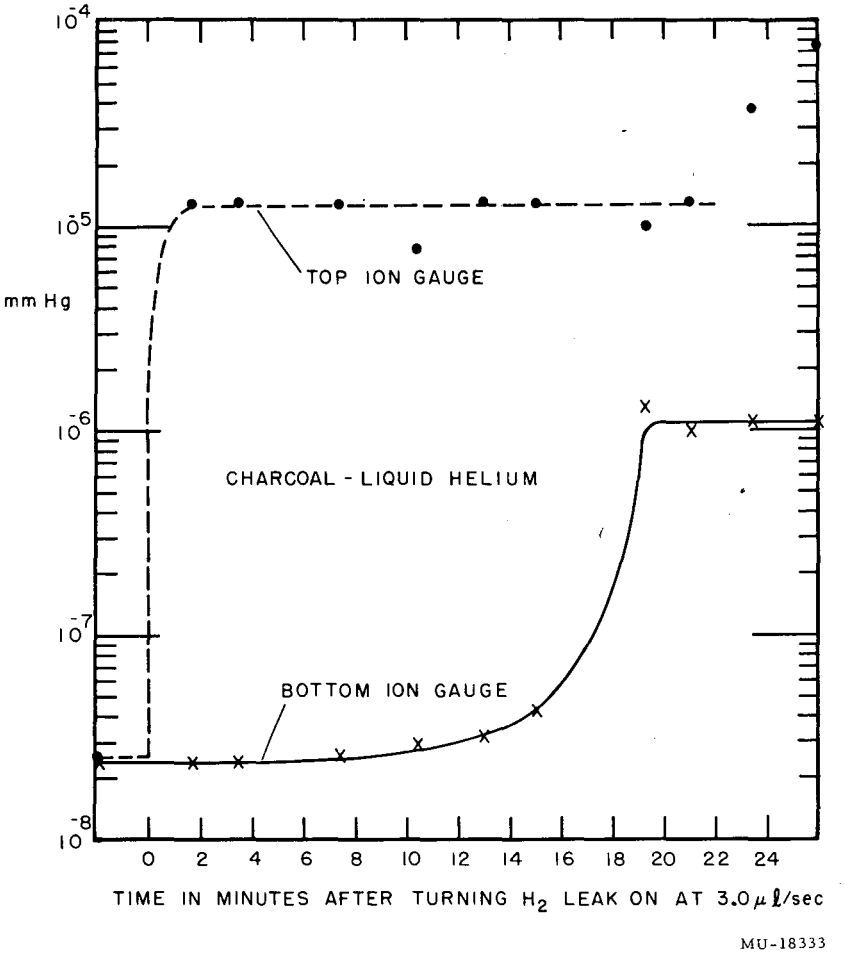

Fig. 30. Results of pumping test - second run.

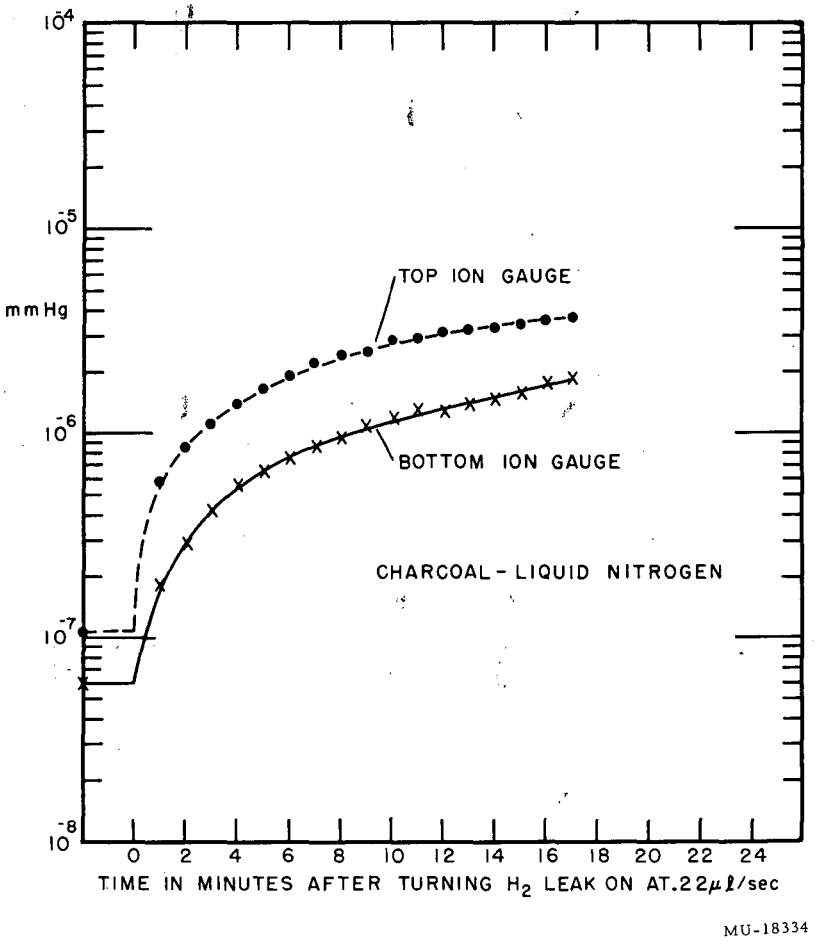

Fig. 31. Results of pumping test - third run.

MECHANICAL ENGINEERING DEVELOPMENT

Thomas H. Batzer

Beta-Ray Experiment

J. Ralph Ullman

Modifications are being made to the mirror-coils support structure which will allow one of the coils to be displaced ± 6° about a horizontal or vertical axis. Such an arrangement will permit the study of the containment properties of asymmetric mirror fields.

Liquid Helium Experiment

J. Ralph Ullman

An attempt was made to cool the activated charcoal trap to liquid helium temperature. Approximately 270 liters of liquid helium was transferred to the trap. The run lasted approximately 36 hr. The operating pressure of the trap at ambient temperature, prior to the run, had been holding between 10^{-8} and 10^{-9} mm Hg for several weeks. The trap was then cooled to liquid nitrogen temperature and held there for several days prior to removing the liquid nitrogen and beginning the transfer of liquid helium. During the early part of the run the high-pressure compressor of the gas-collecting system failed and the gas was thereafter vented to the atmosphere.

The first three Dewar containers (averaging 45 liters each) were exhausted with no apparent transfer of liquid, apparently because of poor design of the transfer line. A second transfer line, having a larger capacity and superior insulating qualities, was substituted. The liquid-level indicator gave a reading of 2 to 6 in. of helium in the trap after all the Dewars were exhausted. With the trap cooled to this extent, the hydrogen leak to the trap was begun. Data were taken at an initial leak setting for an 8-min run. The ion gage at the opposite end of the trap from the incoming hydrogen leak failed to see any pressure increase during this interval.

Continuing plans call for:

1. Putting the Worthington compressor back into reliable operation.
2. Fabrication of a new transfer line to reduce the heat piped to the liquid helium.
3. Determination, from observation of liquid nitrogen boil-off rates, of the
   (a) trap heat capacity,
   (b) trap steady-state heat gain from surrounding atmosphere,
   (c) trap steady-state heat gain due to each ion gage.
4. A second run allowing hydrogen to leak in, with the charcoal trap at liquid nitrogen temperature.
5. A third run, allowing hydrogen to leak in, with the charcoal trap at liquid helium temperature.

Dissociation of D_2^+

J. Ralph Ullman

The several different pieces of mechanical equipment necessary to the support of this investigation are in various stages of engineering. Most of the parts for the D_2^+ analyzer have been received and assembly can proceed. In design is a vacuum system, which is to be used to evacuate the volume around a target arc where it intersects the Cockcroft-Walton beam. The arc will be the PIG reflux type and the beam will be D_2^+ from the Cockcroft-Walton accelerator. The pump box will be 1×2 ft by 6 ft long, and pumping on it will be a 20-in. mercury diffusion pump suitably backed and trapped. As the system must go to air frequently, a 20-in. valve will be used for isolation. The complete system will be assembled as a portable unit for installation in the Cockcroft-Walton pit. Further, since the Cockcroft-Walton beam tube is inclined at 26° with the horizontal, a bending magnet will be required to bring the D_2^+ beam into the machine at the proper angle.

A proposal has been made for a versatile experimental apparatus that would permit study of large arcs in environments varying from high to ultra-low pressures. Solenoid confining fields would vary from 7 to 12 kilogauss and would require up to 1.8 Mw of power supplied to 20 modular coils. The arc would be the PIG reflux type with the filament and gas source separately pumped. The main arc tube would be bakable. The design speed of the pumping system would be approximately 10,000 liters/sec. Work on the machine arrangement has begun and preliminary engineering design is in progress.

Hard-Core Pinch

Raymond E. Keyes

The main obstacle in the way of completing the design for the toroidal hard-core pinch is the 0.007-in.-thick corrugated toroidal liner. Because of the extremely high bids we have received on the fabrication of the liner it has been decided to back off somewhat on the specifications. The alternate specifications will make no change in material requirements, but will allow the corrugated torus assembly to be made by bending straight bellows. The outer periphery of the liner would have the same corrugation amplitude as specified originally, but the inner periphery would have an amplitude about three times as great. There are physical objections to this change but for the sake of cost and better delivery time, it is acceptable. The bent-bellows design would be stronger in resisting pulsed fields and more flexible during bake-out.

A feasibility study is being conducted on a second alternate liner for the Levitron or toroidal hard-core pinch. The proposed liner would consist of a metalized plastic laminate which would completely cover and be bonded to the bore surface of the external copper shell halves. Only the metalized surface would be exposed to the pinch discharge.

Unipolar Generator

Raymond E. Keyes

A trip was made to the Milwaukee plant of Allis-Chalmers to review the design of the unipolar generator. Although the unit is designed for steady-state operation, we plan to pulse it to achieve momentary high currents. The terminals, being close together at the center section, exert high axial loads on the outboard stator sections. The main mechanical engineering problem has been to devise the means to withstand the axial loads and to minimize the displacement of the sections. We proposed that a ring of prestressed bolts be added to the unit to tie the terminal plates together. We also proposed that an existing circle of 12 stay bolts be prestressed in order to contain the axial load of the brushes.

Table Top

John R. Benapfl

Design is in progress on an accel-decal analyzer. This device is essentially a magnetically shielded vacuum chamber about 3 ft long and 1 ft in diameter containing three electrodes, cylindrical in shape, capable of standing off 150 kv. One end has an entrance slit which connects to the Table Top machine. On the other end is a scintillator, light pipe, and photomultiplier combination to pick up the signal. The only major problem encountered so far has been in obtaining a 50% nickel-iron sheet or tube for the combination magnetic shield and vacuum chamber.

Low-Energy Neutral-Beam Experiment

William S. Neef, Jr. and James F. Ryan, Jr.

Most of the components of the Alice vacuum chamber had been designed in detail. The copper conductor for the coils has been received and a special machine to straighten and tape the conductor is in the final stages of assembly. The large furnace for curing the epoxy-potted coil assemblies is in place and is ready for operation. Coil fabrication should begin no later than about September 1, 1959.

The Linde Company will begin construction of a concrete pad for their liquid nitrogen storage cylinder during September. Their installation will include two discharge points, one from a 40-gpm pump and the other for Dewar filling on the outside of the building.

All the demountable flanges on the Alice vacuum system are of the copper-pinch-gasket type. They range in size from 2 in. in diameter up to 20 in. in diameter. Recent experience in the use of pinch gaskets in the larger sizes has shown conflicting results. In the light of this, a decision was made to set up several small vacuum systems that could be quickly thermocycled in order to determine, with reasonable statistics, whether the failures are due to faulty design or poor techniques.

Mechanical Switch

James F. Ryan, Jr.

A current drawing of the switch is shown in Fig. 32. The first successful contact cylinder and finger array had a useful life of about 2000 pulses on the Table Top capacitor bank. A replacement contact assembly failed in preliminary tests after about 20 pulses at relatively low voltages (less than 20 kv across the switch). The failure appears to have been the result of low contact pressure between the fingers and the contact cylinder.

A new contact assembly using silver-tungsten alloy on the leading edge of the cylinder and on the finger tips was fabricated. These contacts have been used for about 150 pulses. In that time there have been two stoppages due to external circuit defects and one stoppage apparently caused by sticking of the contacts. The contacts were dressed and operation mechanically has been satisfactory. The switch is out of the circuit, as it is not required for current experiments. The mechanical reliability of the switch appears to be satisfactory. Further development will be centered on increasing the reliability and useful life of the contacts.

Astron

Charles A. Hurley and James E. Blades

Assembly of the traveling-wave-line experiment of the Astron model has been stopped. Work on the components of the 5-ft-long traveling-wave line being fabricated in the Mare Island shops has also been stopped. These stoppages were based on a decision to redesign the electron gun and also design an accelerator to be placed between the electron gun and the injector.

The present electron gun (see Fig. 33) used in the dc test has undergone some modifications. The connection between the cathode and the top turn of the transformer secondary was changed in order to simplify changing cathodes. The ceramic stack assembly, which supports the accelerating column, was redesigned in an attempt to eliminate voltage breakdown between the focusing-plate supports. The beam focusing plates were redesigned to allow better vacuum pumpout, reduce heat distortion, and simplify alignment.

Atomic and Molecular Beam Cross-Section Measurements

Charles A. Hurley

Approximately 40% of the required hardware is being fabricated and will be delivered by September 1, 1959. The oven holder has been designed and released for fabrication. Work is progressing on the beam chopper, beam flag, mass spectrograph, ion-source support, spectroscope light pipe, and handling equipment.

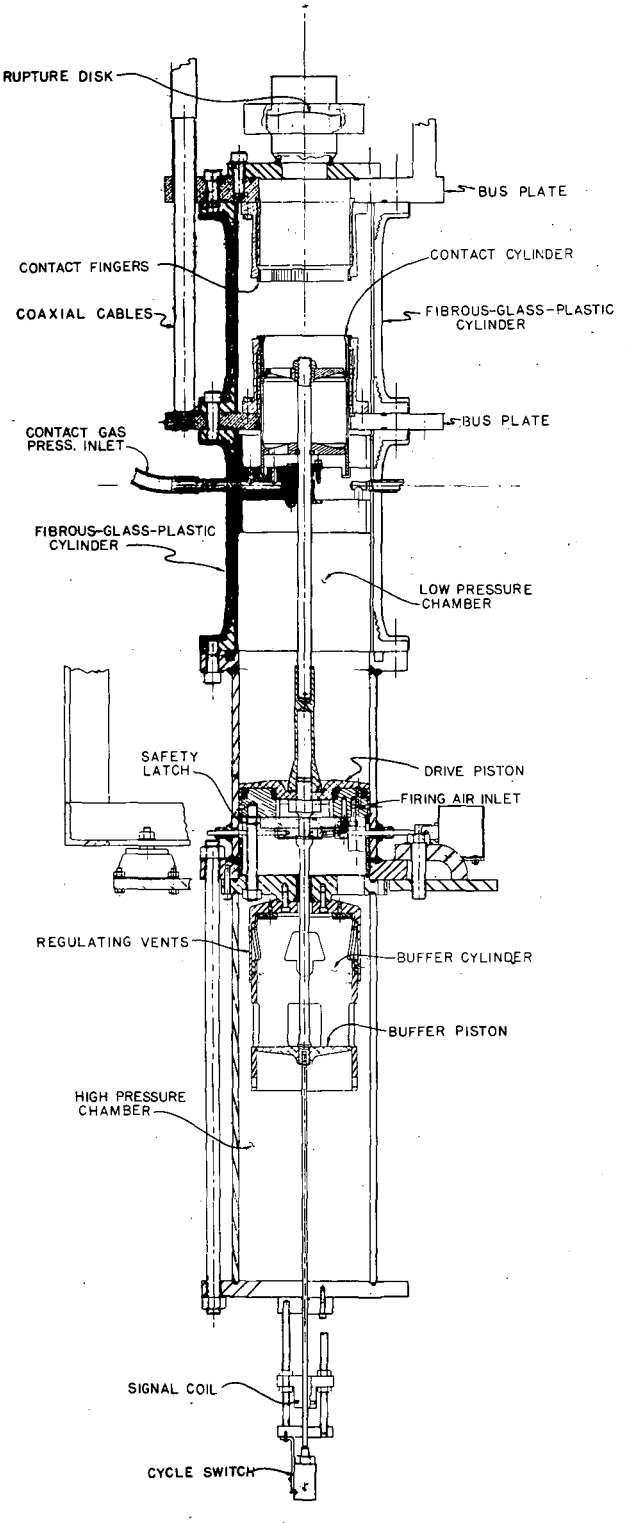

Fig. 32. Switch used in Table Top experiment.

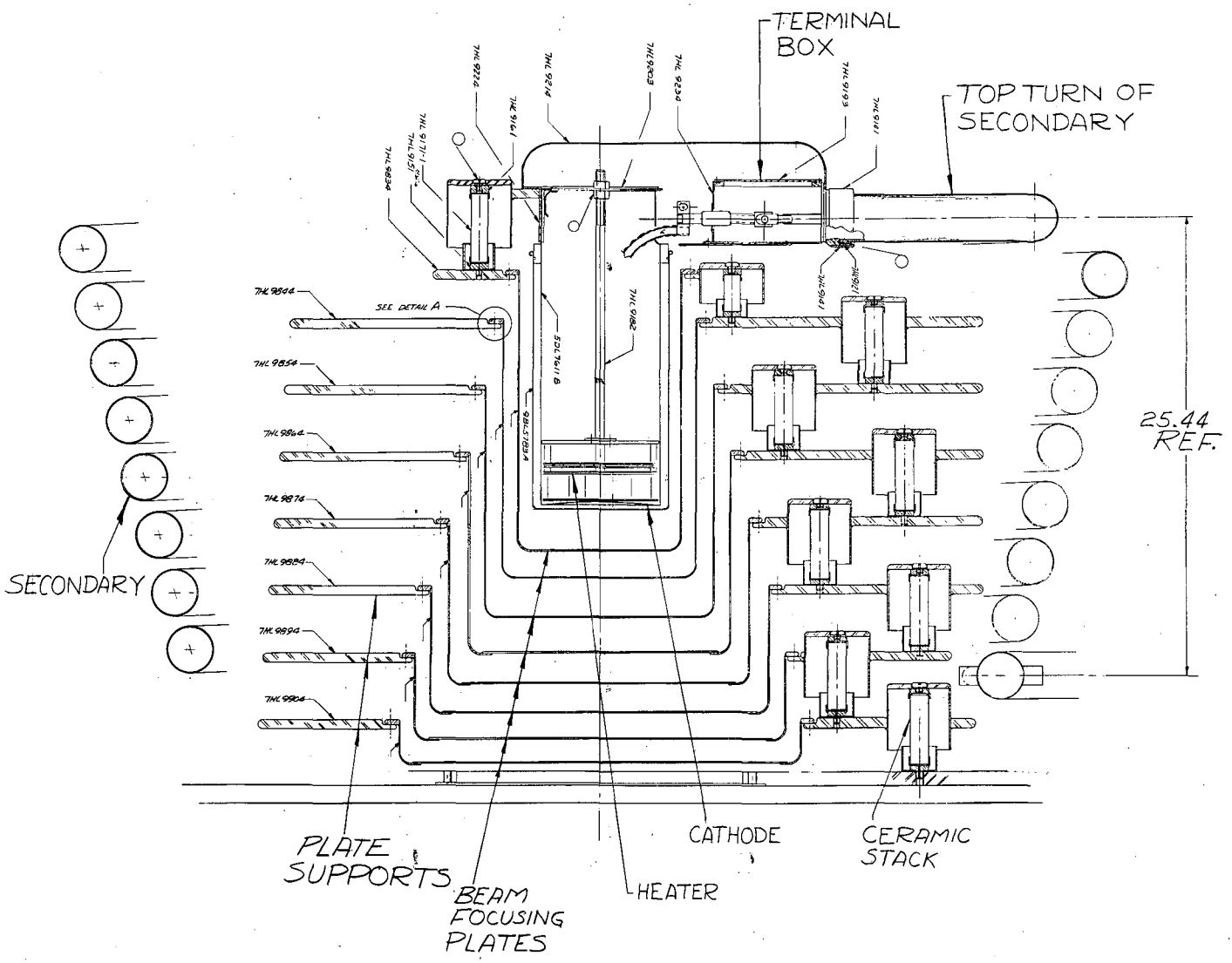

ELECTRON GUN REDESIGN

MUB-313

Fig. 33. Electron gun redesign.

Low-Temperature Refrigeration

Clyde E. Taylor

The three-stage cascade refrigerator No. 2 has operated continuously since April 13, maintaining the baffles of two 20-in. mercury diffusion pumps at about -285°F. No serious operating difficulties have been found. During this period a number of emergency power shutdowns occurred. The two diffusion pumps are operating in the 10^{-9} mm range above the baffles.

The new three-stage cascade refrigerator No. 3, which incorporates many design improvements, is nearly completed. This design includes an entirely new concept of compressor operation and is contained in a compact package (see Fig. 34).

Cryogenic Coils

Clyde E. Taylor, Robert L. Nelson, Joseph C. Behne, Arturo Maimoni, and Richard Mallon

Much of the work on the cryogenic coil project, to date, has been of the nature of preliminary design. This is because much new technology is involved. The main problems now being considered are listed below along with brief comments as to the status of each problem.

1. Conductor Material

(a) Sodium

A small still, of the type operated by Horsley,[1] has been constructed and operated. Several samples have been cast in small stainless steel tubes and the electrical resistance measured at the NBS Boulder laboratories.

Satisfactory purity has not yet been obtained; however, techniques of still operation are being improved. Residual resistivity at liquid helium temperature of commercial undistilled sodium, after rather crude melting techniques, has been found to be 7×10^{-9} ohm-cm. This is only a factor of 10 higher than the value required for coil construction. It is believed that this residual resistivity is nearly proportional to the impurity fraction.

A high-temperature fractionation-type still, capable of producing 100 lb per day of pure sodium, has been roughly designed. Decision on this equipment will be made after some definite results are obtained with the present still.

(b) Aluminum

Aluminum samples of 99.999% and 99.9999% purity have been obtained and a sample of the 99.999% material in the form of 24-gage wire is being prepared for resistivity measurements.

---

[1] G. W. Horsley, The Corrosion of Iron by Oxygen-Contaminated Sodium, AERE-M/R-1441, April 1954.

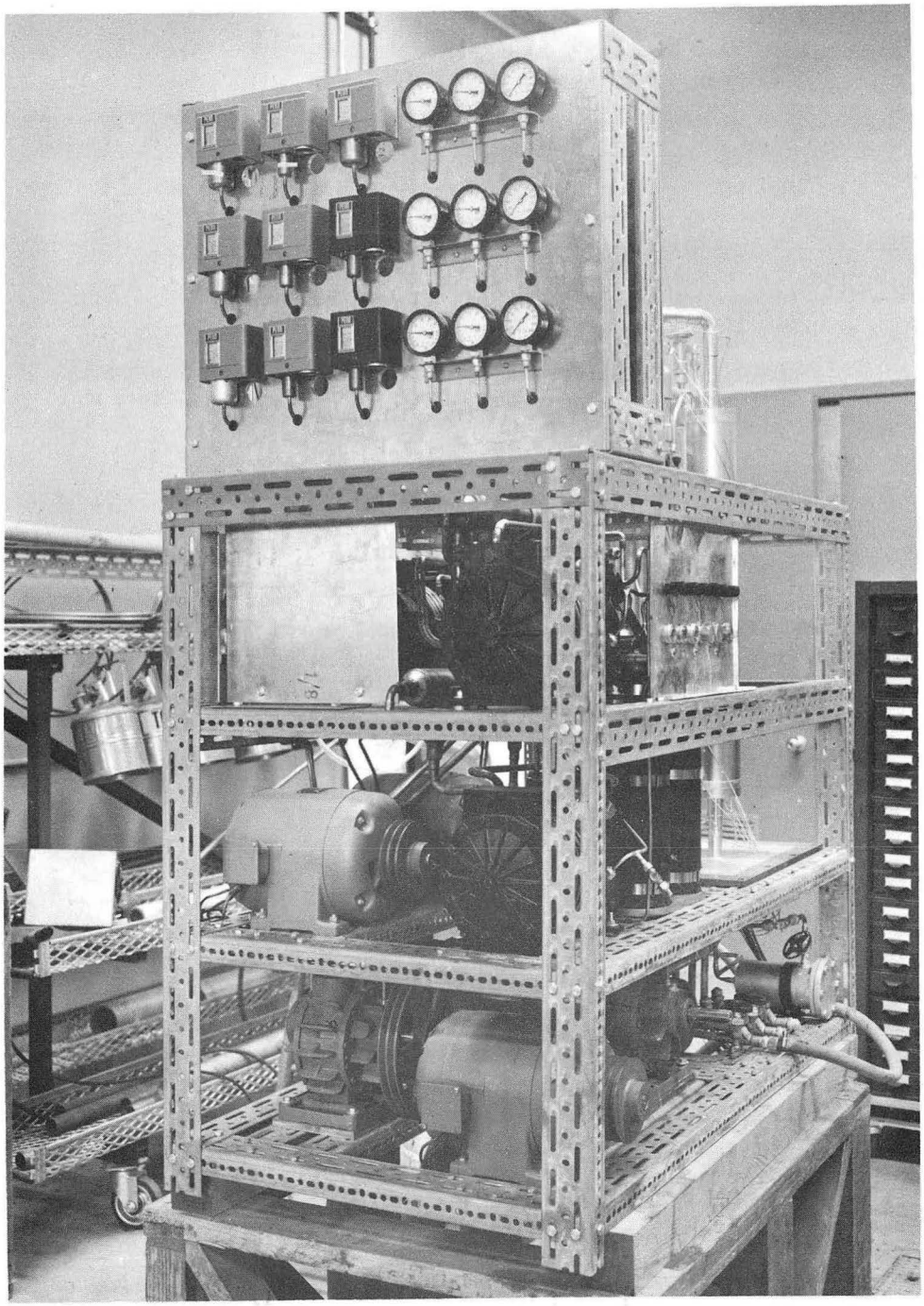

ZN-2238

Fig. 34. Three-stage cascade refrigerator.

2. General Parameter Study

Calculations of magnetic forces, optimum coil proportions, heat transfer, electrical leads, coolant pressure drop, temperature stability, and controllability have been completed and no fundamental limitations have been found.

3. Power Supply

Preliminary cost estimates have been requested for a 20,000-amp 0.5-v power supply for testing an 8-in.-diam coil.

4. Fabrication Techniques

The design of a cryogenic magnet coil for test purposes is now in progress. The coil will be approximately 12 in. long, 8 in. i.d. and 19 in. o.d. It will consist of six layers of windings with 18 turns per layer. The conductor will be sodium, which will be cast in a preformed stainless steel tube.

Laboratory tests indicate that stainless steel tube, 0.5 in. square with 0.010-in. wall, can be bent around a 4-in. radius and will withstand the magnetic pressure of the sodium when forced outward against the coolant grooves, as shown in Fig. 35. Techniques for butt-welding short lengths of this thin-wall tubing are being developed.

5. Low-Temperature Refrigeration-Cycle Analysis

A typical helium gas refrigeration cycle utilizing two expansion engines and operating the compressors at room temperature was calculated. A refrigeration load at 10°K was assumed. This calculation was then coded so that the IBM 704 machine could be used to analyze the cycle and allow variation of the many parameters required to obtain maximum isentropic efficiency. A machine run for this cycle of 600 solutions required only 3 min. All parameters were varied--within reasonable limits--with the exception of compression ratio, which was fixed at 5 to 1. To appreciate the capability of the 704 calculator for this type of engineering calculation, it should be mentioned that 600 typical solutions of the type run on the 704 in 3 min, after coding, would have required more than one man-year of engineering time.

The code is now being changed to allow

(a) a greater number of expansion engines,

(b) variation of compression ratio,

(c) printout of thermodynamics properties at each state point,

(d) calculation of cycle irreversibility.

An analysis of helium cycle with the compressor operated at low temperatures and the heat rejected through a condenser operated at liquid nitrogen temperature was also made. The extremely high consumption of liquid nitrogen and the mechanical difficulties encountered in operation of a compressor at 10°K makes this solution unattractive.

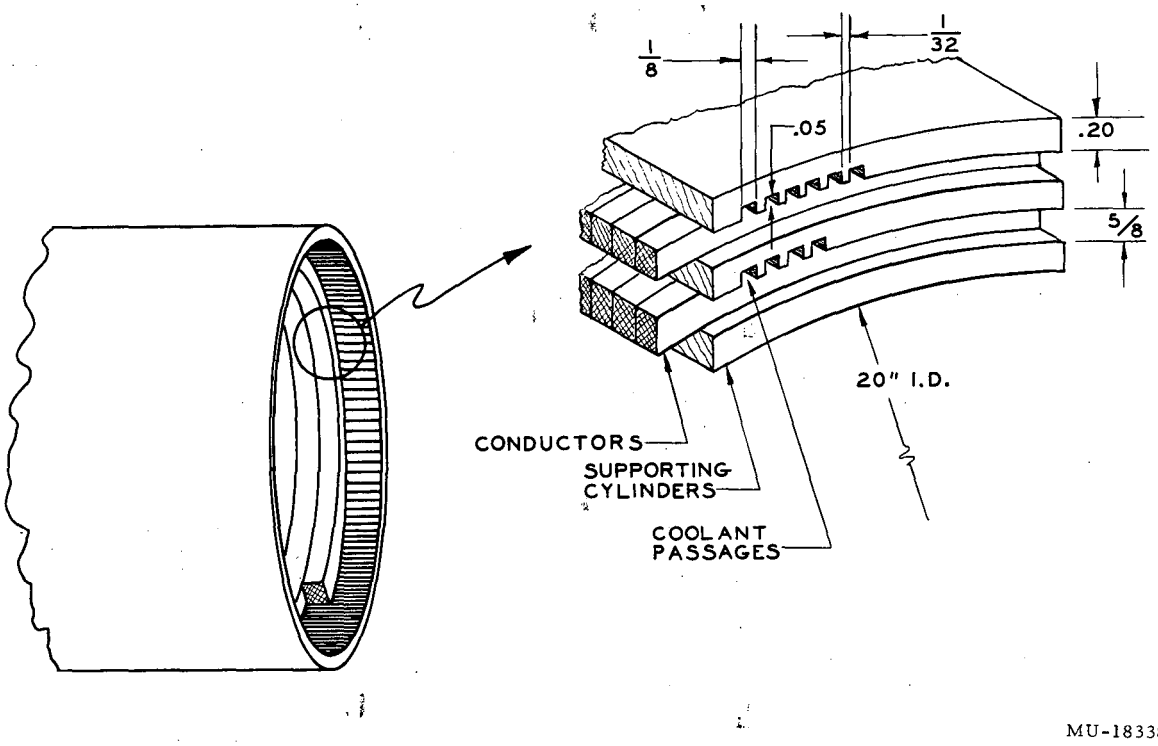

Fig. 35. Conductors and supporting cylinders.

ELECTRICAL ENGINEERING DEVELOPMENT

Vernon L. Smith

Pyrotron

David R. Branum

Table Top II

During the past three months, there has not been a fault in the capacitor bank, coil assembly, or switching chain.

The present chain of crowbar switches, sixteen type-WL-5555 ignitrons, still hold test voltages up to 20 kv rms. The crowbar tubes have been in service since January 1958 and have sustained 19,156 pulses on the machine at an average bank voltage of ± 8 kv. The bank has had peak voltages up to ± 16 kv during this time. The series switches, eight type-WL-5555 ignitrons, have been in service for 48,000 pulses.

Tests of a mechanical switch that closed a short circuit around the crowbar tubes after they had shorted the coil were continued this quarter. There was considerable down time, some 5 weeks, because of failure of the various switch elements. The L/R or decay time of the field in the crowbarred or shorted coil increased from 8 msec with the crowbar tubes alone to 14 msec with the tubes plus the switch. The longer L/R time was desired for the physics experiment now on the machine, therefore any switch failure stopped the experiment; this accounts for a rather low machine operation of only 1,765 pulses at ± 10 kv for this quarter. The normal field-decay time of 8 msec is now long enough for the physics experimenters, so that the mechanical switch has been decoupled from the machine.

In addition to electronics engineering effort on the machine itself, some time was spent on the development of and application of small transitorized scintillation detectors. During this time the signal desired at the output increased in amplitude and time duration, so that the developed detectors were being used beyond their design specifications. New detectors with the new specifications of linear output signals to 40 v and time durations of 20 msec are now in the design stage.

Considerable effort has been expended on the electronic control and swtiching chassis for the 50-kv 1-ma electron gun now under development by the physics group of Table Top II. A temporary 5-kv switching circuit is now being designed and built in order to test the first attempt at the electron gun itself.

There was also considerable engineering effort this quarter spent in assisting the contract physicist from Stanford Research Institute. This effort consisted of designing and having constructed a special shielded low-noise- output source pulser, and then aiding in eliminating or decreasing to an allowable level all transients in the experimental signal-detection system.

Toy Top II

There was continuing engineering effort in the development of the electronics for accurate triggering of multiple pulsed plasma sources and for a system to handle the data-reduction problem of the multiple-output analyzers under development by the physics group.

The machine has been in a period of dc field runs only, so that there has not been any capacitor-bank problem.

Two new 300-kw dc 2,000-amp power supplies for the dc field have been added, and the external connecting cables from the power-supply building to the machine are now under construction. This will give Toy Top a total of five 300-kw dc power supplies--a continuous power of 1.5 Mw or a pulsed power of 2.7 Mw. An additional 500,000-circular-mil cable run between Toy Top II diagnostic room and source-test room is also being constructed. This will allow both areas the use of the two new 300-kw dc supplies.

In addition to the new dc supplies, two high-voltage charging supplies of the kenotron type are under construction. This will give Toy Top two 20-kv 2-amp dc supplies to charge the four main capacitor banks instead of the two 20-kv 200-ma supplies used for the last three years. The allowable pulse rate of the machine could be increased from once every 10 to 12 min to once a minute if desired.

P-4

A new additional arc or beam current-limiting resistor band was designed and is now ready for construction. The unit consists of a series parallel arrangement of eighty 1-kw incandescent lamps.

Some effort was also spent in developing a system of recording the photomultiplier outputs from the large spectrograph used on the machine. A dual-function amplifier-recorder system is desired in order to adequately display the spectral lines of the P-4 beam on a chart recorder. Both a linear and a log function are desired.

Pyrotron–Miscellaneous

H. W. Van Ness

Felix Area

An "out-bakable" high-vacuum mass spectrometer has been rebuilt and put into operation in this area.

Grid Source Development

An arc current regulator system (controlling cathode emission) has been designed and put into successful operation.

A voltage-regulator system for the arc high-voltage supply is being designed.

Getter-Pump Development

Design and successful operation of an electron bombardment current limiter has been achieved.

A high-speed solenoid gas valve has been designed and produced for tests in this program.

Pinch and Collapse

H. W. Van Ness

Gamma Bank Area

Fuses for the charging circuit of the bank have been developed and will be installed as soon as down time is available.

Pulse tests of nickel-plated liner sections for the Levitron toroidal pinch experiment are starting.

Fusing for the electrolytic capacitor banks has been developed and is being installed.

Plasma Acceleration Experiment

A prototype capacitor and ignitron "module" for a fast bank is completed and undergoing tests. Control-system installation for the bank is essentially complete.

Sodium Radiofrequency Analog Experiment

A 5-kw 20-kc relaxation oscillator system has been constructed and checked out for this experiment.

300-kv Marx Bank Area

Excessive premature failures of five out of forty-five Tobe Deutschmann capacitors occurred during operation in a three-file test section of bank. Failure appears to be due to poor construction of capacitors, and a conference with the manufacturer is being arranged. Capacitor internal connections open up because of magnetic and thermal forces, which are applied during each pulse operation. Series connection of capacitors appears to aggravate this situation and causes more rapid deterioration than for conventional parallel bank operation.

Tests are starting to determine if paralleling cross ties between files can reduce or eliminate this problem without introducing other operational difficulties.

Energy-Storage-System Investigation

A trip by engineering personnel to the Allis-Chalmers factory revealed some unsolved design problems of unipolar generators. An adequate scheme of staybolts to withstand the explosive stresses during pulse operation must be determined. Several proposals were discussed and it appears a solution is near at hand. Delivery of the unit is postponed to October 15 because of loss of work time resulting from a strike.

System design and tests on elements such as a 1.5×10^6-amp switch, current-measuring "Hall" semiconductor devices, etc., are in progress at Livermore in anticipation of delivery.

Switch Development

D. B. Cummings

Mechanical Switching

The fast mechanical crowbar relief switch has been used with mixed success on Table Top. We have believed for more than 8 months that silver-tungsten or copper-tungsten would be the best contact materials. Makeshift combinations have been used because of protracted delays in the delivery of satisfactory parts. More than 2,000 operations have been obtained at currents up to 90 ka, although with numerous shutdowns required. The switch is not at present in operation. It will be returned to service as soon as the desired refractory contact assemblies are delivered.

Ignitron Development

Tube Tests

The most attractive approach recently has been tubes with molybdenum anodes. Some have gone through more than 4,000 operations at 25 kv. Unfortunately enough molybdenum is vaporized to cause extensive wetting of the ignitor. This produces a greatly decreased ignitor resistance, resulting in firing failures. Experiments were carried out to match impedances with a step-down pulse transformer with a very stiff circuit. This cleaned up wetted ignitors and kept clean ones from wetting. Unfortunately it also broke off ignitor tips. We must find out if there is a power level that can keep ignitors clean without breaking them. Westinghouse hollow ignitors did not break, but they would not fire after about 100 shots. It is hoped that when suitable ignitors and (or) ignitor-firing circuits are developed a reliable 20-kv tube will have been realized.

Ignitron Mechanisms Investigation

Numerous Kerr-cell photos have been taken of a pulsed glass ignitron. The velocity of arc-spot ring propagation varies with voltage from 4×10^5 to 2×10^5 cm/sec. The growth appears velocity-limited at higher peak currents, rather than following the current. The maximum velocity attained at a given voltage level appears proportional to about the 0.7 power of the peak current at that level. Tests are being made to determine the dependence on

temperature and circuit parameters. We are gaining a much better comprehension of the whole breakdown mechanism.

Microwave Diagnostic Experiments

Harlin L. Bunn

P-4 Experiment

1. Swept Frequency Receiver

An S-band swept frequency receiver was designed for studying electron cyclotron radiation from the P-4 machine. A magnetic field of 1,000 gauss requires a receiver frequency of 2800 Mc. A Raytheon QK 518 backward-wave oscillator with circuit provisions for leveling was used for the local oscillator. Noise figures on the order of 6 to 10 db were obtained over a 1000-Mc band width. The receiver was installed on the experiment, and evidence of radiation over a band centered at 2800 Mc was noted. The antenna used for receiving this radiation was an open-ended wave guide extended to within a few inches of the plasma.

The receiver initially was installed in close proximity to the machine. Work is now in progress to relocate the receiver at the machine console, using a waveguide run to the machine. Future efforts will include a properly designed antenna and a very-low-level detector because of the low power levels being radiated.

2. Interferometers

A 4-mm interferometer using a Phillips DX 151 klystron was installed. This is being used to study the decay of the P-4 beam. Additional work in the method of presentation is required.

The 8-mm interferometer presently in use has been modernized to use the R 9521 klystron. Considerably greater power and frequency coverage are realized through its use. PRD Type-6606 ridge guide detectors were used. These detectors use IN 53 crystals and are superior in performance to other detectors used.

3. 4-mm and 8-mm Antennas

Because of shift in position of the P-4 beam, adjustable antennas are required. On the basis of design requirements provided by A. Gardner, a device was built which allows manual shifting in position of the 8-mm and 4-mm antennas used with the respective interferometers. This has been installed and is presently in use.

Table Top Experiment

A K-band interferometer was assembled and installed on Table Top, using the single-frequency fringe presentation. Because of the pulsed operation of this machine, it has been difficult to obtain meaningful results because the plasma is too dense and cuts off K-band transmission. It is also suspected that the plasma column is pinched to such a small size that the

microwave energy scatters around the column, upsetting the requirement of a large slab geometry, a condition assumed by Wharton and Slager in their initial work on interferometers.

Because of the difficulties enumerated in the above paragraph, an 8-mm interferometer was installed on Table Top. Somewhat better results were obtained, but the preamplifier requires some modification to improve its performance. The problem of scattering around the column does not appear to have improved, and some future work on design of a narrow beam radiator is necessary.

Toy Top Experiment

Two superheterodyne receivers are required for studying radiation from the Toy Top machine at different points along the machine. Fields used will be 395 gauss and 593 gauss, requiring frequencies of 1100 Mc and 1660 Mc. Very-broad-band antennas with maximum diameters of 4 in. are required because of the geometry. Helical antennas with gains of 13 db, beam widths of 45 deg, and band widths of 50% have been designed and are being fabricated. An Amerac cavity Model 198A, using a 6BM6 klystron, will provide local oscillator power. Mixing of the L. O. and signal will occur in a coaxial mixer and the difference frequency will be fed to a conventional intermediate-frequency amplifier.

The X-band, K-band, and Ka-band (8-mm) interferometer chassis have been tidied up with better mechanical layout.

Advanced Development

1. Harmonic Receiver

A study of synchrotron radiation is desired by Toy Top physicists, requiring the use of a multiharmonic superheterodyne receiver. Theoretically, radiation should occur at the electron-cyclotron frequency and at its harmonics. Since the harmonics occur at exact multiples of the electron-cyclotron frequency, it would be highly desirable to have one power source to provide fundamental and harmonic local oscillator energy. This is accomplished by splitting the power output of a 23-kMc-klystron into three separate paths by means of a directional coupler and wave-guide tee. Output from the directional coupler would provide local oscillator energy at 23 kMc. Power split by means of the tee would be used to drive two separate crystal multipliers, providing 46 kMc and 69 kMc local oscillator energies. Such a receiver has been demonstrated.

2. Temperature Monitor

A circuit has been designed for monitoring the bulb temperature of a DX 151 klystron and for shutting off the voltage to the tube should the maximum temperature be exceeded. A bridge circuit using a thermistor sensing element was used. This will be installed on each DX 151 in use.

3. Telemetering Circuits

Transistorized circuits for monitoring high-voltage probe currents are being developed. This would consist of an FM or PM system using diode modulators. This design has not been successfully demonstrated at present.

4. Transistorized Preamplifier

A transistorized version of a preamplifier used in current equipment has been designed. Band width achieved is .3 Mc. Some more work on the noise level and input impedance is necessary.

5. Low-Loss Wave Guides

a. TE_{01} Wave Guide

Successful development of very dense plasmas requires the use of wave lengths on the order of 3 or 4 mm. Increasing frequency results in greater loss per unit length in standard rectangular wave guides because of skin losses. There are two available sources of power at 70 kMc. One of these, a DX 151 klystron, has an output power of about 100 mw. The other, a classified tube, has considerably less power. A 4-mm interferometer using these tubes has been installed. The installation had to be made in immediate proximity to the machine because the long runs of wave guide from the machine console attenuated the signal so that the interferometer would not work. It is therefore evident that low-loss wave-guide transmission is extremely important. The use of the Multimode TE_{01} type of transmission is being considered. A section of Helix Waveguide for use as a mode filter is being built here by using data from The Bell Laboratories. The Bell Transition from rectangular to circular TE_{01} wave guide has previously been built here but has not performed satisfactorily. Dr. H. E. Rowe of Bell Laboratories indicates that the transition was too short and the method of manufacture was incorrect. An attempt will be made to fabricate this design correctly, either at this laboratory or an outside concern.

A second type of transition, invented by Marie in France, will be fabricated. This is different from the Bell transition in that all machined surfaces are planes, instead of curved surfaces as in the Bell transition. This results in an inherently simple mandrel to be used in electroforming.

A transition designed by Microwave Associates will also be tried. The disadvantage is that the band width is only 6% as compared to a full-wave-guide band for the other two transitions. A guide size of 0.634 in. i.d. will be used for all three transitions, as this prevents all TE_{0n} modes above TE_{01} from being transmitted. This results in a somewhat higher loss, but for the length of runs expected the loss is not too important.

When these components are completed, installation will be made on the P-4 machine because an operating 4-mm interferometer is being used there.

b. H Guide

A new type of wave guide consisting of two parallel planes separated by a dielectric strip exhibits the same property of decreasing loss with increasing frequency as does the TE_{01} mode. Studies of this mode, predicted in 1956 by Tischer, have been made at the Microwave Research Institute, Polytechnic Institute of Brooklyn. These studies indicate that the mode does indeed show decreasing loss with increasing frequency in the range of frequencies studied (25 kMc to 50 kMc). A simple rectangular horn is used for launching the mode from rectangular wave guide.

6. Gas Discharge Tube

A study is being made of the possibility of generating 4-mm power from a 35-watt 8-mm Elliot Brothers klystron, using the gas discharge tube developed by Baird at the University of Illinois Ultra Microwave Laboratory. Late data just received indicate successful generation of 6 milliwatts at 70 kMc, and expectation of improved conversion efficiency with further effort. Use of this device would result in a source of 4-mm power costing about half that of DX 151, although not as much power. Construction of the gas discharge tube has been completed and testing will take place next quarter.

7. Frequency Multiplication

Studies are being made of schemes of frequency multiplication. These include crystal multiplication using standard techniques, and the possibility of achieveing frequency multiplication by means of plasmas. In conjunction with this, an Oak Ridge-designed Von Ardenne Duo Plasmatron is being constructed, and a power supply for powering this unit has been designed and is under construction. Studies will be made to see if frequency multiplication can be achieved with plasmas.

8. Neutron-Detection Experiment

A scheme generated by C. B. Wharton for detecting neutrons by using a microwave cavity filled with combinations of certain gases has been successfully demonstrated. Measurement of the shift in resonant frequency and change in "Q" of the cavity indicates the flux density of a neutron source. This was evaluated on the Laboratory boiling-water reactor. The result is a device, having practically no dead time, that can be used for detecting neutrons. This can be used with future Sherwood machines that create fusion and emit neutrons.

Astron

Kris Aaland

Pulse-Forming Network (PFN) Charging Supply

The polarity was reversed to negative on the PFN. This eliminated a recurring voltage-breakdown condition involving a filament-supply isolation transformer. The filaments can now be run at ground potential.

Main Field Supply (66 kw, 0.1% current regulated)

A fast-response (0 to 30 kc) dc current transformer of 4000 to 1 ratio has been added to the shunt circuit. This increases the over-all loop gain and eliminates a 2-sec thermal time constant encountered with the previous system, which utilized low-voltage light bulbs.

Electron Gun (750 kv)

Design proposals are being worked up. An effective accelerating voltage of 750 kv for 0.25 μsec is required. The two proposals under study are

(a) Marx generator,

(b) induction accelerator, utilizing pulsed magnetic cores with the electron beam as a secondary.

Induction Accelerator

The 750-kv beam developed by the electron gun mentioned above will be accelerated 2 Mev by an induction accelerator.

Tests under pulse conditions have been made on tape-wound silicon steel cores 1 mil and 2 mils thick. Additional tests to determine peak current and rates of rise will be made with a 1257 glass thyratron and a type-GL-7093 low-inductance ceramic thyratron.

Cross-Section Atomic and Molecular Beam Measurements

David R. Branum

A temporary experimental setup was built for cross-section measurements using the crossed-beam technique. The setup consisted of small ac and dc power supplies, voltage regulators, and recorders.

Design and construction are now under way for the experimental area in Building 180. The racks and vacuum control power are now under construction.

Some effort is being applied to the design of a 100-cycle chopper that has to run in a vacuum of 10^{-6} mm of Hg with variation of only one-half cycle. A 100-cycle-response electrometer amplifier is now being purchased and a 100-cycle phase comparator is now ready for construction.

TALKS AND PUBLICATIONS

IV International Conference on Ionization Phenomena in Gases, Uppsala, Sweden, August 17 - 21, 1959:

C. B. Wharton, Microwave Radiation Measurements of Very Hot Plasmas (UCRL-5514 Abstract, March 1959).

D. H. Birdsall, S. A. Colgate, and H. P. Furth, The Hard-Core Pinch. I (UCRL-5599, July 1959).

D. H. Birdsall, S. A. Colgate, and H. P. Furth, The Hard-Core Pinch. II (UCRL-5602, July 1959).

R. F. Post, Some Aspects of High-Temperature Plasma Research with the Mirror Machine (UCRL-5604-T Abstract, June 1959).

W. R. Baker, A. Bratenahl, A. W. DeSilva, and W. B. Kunkel, Viscous Effects in Highly Ionized Rotating Plasmas (UCRL-8861, August 1959).

University of California, Berkeley, California, Alumni House; July 15, 1959:

R. F. Post, Thermonuclear Energy (invited paper).

University of California at Los Angeles, Los Angeles, California, Mathematical Sciences Building, July 17, 1959:

R. F. Post, Thermonuclear Energy (invited paper).

Sacramento State College; Sacramento, California, July 27, 1959:

H. P. Furth, Controlled Thermonuclear Reactions (invited paper).

Space Technology Laboratory, Los Angeles, California, August 7, 1959:

H. P. Furth, Hard-Core Pinch (invited paper).

U. S. Naval Base, Treasure Island, California, August 19, 1959:

Warren Heckrotte, Plasma Physics Research in the Sherwood Project (invited paper).

Journal Publications

The Physics of Fluids:

F. H. Coensgen, W. F. Cummins, and A. E. Sherman, Multistage Magnetic Compression of Highly Ionized Plasma July-August issue.

S. A. Colgate, Collisionless Plasma Shock, September-October issue.

Annual Review of Nuclear Science:

R. F. Post, Thermonuclear Reactions, 9, (1959).

Information Division
sa